Computational Fluid Dynamics: Past, Present and Future

Prof. Antony Jameson

Department of Aeronautics & Astronautics
– *Aerospace Computing Laboratory* –
Stanford University
jameson@baboon.stanford.edu

Future Directions in CFD Research
National Institute for Aerospace
August 6–8, 2012, Hampton, VA

Outline

Outline

History of CFD in Van Leer's View

Emergence of CFD

- In 1960 the underlying principles of fluid dynamics and the formulation of the governing equations (potential flow, Euler, RANS) were well established
- The new element was the emergence of powerful enough computers to make numerical solution possible – to carry this out required new algorithms
- The emergence of CFD in the 1965–2005 period depended on a combination of advances in computer power and algorithms.

Some significant developments in the '60s:

- birth of commercial jet transport – B707 & DC-8
- intense interest in transonic drag rise phenomena
- lack of analytical treatment of transonic aerodynamics
- birth of supercomputers – CDC6600

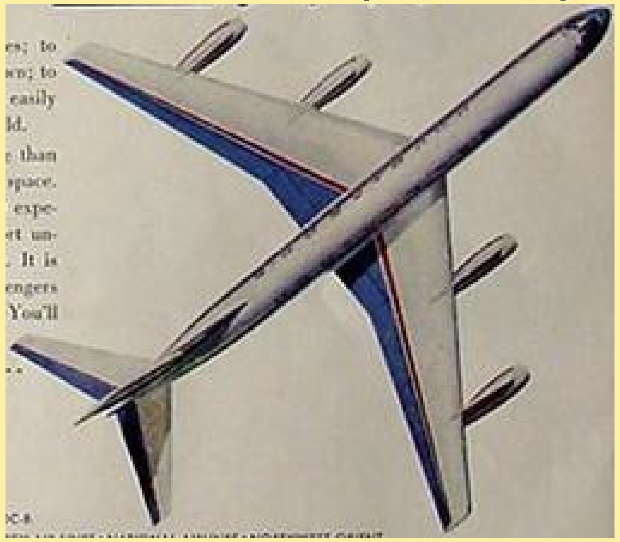

DC-8

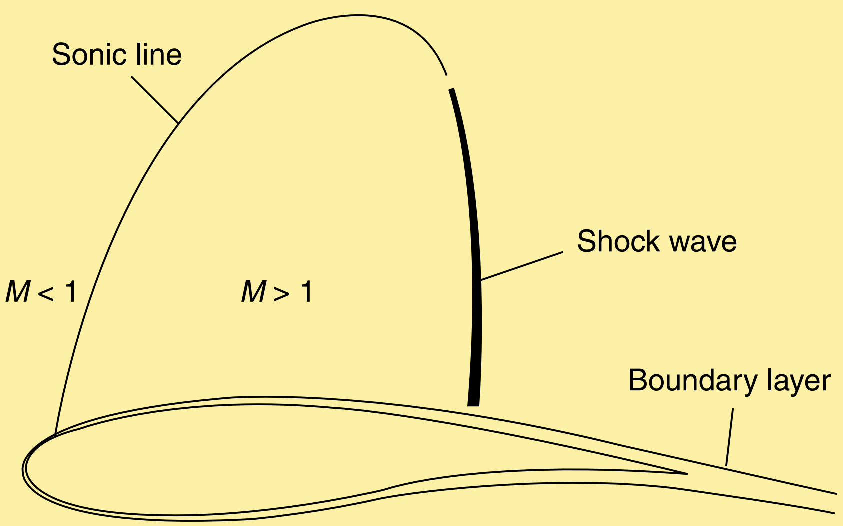

Transonic Flow

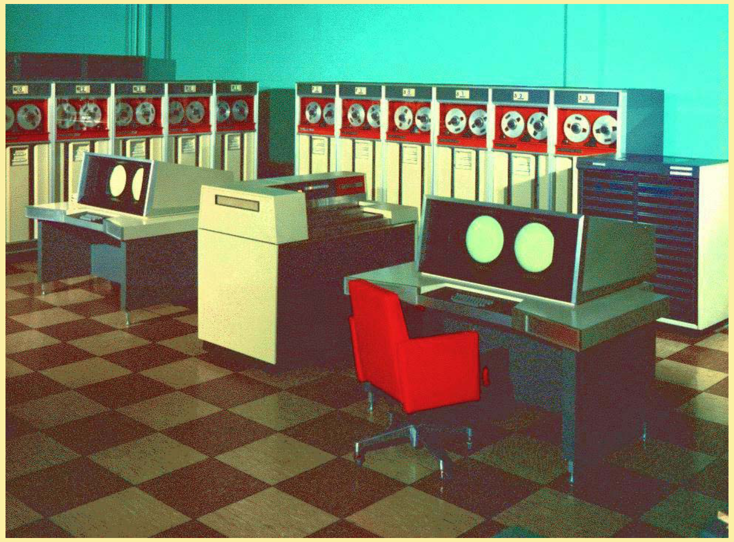

CDC6600

Multi-Disciplinary Nature of CFD

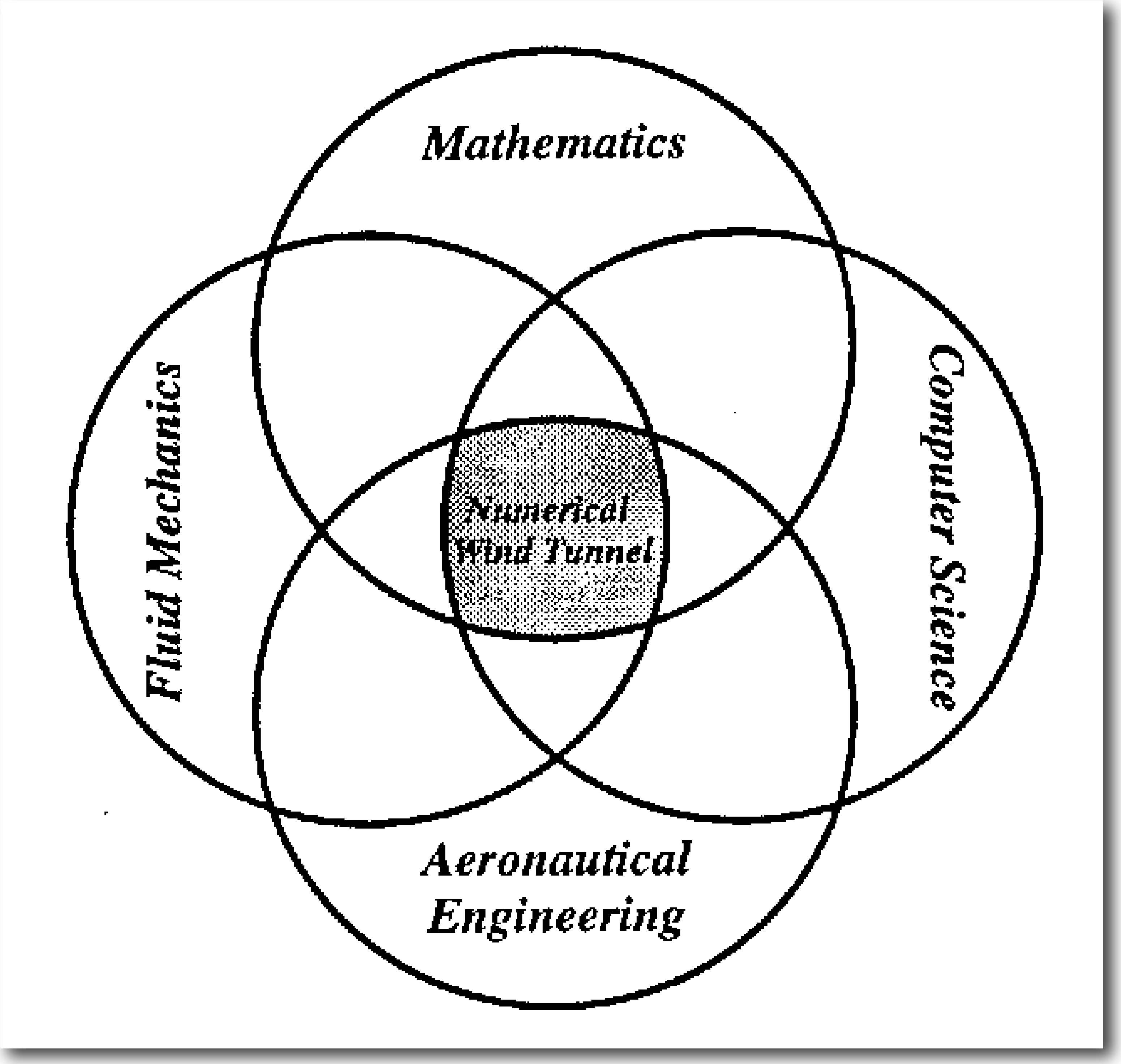

Hierarchy of Governing Equations

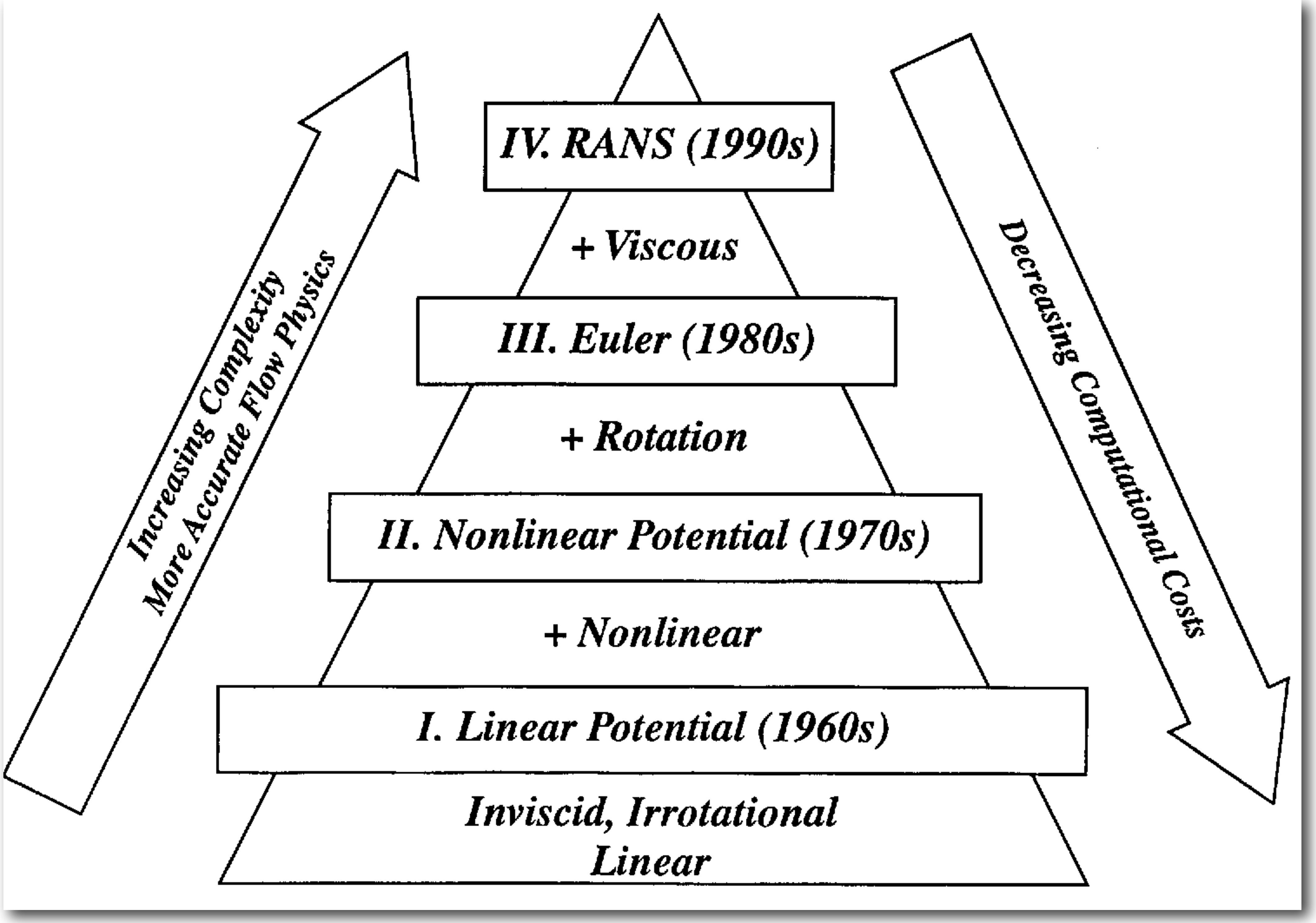

50 Years of CFD

- 1960–1970: **Early Developments**

  Riemann-based schemes for gas dynamics (Godunov), 2nd-order dissipative schemes for hyperbolic equations (Lax-Wendroff), efficient explicit methods for Navier-Stokes (MacCormack), panel method (Hess-Smith)

- 1970–1980: **Potential Flow Equations**

  type-dependent differencing (Murman-Cole), complex characteristics (Garabedian), rotated difference (Jameson), multigrids (Brandt), complete airplane solution (Glowinsky)

- 1980–1990: **Euler and Navier-Stokes Equations**

  oscillation control via limiters (Boris-Book), high-order Godunov scheme (van Leer), flux splitting (Steger-Warming), shock capturing via controlled diffusion (Jameson-Schmit-Turkel), approximate Riemann solver (Roe), total variation diminishing (Harten), multigrids (Jameson, Ni), solution of complete airplane (Jameson-Baker-Weatherill)

- 1990–2000: **Aerodynamic Shape Optimization**

  adjoint based control theory

- 2000–2010: **Discontinuous Finite Element Methods**

  Discontinuous Galerkin, Spectral Difference, Flux Reconstruction, *etc.*

Advances in Computer Power

1970	CDC6600	1 Megaflops	10^6
1980	Cray 1 Vector Computer	100 Megaflops	10^8
1994	IBM SP2 Parallel Computer	10 Gigaflops	10^{10}
2007	Linux Clusters	100 Teraflops	10^{14}
2007	(affordable) Box Cluster in my house Four 3 GHz dual core CPUs (24 Gigaflops peak) $10,000	2.5 Gigaflops	2.5×10^9
2009	HP Pavilion Quadcore Notebook $1,099	1 Gigaflops	10^9
2011	MacBook Pro Quadcore Laptop $2,099	2.5 Gigaflops	2.5×10^9

Outline

The Cost of the Degrees of Freedom

Fluid dynamic problems involve polynomials with large N and fairly large p

Complexity of Fluid Dynamic Simulations - Explicit Schemes

- With $N \approx n^3$ mesh points in 3D and explicit time stepping, each time step requires $O(n^3)$ operations
- The time step of a stable scheme is proportional to the mesh interval h divided by the wave speed, and $h \approx 1/n$, giving complexity $Cn^4 \approx N^{4/3}$ with a constant C depending on the algorithm

Complexity of Fluid Dynamic Simulations - Implicit Schemes

- An implicit scheme requires matrix inversion at each time step with complexity NB^2 where B is the bandwidth $\approx \mathrm{n}^2$, so the cost of a step is $O(n^7)$
- The time step is not limited by the mesh interval, so the number of time steps is independent of n, giving total complexity $\approx \mathrm{n}^7$

Grid Size for a Transport Aircraft Wing

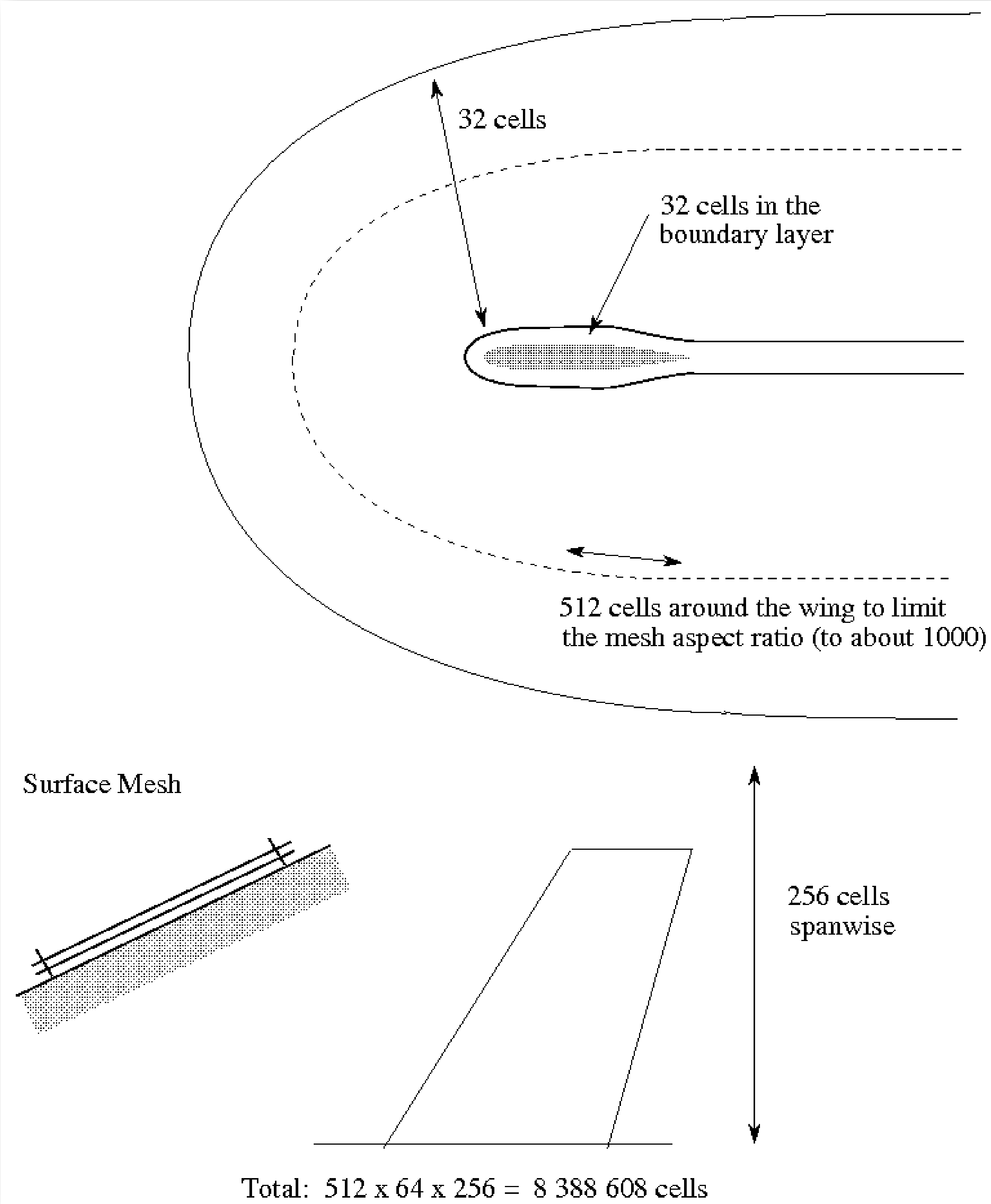

Complexity of CFD in the ‘70s

- The complexity of a 3D prediction of transonic flow is $O(n^4)$ and reasonable accuracy can be obtained with $n \approx 100$
- Calculations could be completed in $O(10^8)$ operations with a CDC 6600 which could achieve $\approx 10^6$ flops
- Thus a useful 3D calculation might be possible in $O(10^2)$ seconds
- The author recognized this in 1971
- Actually FLO22 (Jameson and Caughey), which was the first program which could actually predict transonic flow over a swept wing with engineering accuracy, required about 10,000 seconds for a solution

Complexity of CFD in the ‘80s

- 800,000 mesh cells for a viscous mesh around a wing
- 5,000 flops per solution step using FLO107
- 300 steps for the solution to converge
- $(8 \times 10^5) \times (5 \times 10^3) \times (3 \times 10^2) = 1.2 \times 10^{12}$

Roughly 10^{12} flops for RANS simulation on 0.8 million mesh cells

With a 1 Gigaflop computer, solution takes about 1,000 seconds...

... About 400 seconds with a 2011 MacBook Pro quadcore at 2.5 Gflops

CFD Complexity for Turbulent Flow Simulations

- For a turbulent flow with a Reynolds number *Re*, the length scale of the smallest eddies relative to the integral length scale $\approx Re^{-3/4}$ (Kolmogorov, 1943)
- With a comparable time step, the complexity of the simulations $\approx Re^3$
- For a jumbo jet such as the Airbus A380, $Re \approx 10^8$
- Direct Numerical Simulation (DNS) of the flow over the A380 has a complexity $\approx 10^{24}$ operations
- With a Petaflop computer (IBM Roadrunner, 2008), DNS of the A380 has a complexity of about 10^9 seconds

About 30 Years!

Outline

Impact of CFD on Configuration Lines & Wind Tunnel Testing

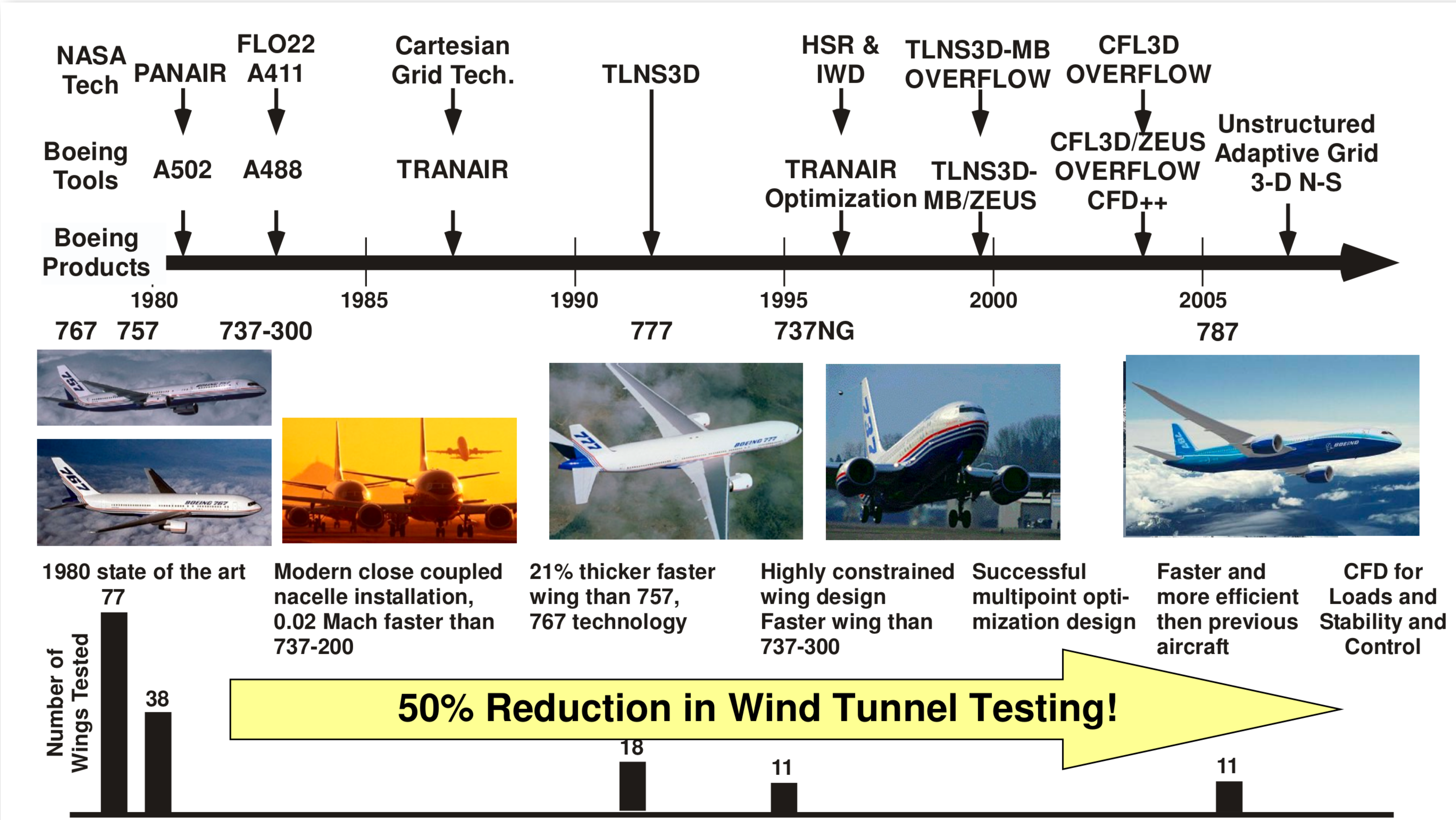

Impact of CFD on B737-300 Program

1975 1976 1977 1978 1979 1980 1981 1982 1983 1984

20 Years of wind tunnel based development indicated nacelles cannot be placed too close to the wing without excessive drag

Joint CFD/Wind Tunnel Studies unlock the secret of nacelle/wing interference drag

707/CFM56 Design & Flight Test validated CFD concepts

737-300 Program initially rejected due to high cost of increasing landing gear length

Go Ahead

Roll Out

Certification

Initial Studies

737-300 Program

McDonnell-Douglas MD-80 Go Ahead

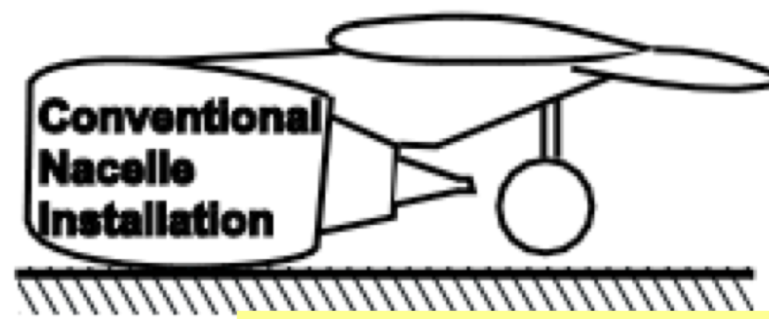

Without the understanding gained from CFD there would not have been a 737-300 Program!

Walt Gillette
Manager, 737 Aerodynamics - then
Vice President, 787 Engineering – retired

5000+ Additional Sales!

Computational Methods at Boeing

TRANAIR:

- Full Potential with directly coupled Boundary Layer
- Cartesian solution adaptive grid
- Drela lag-dissipation turbulence model
- Multi-point design/optimization

Navier-Stokes Codes:

- CFL3D – Structured Multiblock Grid
- TLNS3D – Structured Multiblock Grid, Thin Layer
- OVERFLOW – Overset Grid

N-S Turbulence Models:

- S-A Spalart-Allmaras
- Menter's k-ω SST

CFD Contributions to B787

CFD Development for Aircraft Design

MEGAFLOW / MEGADESIGN
- National CFD Initiative (since 1995)

Development & validation of a national CFD software for complete aircraft applications which

- allows computational aerodynamic analysis for 3D complex configurations at cruise, high-lift & off-design conditions
- builds the basis for shape optimization and multidisciplinary simulation
- establishes numerical flow simulation as a routinely used tool at DLR and in German aircraft industry
- serves as a development platform for universities

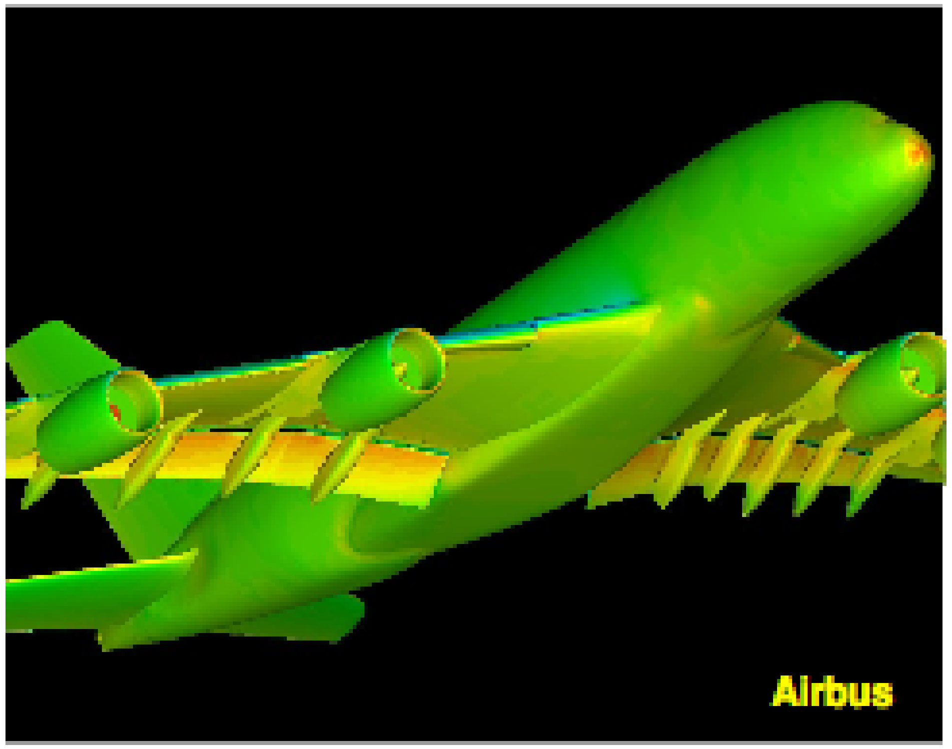

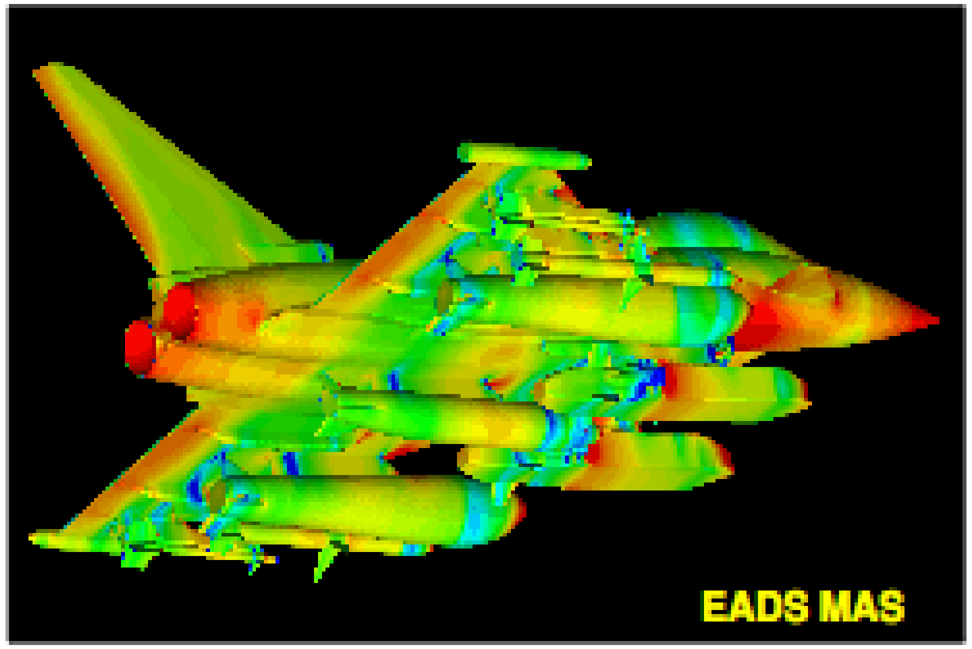

Block-Structured RANS Capability: FLOWer

Efficient simulation tool for configurations of moderate complexity

- advanced turbulence and transition models (RSM, DES)
- state-of-the-art algorithms
  - baseline: JST scheme, multigrid
  - robust integration of RSM (DDADI)
- chimera technique for moving bodies
- fluid / structure coupling
- design option (inverse design, adjoint)

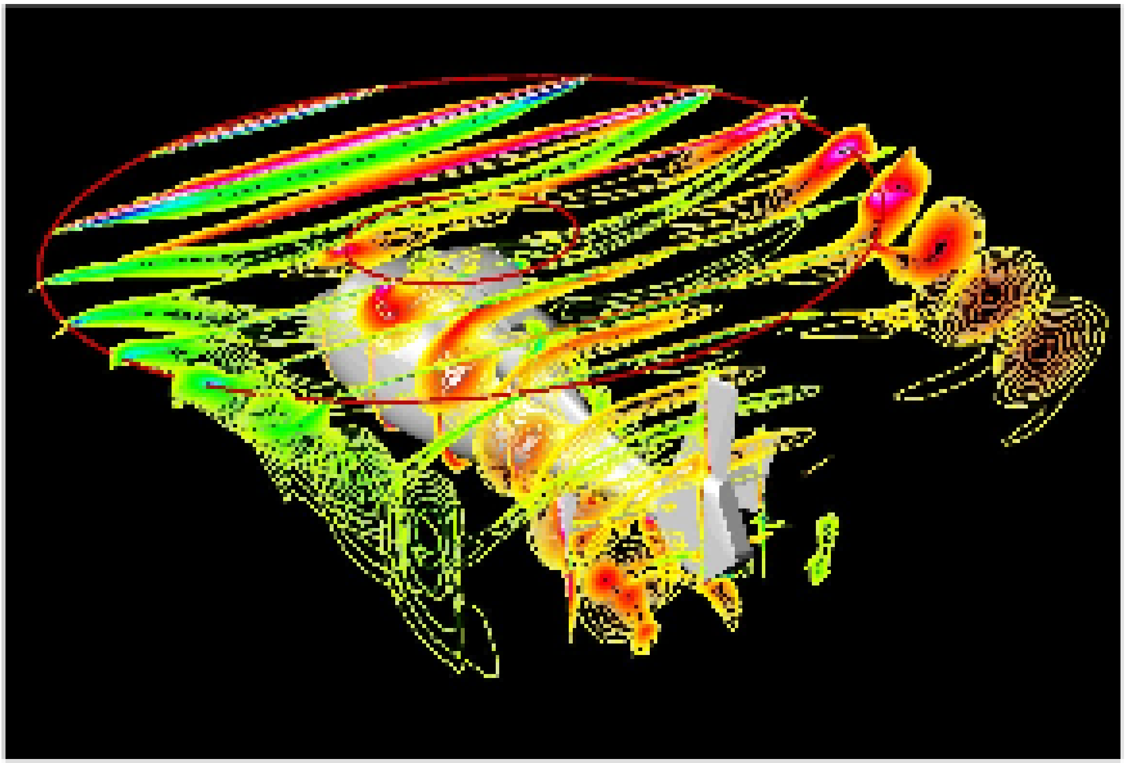

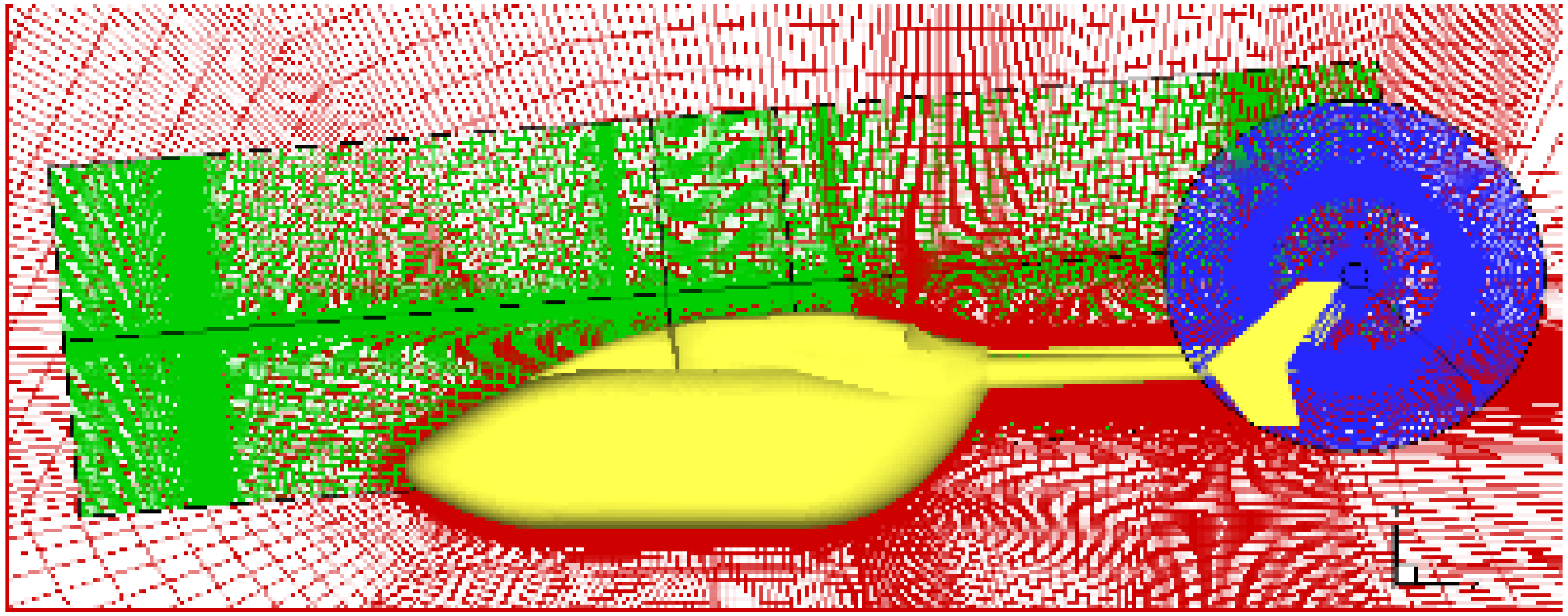

FLOWer-Code

- Fortran
- portable code
- parallelization based on MPI

Unstructured RANS Capability: TAU

Tool for complex configurations

- hybrid meshes, cell vertex / cell centered
- high-level turbulence & transition models (RSM, DES, linear stability methods)
- state-of-the-art algorithms (JST, multigrid, ...)
- local mesh adaptation
- chimera technique
- fluid / structure coupling
- continuous/discrete adjoint
- extensions to hypersonic flows

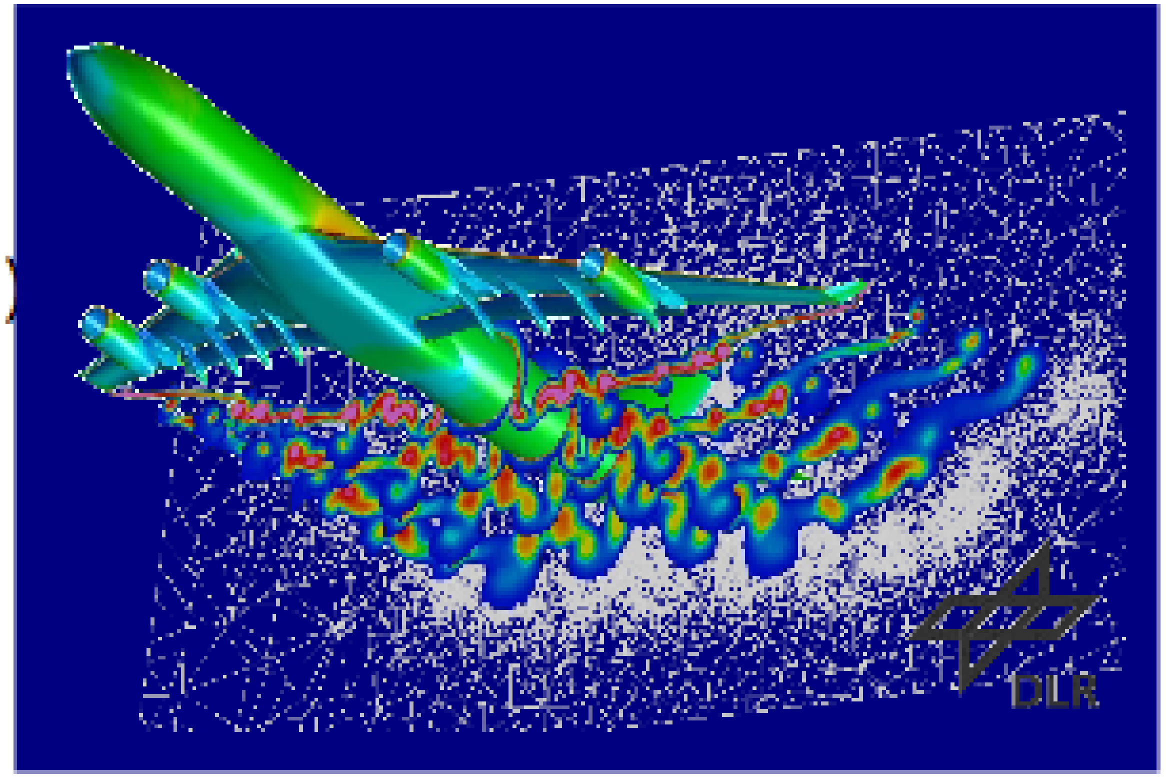

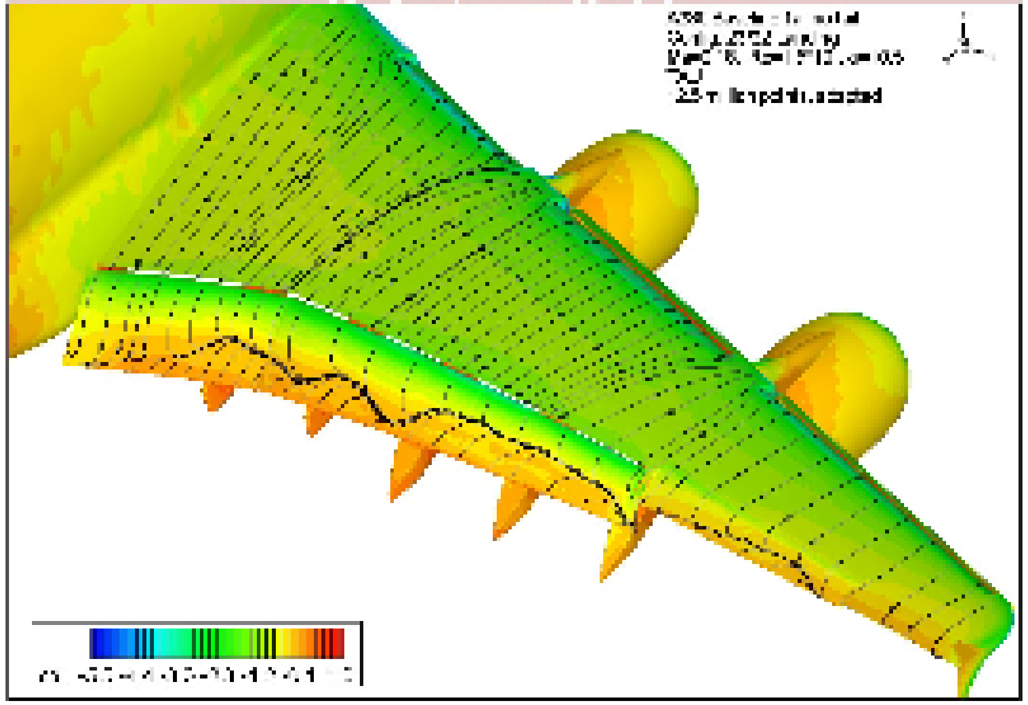

TAU-Code

- unstructured database
- C-code, Python
- portable code, optimized for cache hardware
- high performance on parallel computer

Numerical Flow Simulation

Relation CFD / wind tunnel

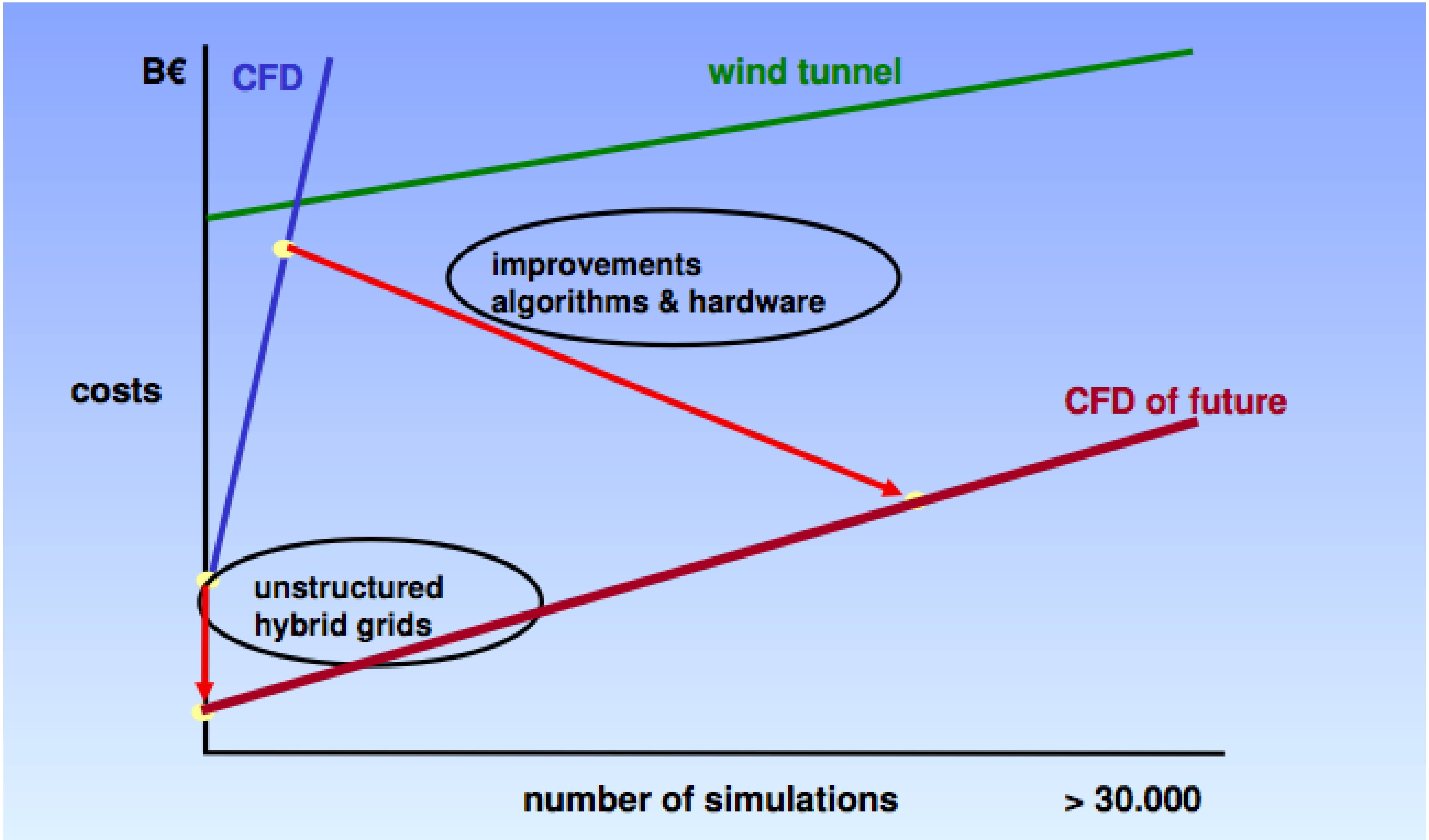

✈ **CFD cost effective alternative**

CFD Contribution to A380

Wing Optimization Using SYN107

State of the Art Wing Design Process in 2 Stages, starting from Garabedian-Korn Airfoil and NASA Common Research Model

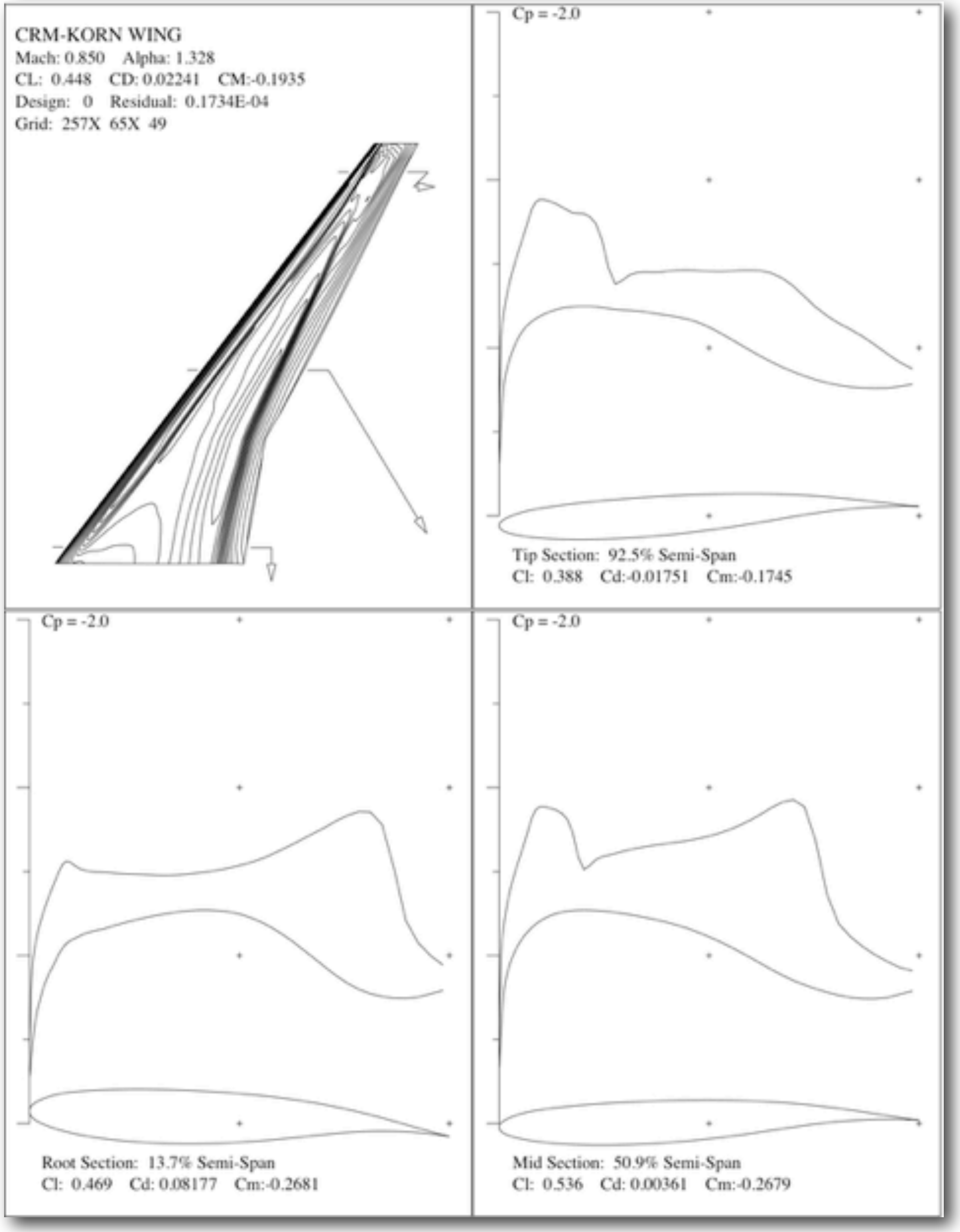

Wing Optimization Using SYN107

State of the Art Wing Design Process in 2 Stages, starting from Garabedian-Korn Airfoil and NASA Common Research Model

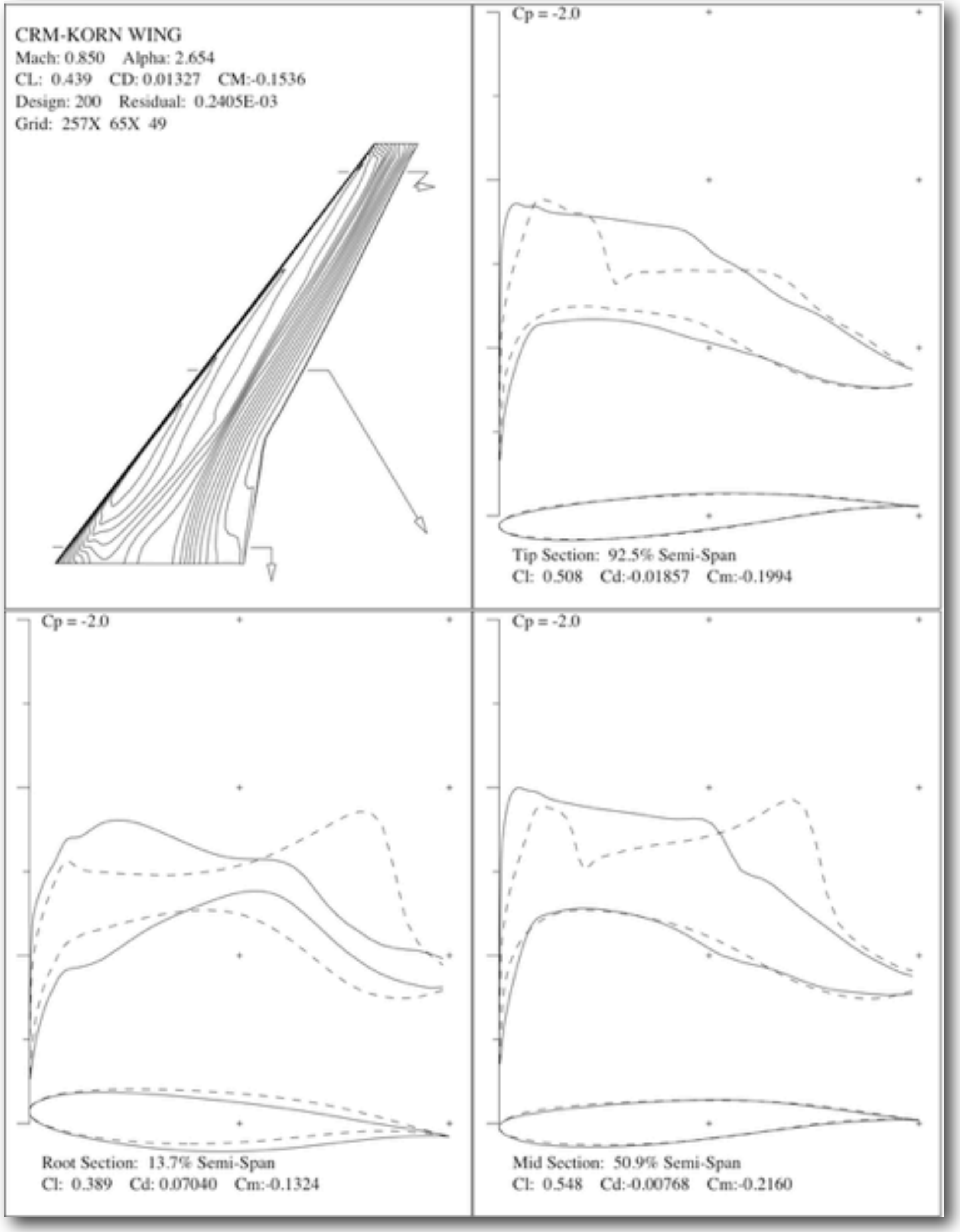

Outline

The Current Status of CFD

- Worldwide commercial and government codes are based on algorithms developed in the ‘80s and ‘90s
- These codes can handle complex geometry but are generally limited to 2nd order accuracy
- They cannot handle turbulence without modeling
- Unsteady simulations are very expensive, and questions over accuracy remain

The Future of CFD (?)

CFD has been on a plateau for the past 15 years

- Representations of current state of the art:
  - Formula 1 cars
  - Complete aircrafts
- The majority of current CFD methods are not adequate for vortex dominated and transitional flows:
  - Rotorcraft
  - High-lift systems
  - Formation flying

Large-Eddy Simulation

The number of DoF for an LES of turbulent flow over an airfoil scales as **$Re_c^{1.8}$ (resp. $Re_c^{0.4}$) if the inner layer is resolved (resp. modeled)**

Rapid advances in computer hardware should make LES feasible within the foreseeable future for industrial problems at high Reynolds numbers. To realize this goal requires

- high-order algorithms for unstructured meshes (complex geometries)
- Sub-Grid Scale models applicable to wall bounded flows
- massively parallel implementation

Chapman (1979), AIAA J. 17(12)

Typical Requirements of CFD

Traditional numerical schemes for engineering problems are too dissipative and do not provide sufficient accuracy for LES and DNS

- **Accuracy:** solution must be right
- **Small numerical dissipation:** unsteady flow features
- **Unstructured grids:** complex geometries
- **Numerical flux:** wave propagation problems
- **High resolution capabilities:** transitional and turbulent flows
- **Efficiency:** code parallelism
- ...

Classic Numerical Methods

Finite Difference

- Structured
- High-order
- Numerical flux

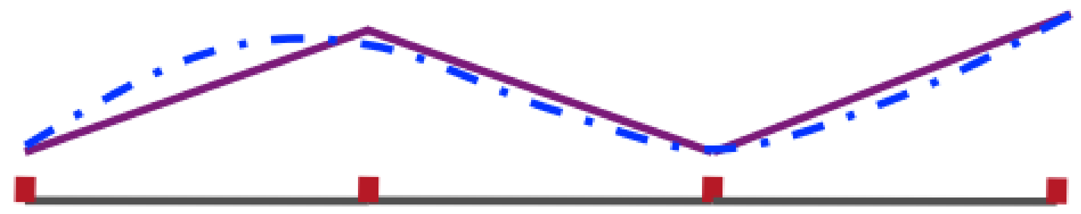

Finite Volume

- Unstructured
- Low-order
- Numerical flux

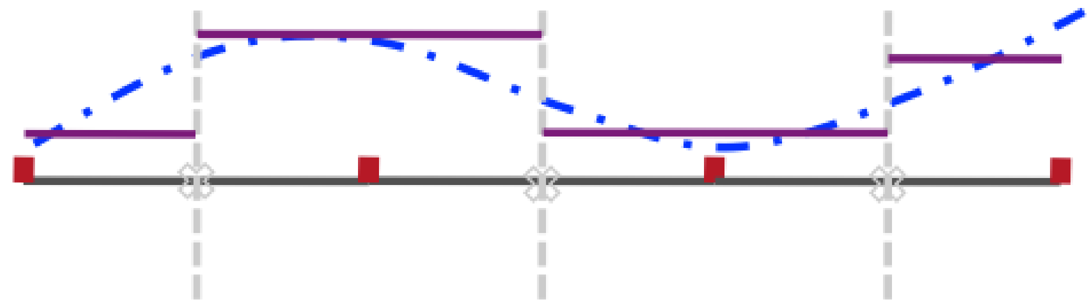

Continuous FE

- Unstructured
- High-order
- No numerical flux

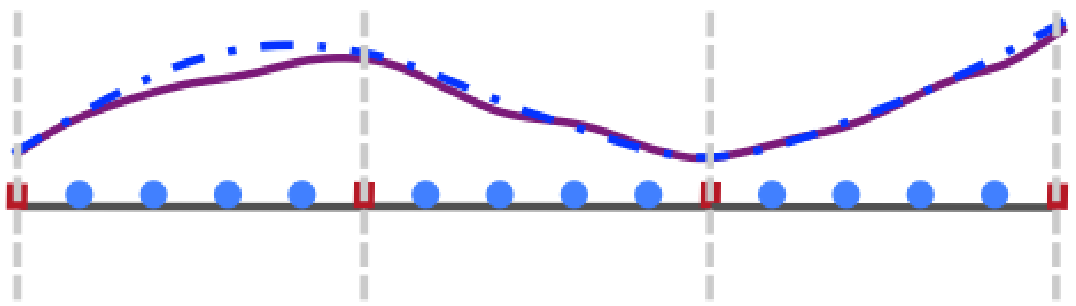

Classic Numerical Methods

Finite Difference

- Structured
- High-order
- Numerical flux

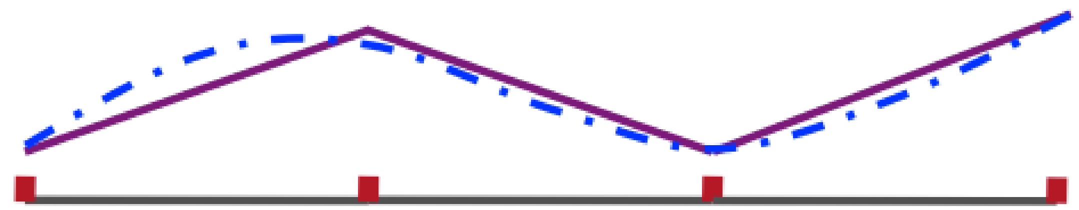

Finite Volume

- Unstructured
- Low-order
- Numerical flux

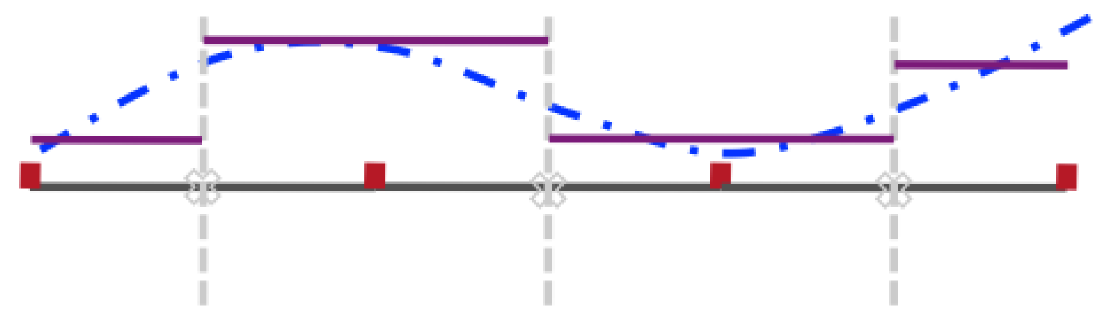

Continuous FE

- Unstructured
- High-order
- No numerical flux

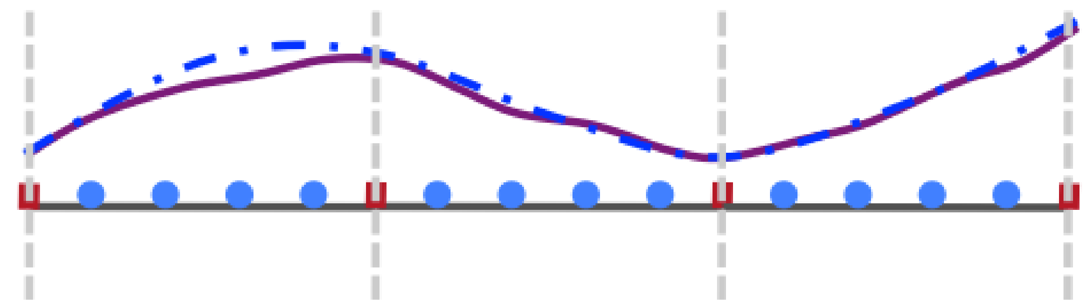

Disontinuous FE

- Unstructured
- High-order
- Numerical flux

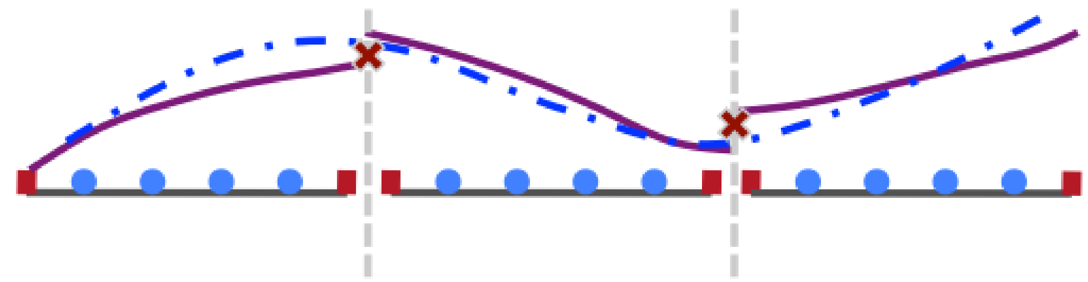

A Review of the Literature

Past Research on DG Schemes:

- Modern development of DG schemes for hyperbolic conservation laws stems from the work of Cockburn & Shu [1989a,1989b,1990,1998,2001]

Recent Research:

Attempts to reduce complexity and avoid quadrature:

- Spectral Difference (SD) scheme by Kopriva & Kolias [1996], Liu, Vinokur & Wang [2006]
- Nodal Discontinuous Galerkin (NDG) scheme by Atkins & Shu [1998], Hesthaven & Warburton [2007]
- Flux Reconstruction (FR) scheme by Huynh [2007,2009]

Cockburn, et al. (1989). J. Comput. Phys., 84(1); Cockburn, Shu (1989). Math. Comput., 52; Cockburn, et al. (1990). Math. Comput., 54(190); Cockburn, Shu (1998). J. Comput. Phys., 141; Cockburn, Shu (2001). J. Sci. Comput., 16; Kopriva, Kolias (1996). J. Comput. Phys., 125(1); Liu, et al. (2006). J. Comput. Phys., 216(2); Atkins, Shu (1998). AIAA J., 36(5); Hesthaven, Warburton, (Springer Verlag, 2007); Huynh, (2007). AIAA P., 2007-4079; Huynh, (2009) AIAA P., 2009-403

Outline

Introduction

- **The following presentation emphasizes development of Huynh's FR approach, and energy stability**
- **Energy stability analysis versus Fourier stability analysis**
  - Energy method is more general and rigorous
  - Energy method enables stability proofs for all orders of accuracy
  - Energy method applies to non-uniform meshes
  - *Fourier analysis provides more detailed information about the distribution of dispersive and diffusive errors*
  - *Fourier analysis identifies super accuracy for linear problems*

The Energy Stable FR scheme (ESFR):

- **Until recently, stable FR schemes identified on an ad hoc basis**
- **We have identified a range of correction functions that guarantee linear stability for all orders of accuracy**
- **Achieved by extending Jameson's proof of stability of an SD scheme for the linear advection equation for all orders of accuracy**

The Flux Reconstruction Scheme

The solution is locally represented by Lagrange polynomial of degree $n-1$ on the solution points:

$$u_h = \sum_{j=1}^{n} u_j l_j(x) \qquad f_h^D = \sum_{j=1}^{n} f_j^D l_j(x)$$

The flux is discontinuous and needs to be corrected in a suitable way

$$\Delta_L = \widetilde{f}_L - f_h^D(-1) \qquad \Delta_R = \widetilde{f}_R - f_h^D(1)$$

$$h_L(-1) = 1, \quad h_L(1) = 0 \qquad h_R(1) = 1, \quad h_R(-1) = 0$$

The continuous flux is obtained from the discontinuous counterpart by adding the correction functions of degree n weighted by the flux corrections

$$f_h^C = \sum_{j=1}^{n} f_j^D l_j(x) + h_L(x)\Delta_L + h_R(x)\Delta_R$$

The continuous flux is finally differentiated at the solution points and the solution is advanced in time

$$\frac{\partial u_i}{\partial t} + \left[\sum_{j=1}^{n} f_j^D \frac{\mathrm{d}l_j}{\mathrm{d}x}(x_i) + \Delta_L \frac{\mathrm{d}h_L}{\mathrm{d}x}(x_i) + \Delta_R \frac{\mathrm{d}h_R}{\mathrm{d}x}(x_i) \right] = 0$$

Huynh, (2007). AIAA P., 2007-4079; Huynh, (2009) AIAA P., 2009-403

The FR Scheme Graphically Illustrated

The solution is locally represented by Lagrange polynomial of degree *n*-1 on the *n* solution points:

$$u_h = \sum_{j=1}^{n} u_j l_j(x)$$

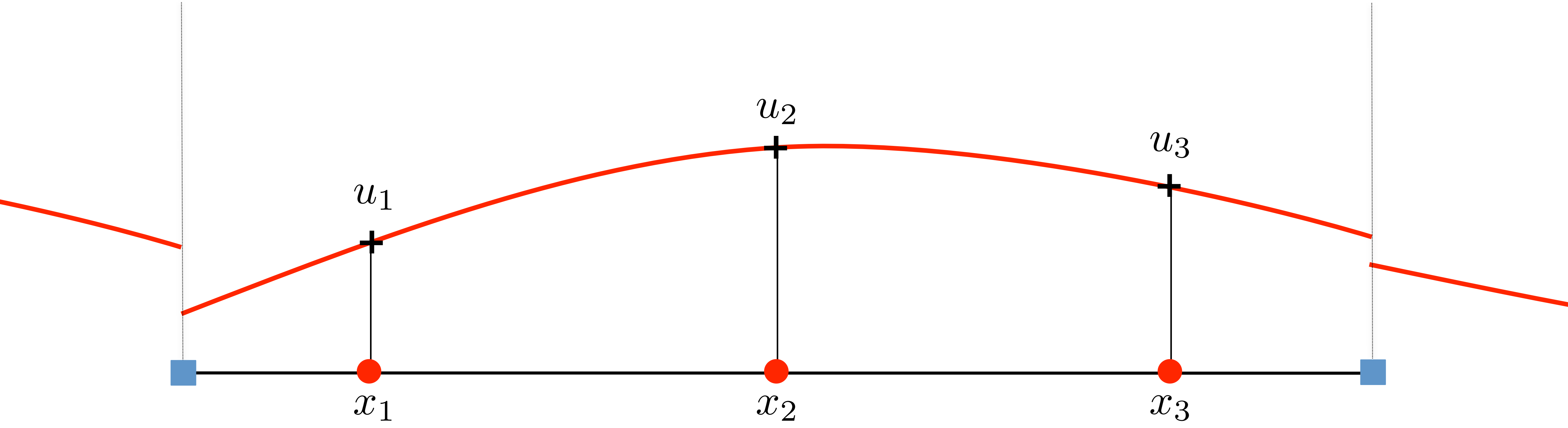

Huynh, (2007). AIAA P., 2007-4079; Huynh, (2009) AIAA P., 2009-403

The FR Scheme Graphically Illustrated

The discontinuous flux is constructed

$$f_h^D = \sum_{j=1}^{n} f_j^D l_j(x)$$

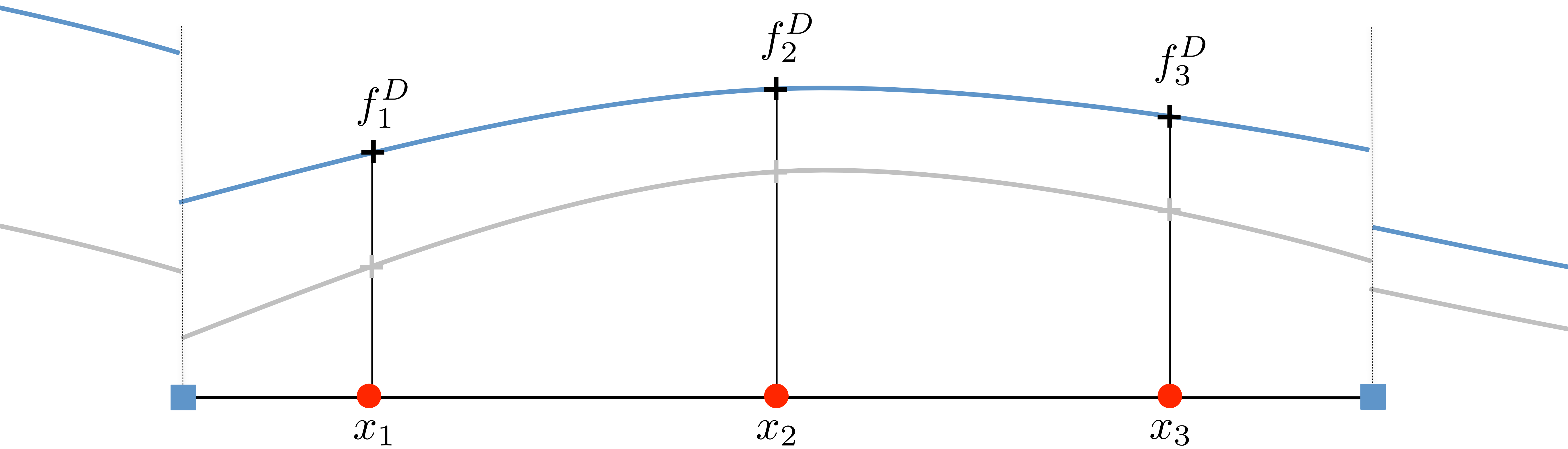

Huynh, (2007). AIAA P., 2007-4079; Huynh, (2009) AIAA P., 2009-403

The FR Scheme Graphically Illustrated

Solution is evaluated at element boundaries

$$u_L = \sum_{j=1}^{n} u_j l_j(-1) \qquad u_R = \sum_{j=1}^{n} u_j l_j(+1)$$

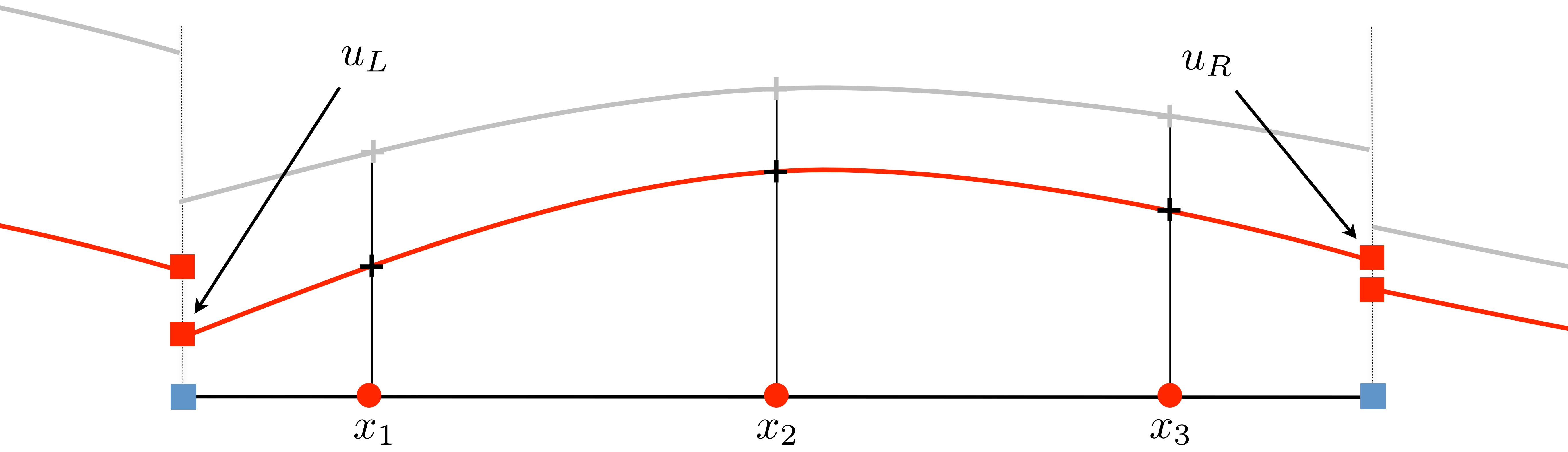

Huynh, (2007). AIAA P., 2007-4079; Huynh, (2009) AIAA P., 2009-403

The FR Scheme Graphically Illustrated

The common interface flux is computed from multiply defined values at each interface (FV-type numerical flux such as approximate Riemann flux)

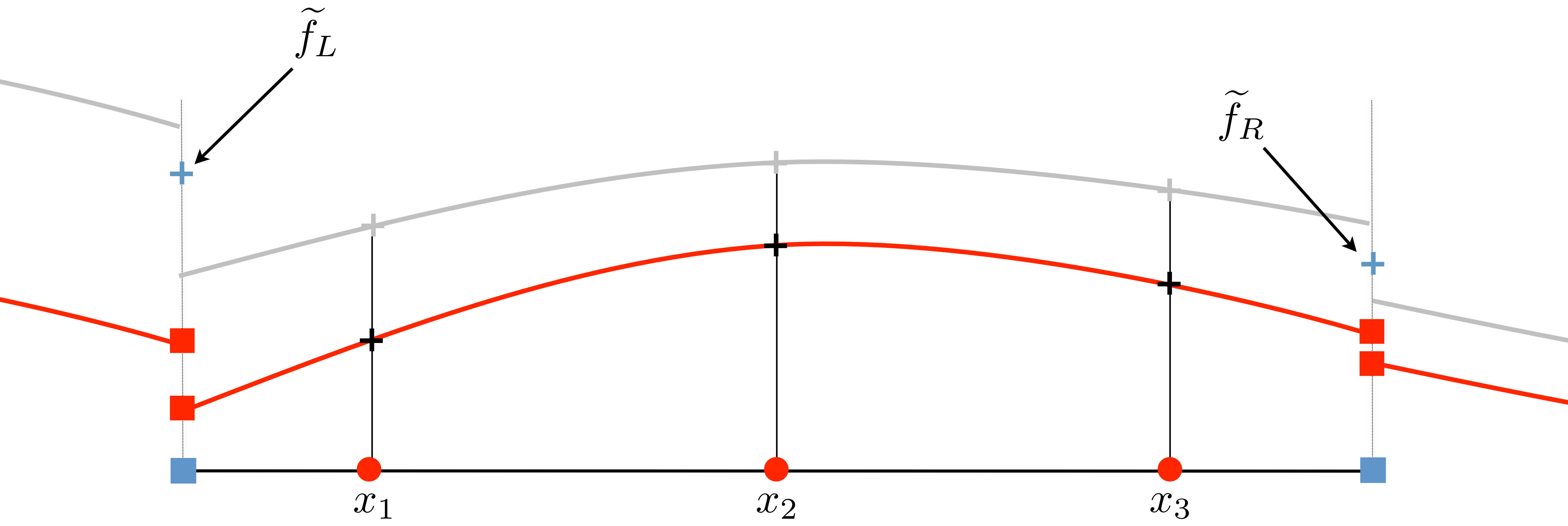

Huynh, (2007). AIAA P., 2007-4079; Huynh, (2009) AIAA P., 2009-403

The FR Scheme Graphically Illustrated

The **common** **interface flux is computed from multiply defined values at each interface (FV-type numerical flux such as approximate Riemann flux)**

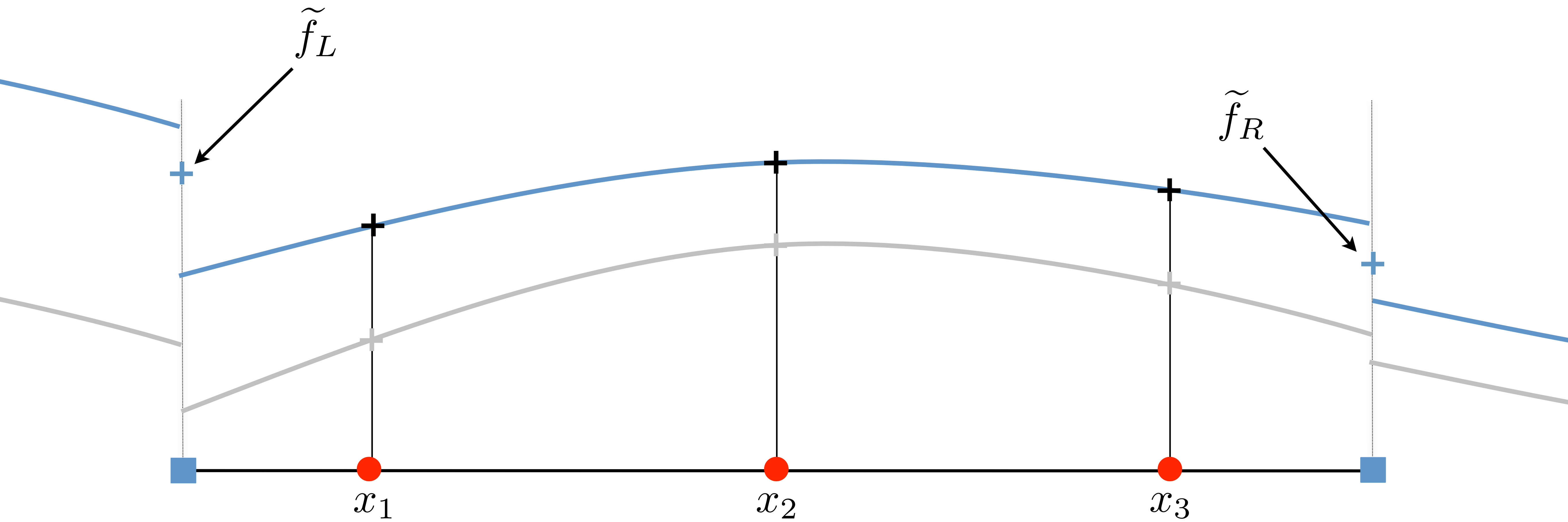

Huynh, (2007). AIAA P., 2007-4079; Huynh, (2009) AIAA P., 2009-403

The FR Scheme Graphically Illustrated

Correction functions of degree *n* are introduced

$$h_L(-1) = 1, \quad h_L(1) = 0$$

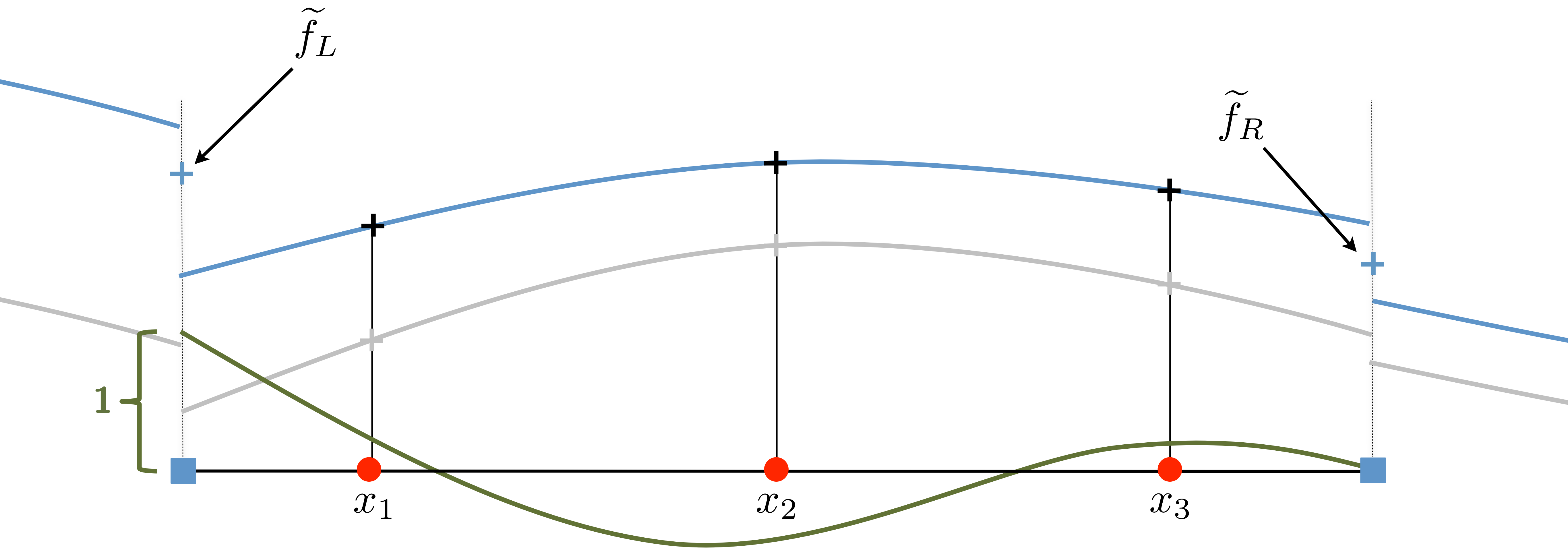

Huynh, (2007). AIAA P., 2007-4079; Huynh, (2009) AIAA P., 2009-403

The FR Scheme Graphically Illustrated

The correction functions are scaled

$$\Delta_L = \widetilde{f}_L - f_h^D(-1)$$

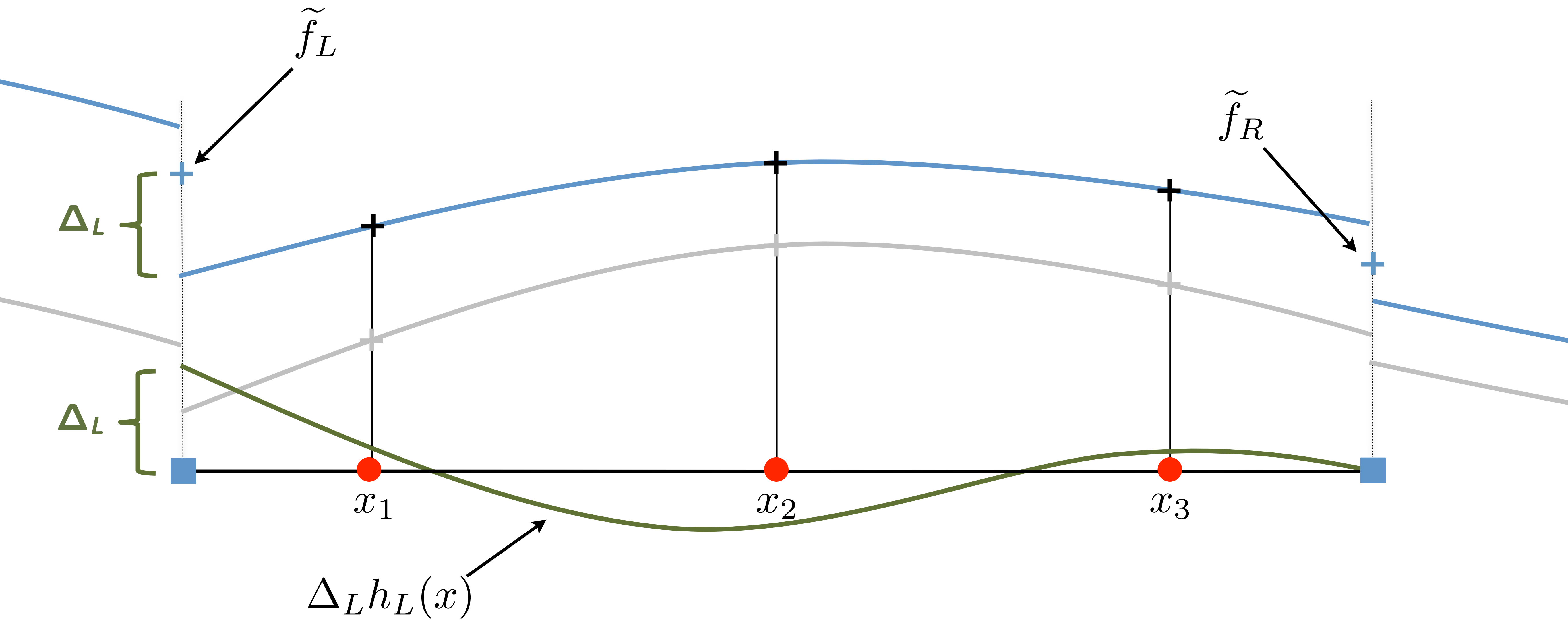

Huynh, (2007). AIAA P., 2007-4079; Huynh, (2009) AIAA P., 2009-403

The FR Scheme Graphically Illustrated

The correction is added to the discontinuous flux

$$f_h^* = \sum_{j=1}^{n} f_j^D l_j(x) + h_L(x)\Delta_L$$

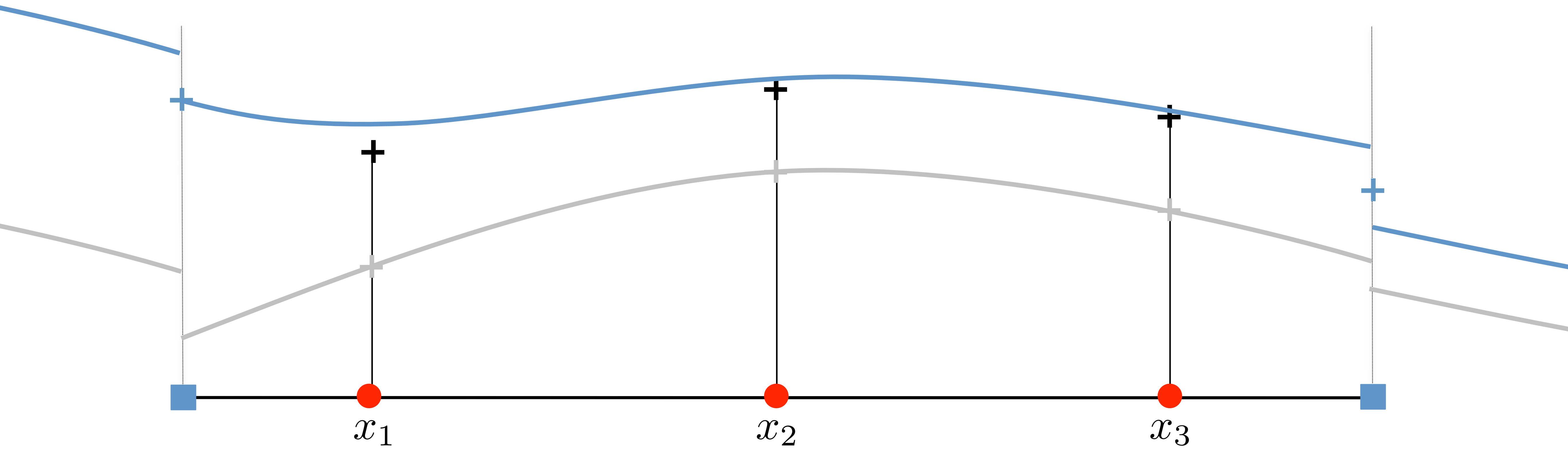

Huynh, (2007). AIAA P., 2007-4079; Huynh, (2009) AIAA P., 2009-403

The FR Scheme Graphically Illustrated

The right boundary is corrected the same way

$$h_R(1) = 1, \quad h_R(-1) = 0$$

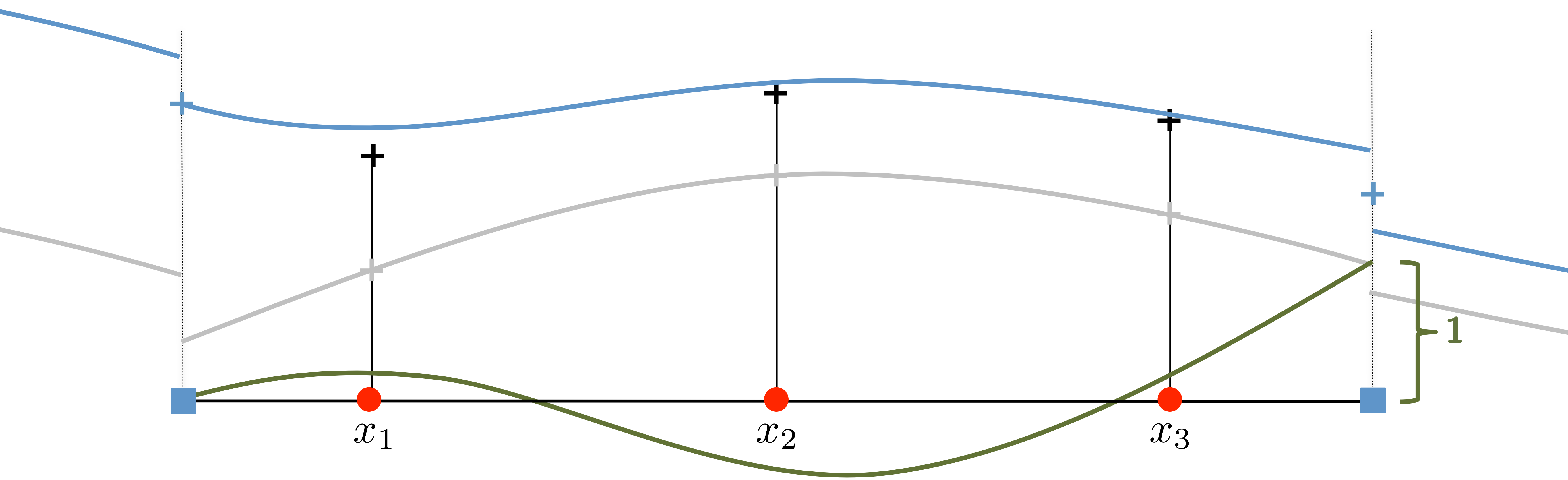

Huynh, (2007). AIAA P., 2007-4079; Huynh, (2009) AIAA P., 2009-403

The FR Scheme Graphically Illustrated

The correction is scaled...

$$\Delta_R = \widetilde{f}_R - f_h^D(+1)$$

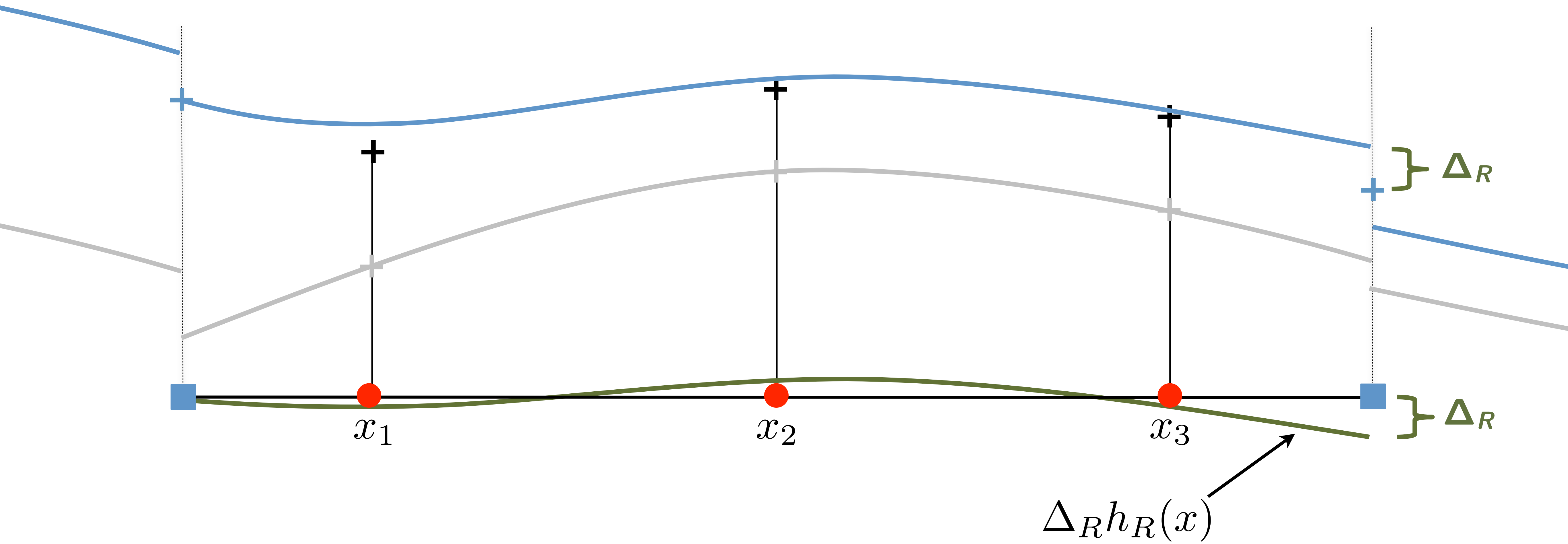

Huynh, (2007). AIAA P., 2007-4079; Huynh, (2009) AIAA P., 2009-403

The FR Scheme Graphically Illustrated

And added to the discontinuous flux

$$f_h^C = \sum_{j=1}^{n} f_j^D l_j(x) + h_L(x)\Delta_L + h_R(x)\Delta_R$$

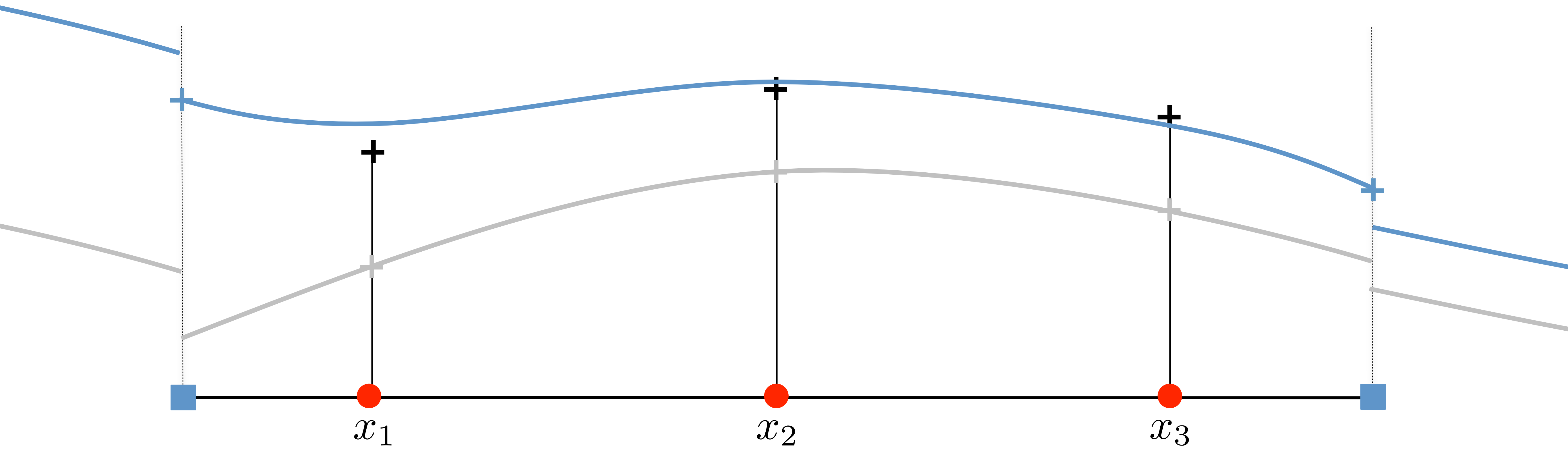

Huynh, (2007). AIAA P., 2007-4079; Huynh, (2009) AIAA P., 2009-403

The FR Scheme Graphically Illustrated

Total approximate continuous flux

$$f_h^C = \sum_{j=1}^{n} f_j^D l_j(x) + h_L(x)\Delta_L + h_R(x)\Delta_R$$

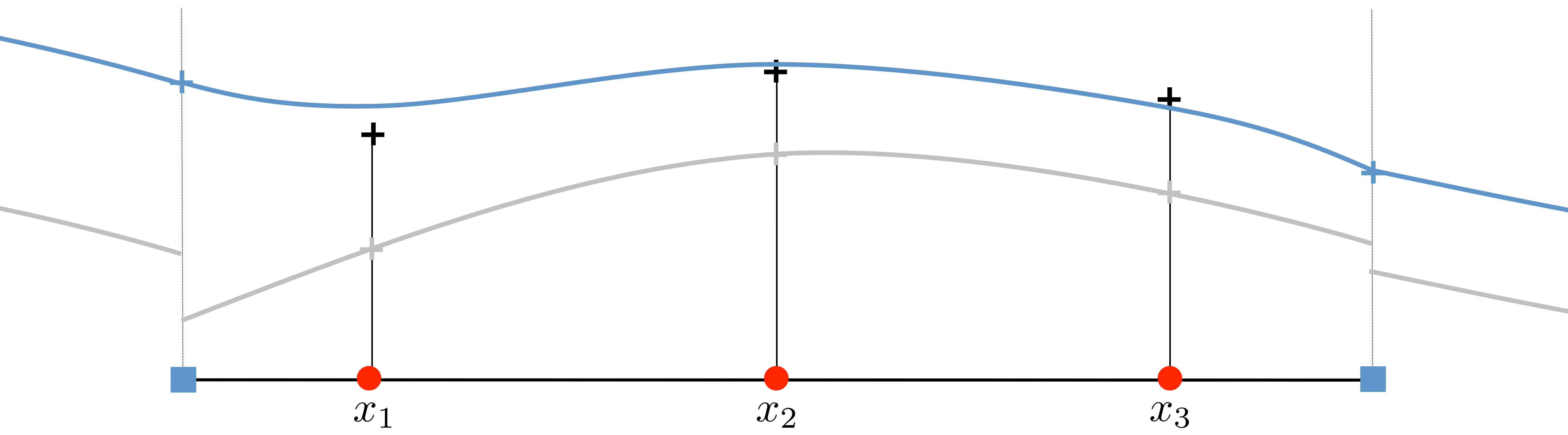

Huynh, (2007). AIAA P., 2007-4079; Huynh, (2009) AIAA P., 2009-403

The FR Scheme Graphically Illustrated

The divergence of the flux is evaluated at the solution points

$$\frac{\partial f^C}{\partial x}(x_i) = \sum_{j=1}^{n} f_j^D \frac{\mathrm{d}l_j}{\mathrm{d}x}(x_i) + \Delta_L \frac{\mathrm{d}h_L}{\mathrm{d}x}(x_i) + \Delta_R \frac{\mathrm{d}h_R}{\mathrm{d}x}(x_i)$$

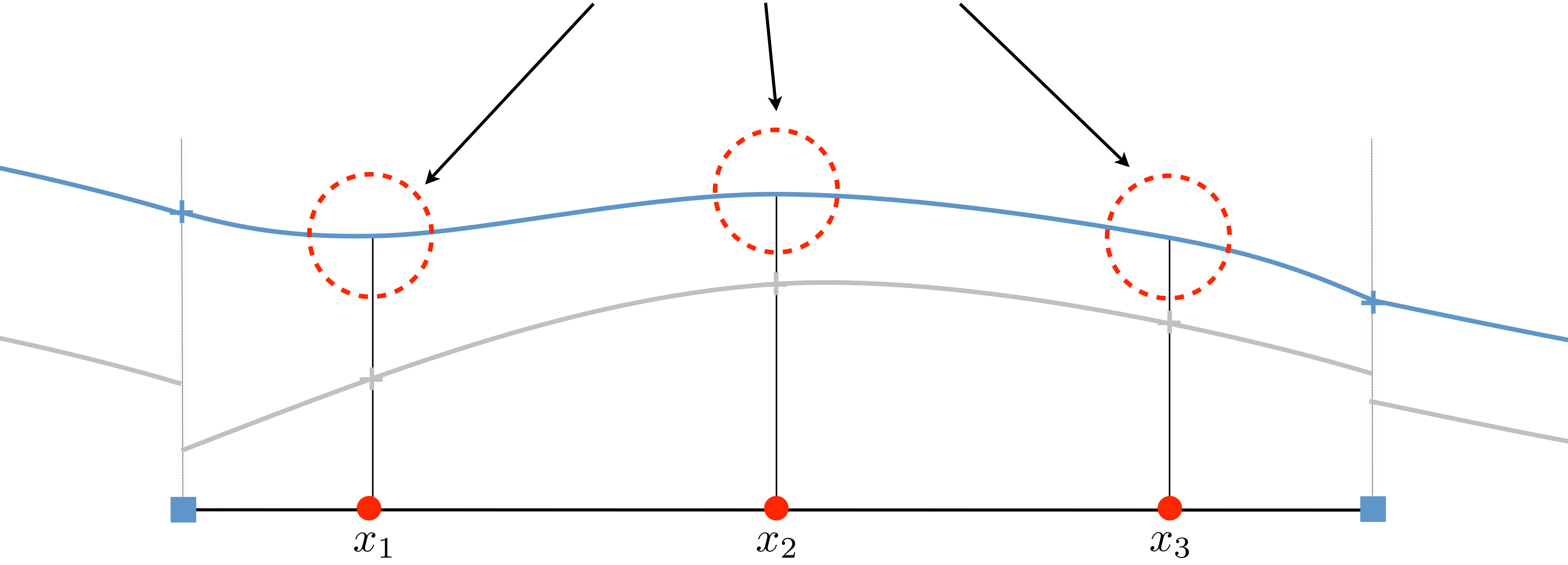

Huynh, (2007). AIAA P., 2007-4079; Huynh, (2009) AIAA P., 2009-403

The FR Scheme Graphically Illustrated

The solution is advanced in time

$$\frac{\partial u_i}{\partial t} + \left[\sum_{j=1}^{n} f_j^D \frac{\mathrm{d}l_j}{\mathrm{d}x}(x_i) + \Delta_L \frac{\mathrm{d}h_L}{\mathrm{d}x}(x_i) + \Delta_R \frac{\mathrm{d}h_R}{\mathrm{d}x}(x_i) \right] = 0$$

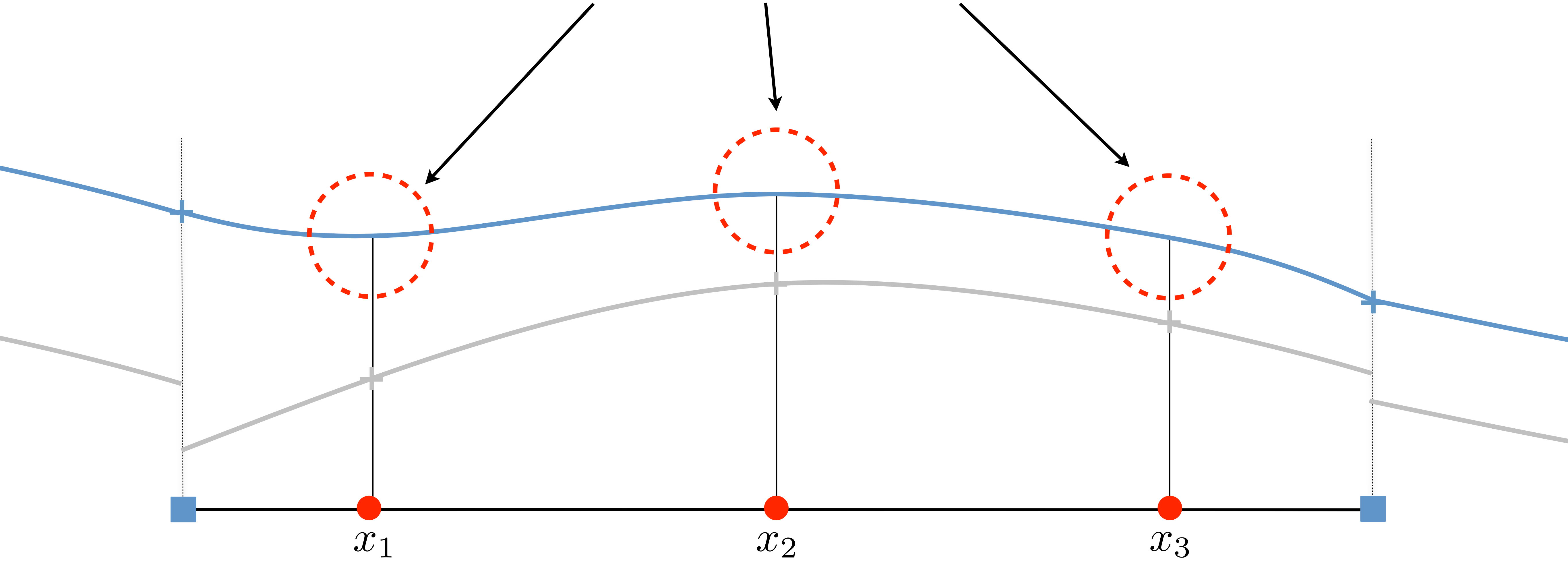

Huynh, (2007). AIAA P., 2007-4079; Huynh, (2009) AIAA P., 2009-403

Energy Stability of the FR Scheme

The FR method defines a family of energy stable schemes in the norm

$$||U^{\delta D}||_{p,2} = \left[\sum_{n=1}^{N} \int_{x_n}^{x_{n+1}} (U_n^{\delta D})^2 + \frac{c}{2}(J_n)^{2p} \left(\frac{\partial^p U_n^{\delta D}}{\partial x^p}\right)^2 \mathrm{d}x\right]^{1/2}$$

The schemes have the form

$$\frac{\partial u_i}{\partial t} + \left[\sum_{j=1}^{n} f_j^D \frac{\mathrm{d}l_j}{\mathrm{d}x}(x_i) + \Delta_L \frac{\mathrm{d}h_L}{\mathrm{d}x}(x_i) + \Delta_R \frac{\mathrm{d}h_R}{\mathrm{d}x}(x_i)\right] = 0$$

where the correction functions in terms of Legendre polynomials are

$$h_L = \frac{(-1)^p}{2}\left[L_p - \left(\frac{\eta_p(c)L_{p-1} + L_{p+1}}{1+\eta_p(c)}\right)\right]$$

$$h_R = \frac{(+1)^p}{2}\left[L_p + \left(\frac{\eta_p(c)L_{p-1} + L_{p+1}}{1+\eta_p(c)}\right)\right]$$

with a single parameter c

$$\eta_p(c) = \frac{c(2p+1)(a_p p!)^2}{2}$$

Vincent, et al. (2010). J. Sci. Comput., 47(1); Vincent, et al. (2011). J. Comput. Phys., 230(22)

A Family of Energy Stable Schemes

Accuracy

Nodal DG:

$$c = 0 \quad \Rightarrow \quad \eta_p = 0$$

$$g_L = \frac{(-1)^p}{2}\left[L_p - L_{p+1}\right], \quad g_R = \frac{(+1)^p}{2}\left[L_p + L_{p+1}\right]$$

Spectral Difference:

$$c = \frac{2p}{(2p+1)(p+1)(a_p p!)^2} \quad \Rightarrow \quad \eta_p = \frac{p}{p+1}$$

$$g_L = \frac{(-1)^p}{2}(1-x)L_p, \quad g_R = \frac{(+1)^p}{2}(1+x)L_p$$

G2 Scheme by Huynh [2007]:

$$c = \frac{2(p+1)}{(2p+1)p(a_p p!)^2} \quad \Rightarrow \quad \eta_p = \frac{p+1}{p}$$

$$g_L = \frac{(-1)^p}{2}\left[L_p - \frac{(p+1)L_{p-1} + pL_{p+1}}{2p+1}\right], \quad g_R = \frac{(+1)^p}{2}\left[L_p + \frac{(p+1)L_{p-1} + pL_{p+1}}{2p+1}\right]$$

Allowable Time-Step

Outline

Numerical Dissipation

N=6

Temporal Mixing-Layer

60×60 DoF

N=2

N=5: 100×200×10 DoF

Numerical Dissipation

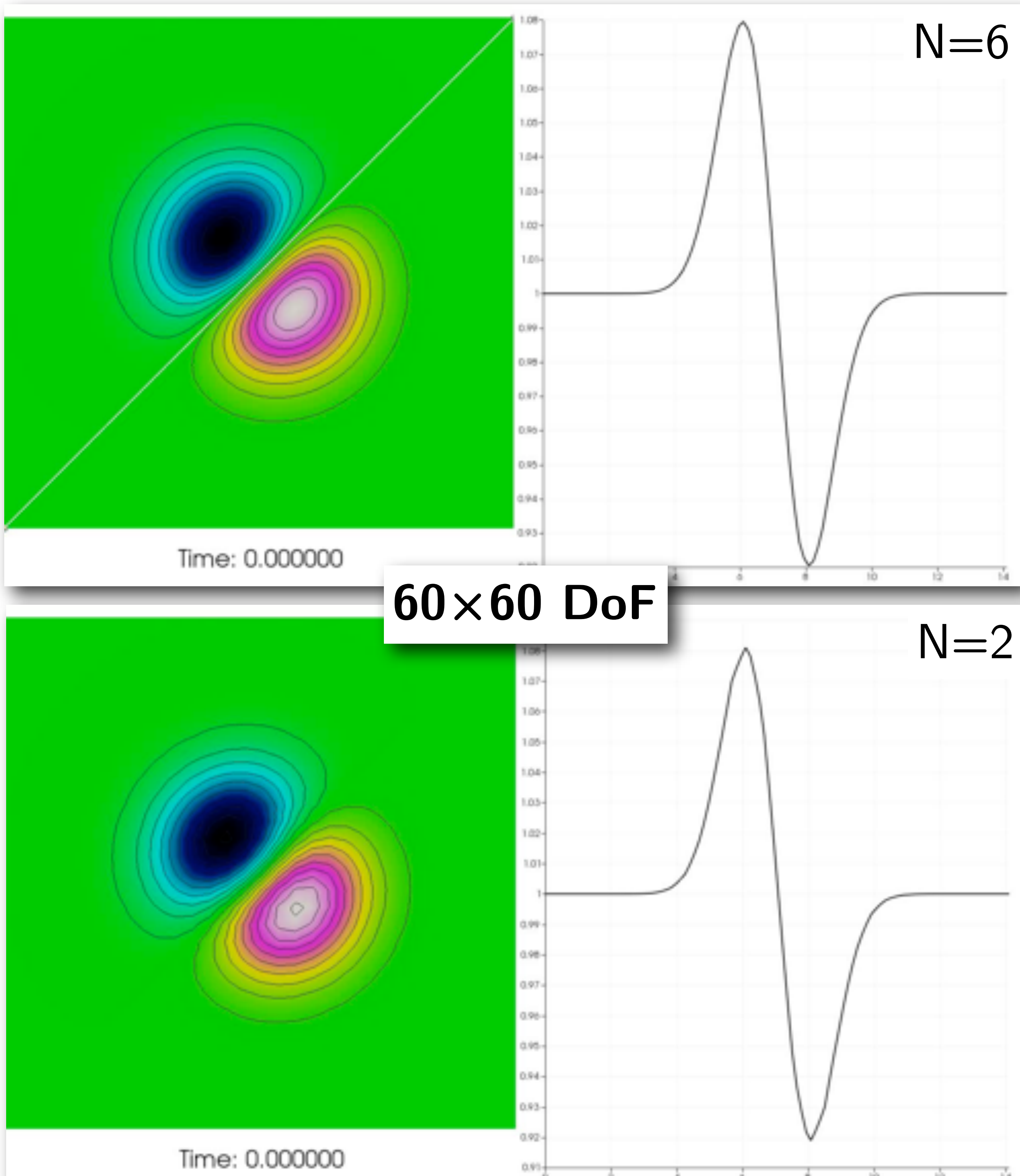

Temporal Mixing-Layer

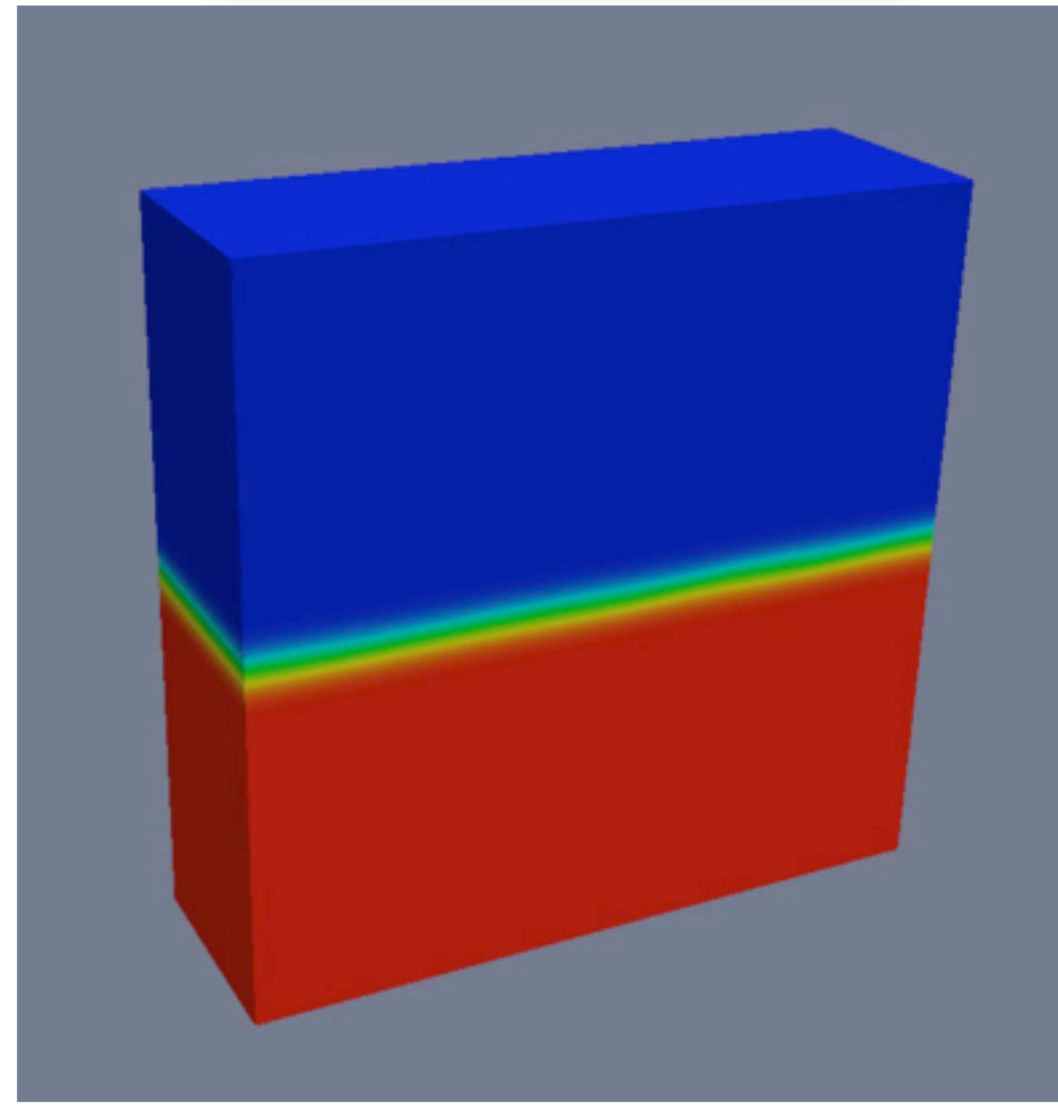

N=5: 100×200×10 DoF

Numerical Dissipation

N=6, $60 \times 60 \times 12$ DoF

Numerical Dissipation

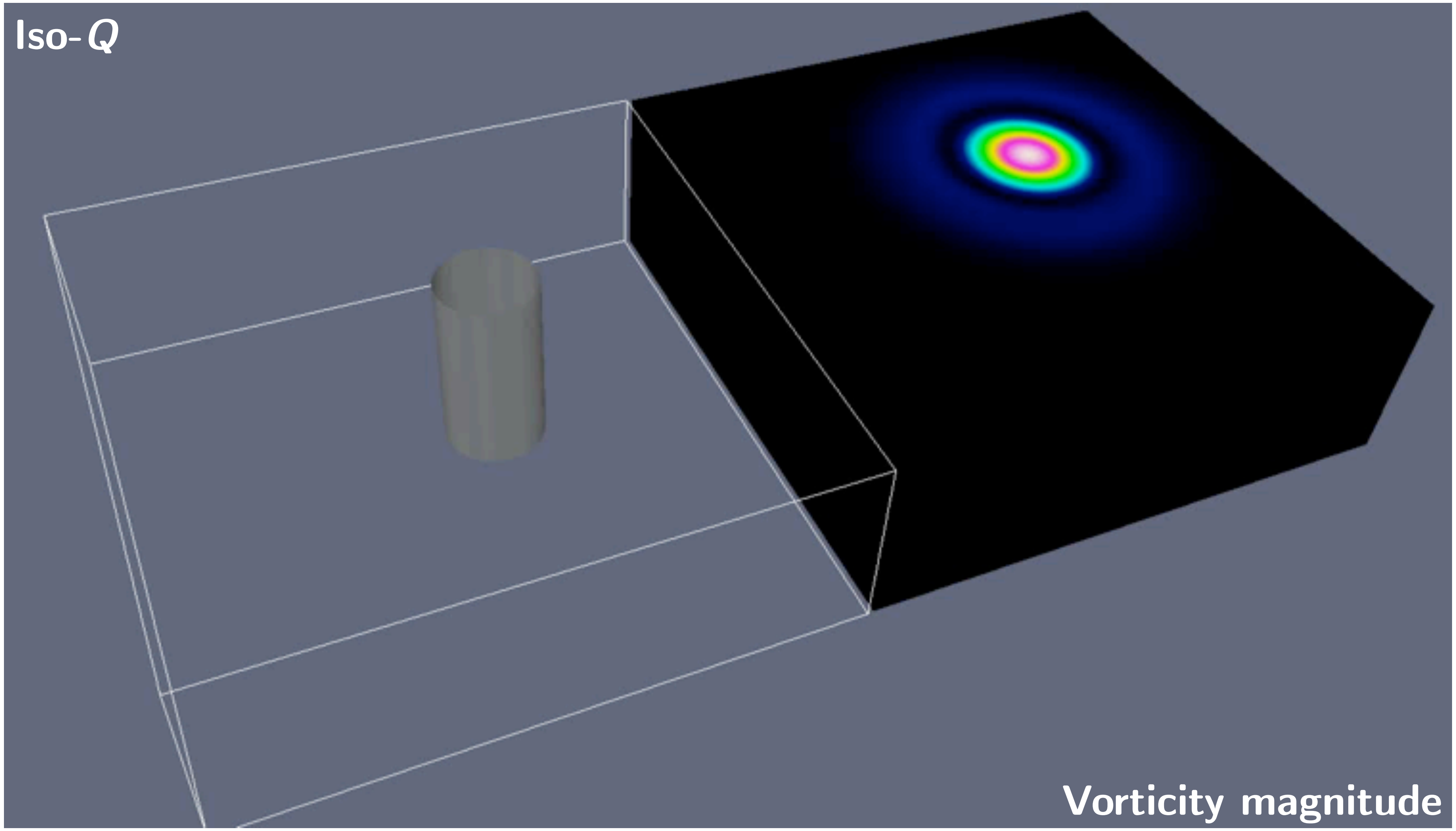

N=6, 60×60×12 DoF

High-Order Boundaries

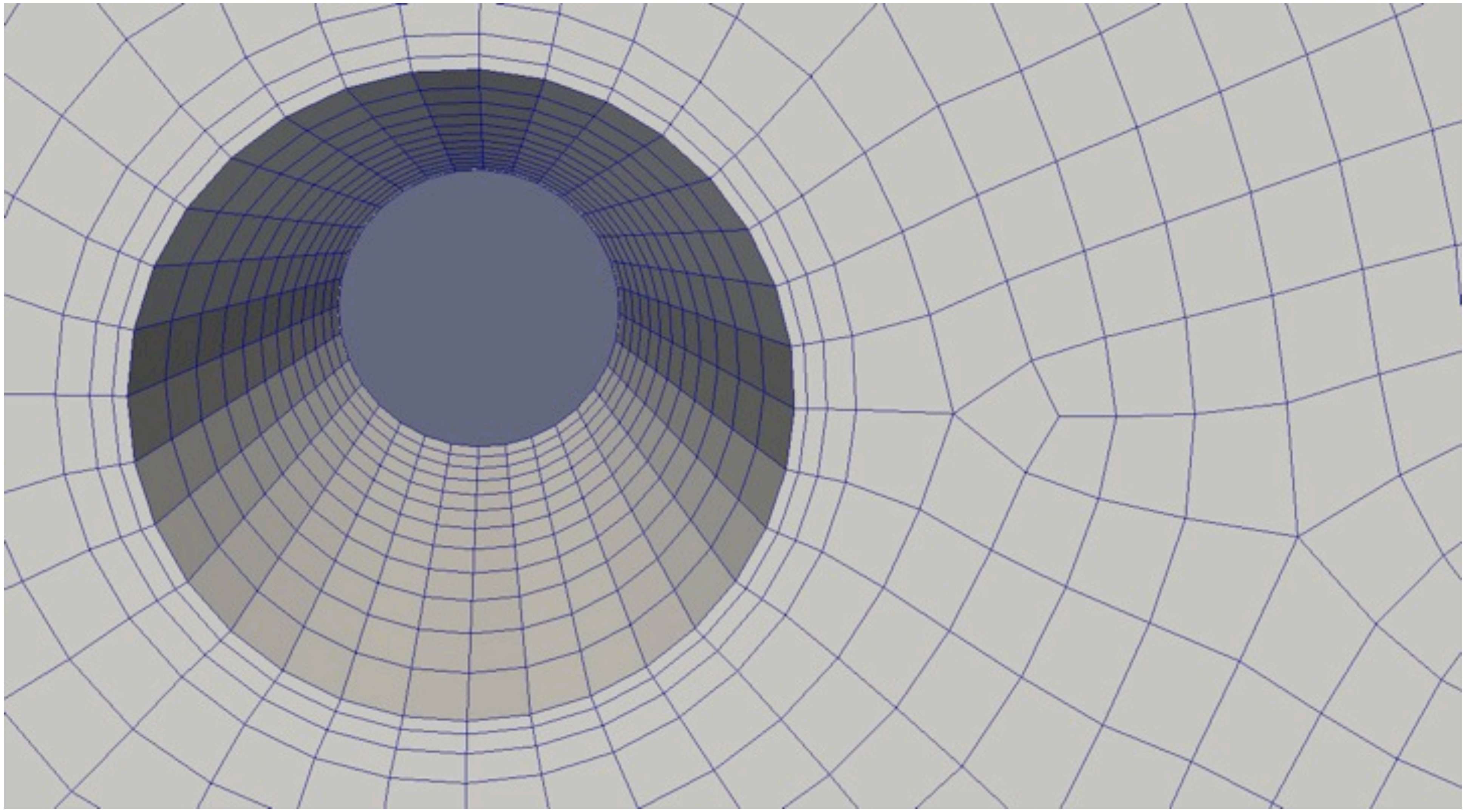

Liang, *et al.* (2009). Comput. Struct., 87; Sun, *et al.* (2007). Commun. Comput. Phys., 2(2)

High-Order Boundaries

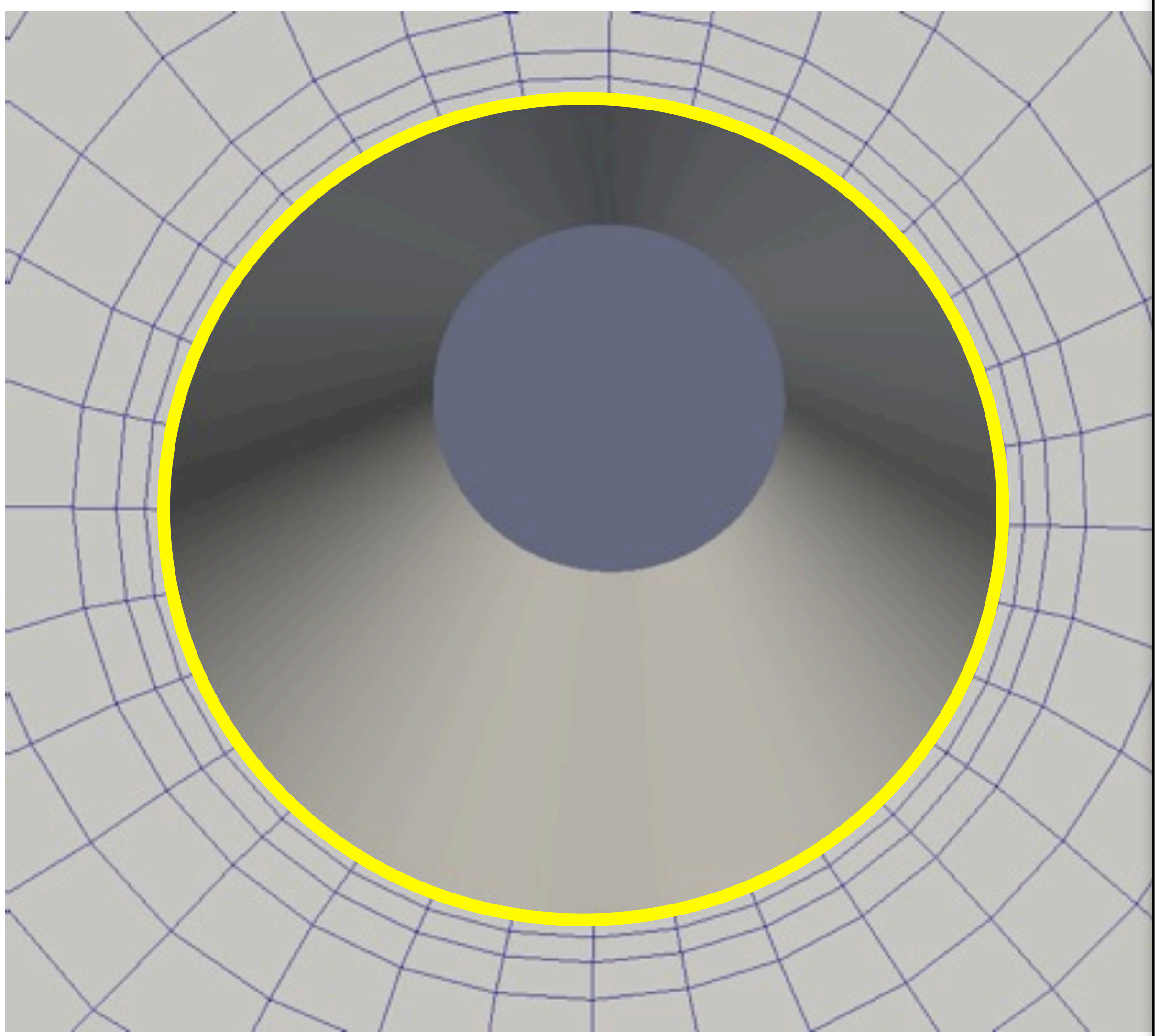

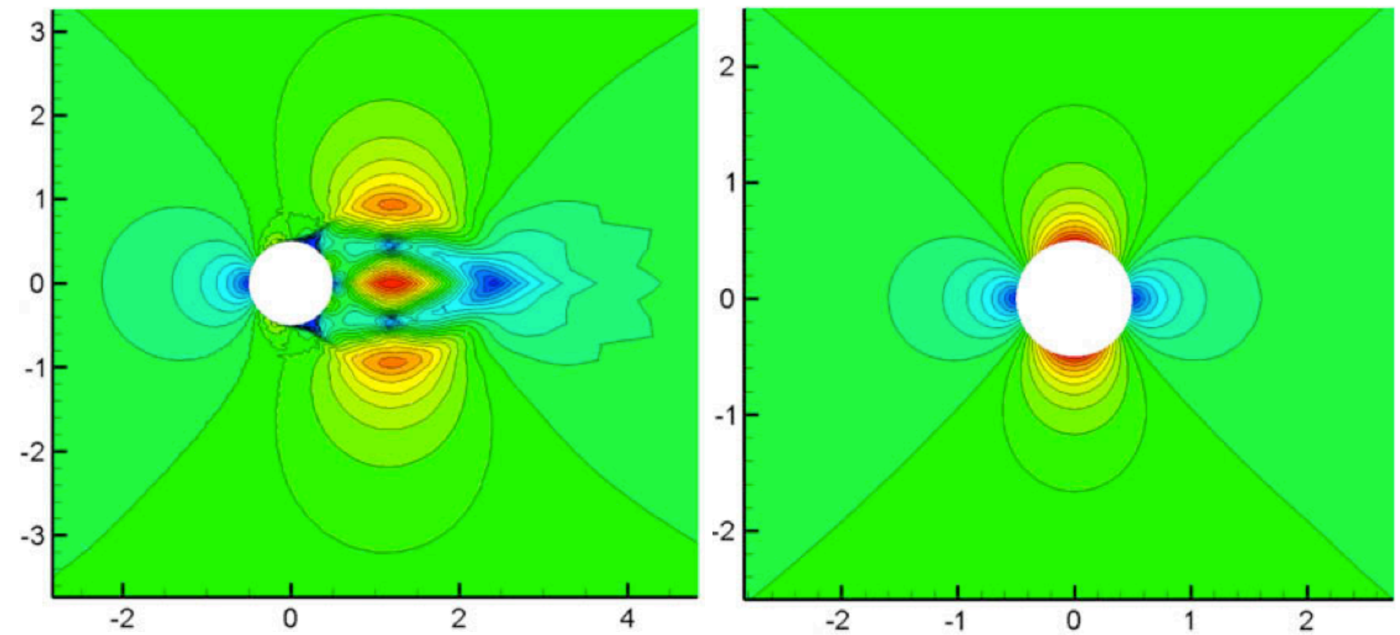

Cylinder: N=4, 32×32, linear *vs.* cubic

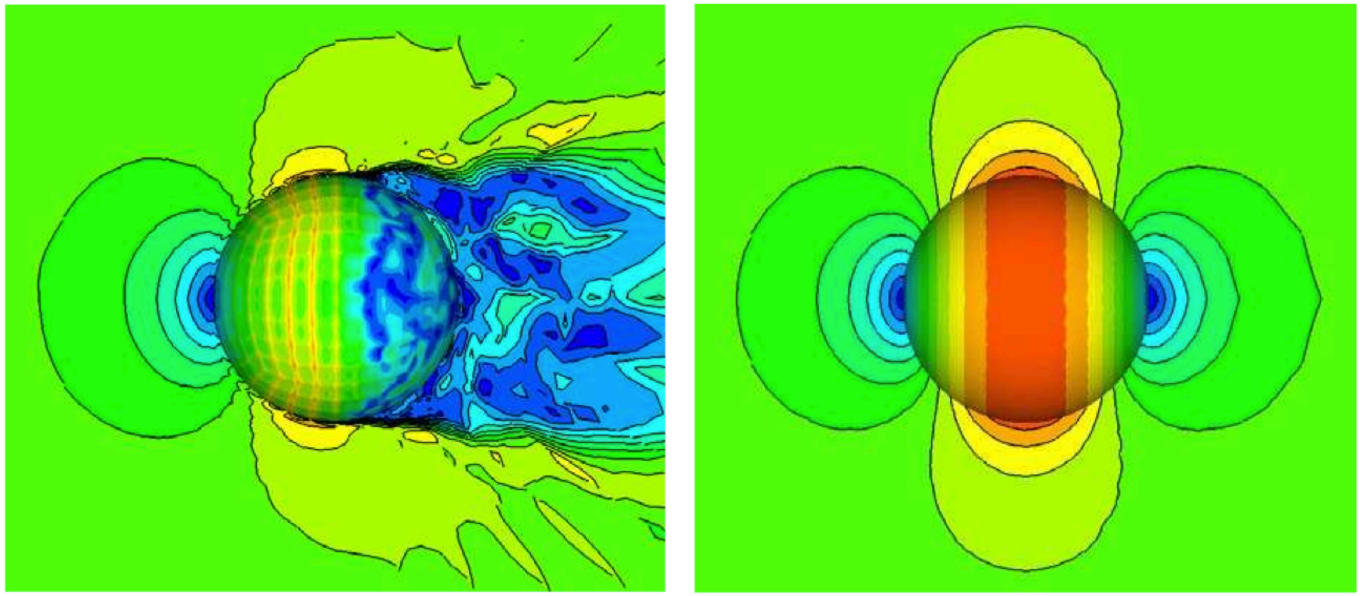

Sphere: N=3, linear *vs.* quadratic

Liang, *et al.* (2009). Comput. Struct., 87; Sun, *et al.* (2007). Commun. Comput. Phys., 2(2)

Transitional Flow over SD7003 Airfoil

	Freestream Turbulence	Separation x_{sep}/c	Transition x_{tr}/c	Reattach. x_r/c
Radespiel et al.	0.08%	0.30	0.53	0.64
Ol et al.	0.10%	0.18	0.47	0.58
Galbraith Visbal	0%	0.23	0.55	0.65
Uranga et al.	0%	0.23	0.51	0.60
Present ILES*	**0%**	**0.23**	**0.53**	**0.64**

Experiments in green

SD scheme, N=4

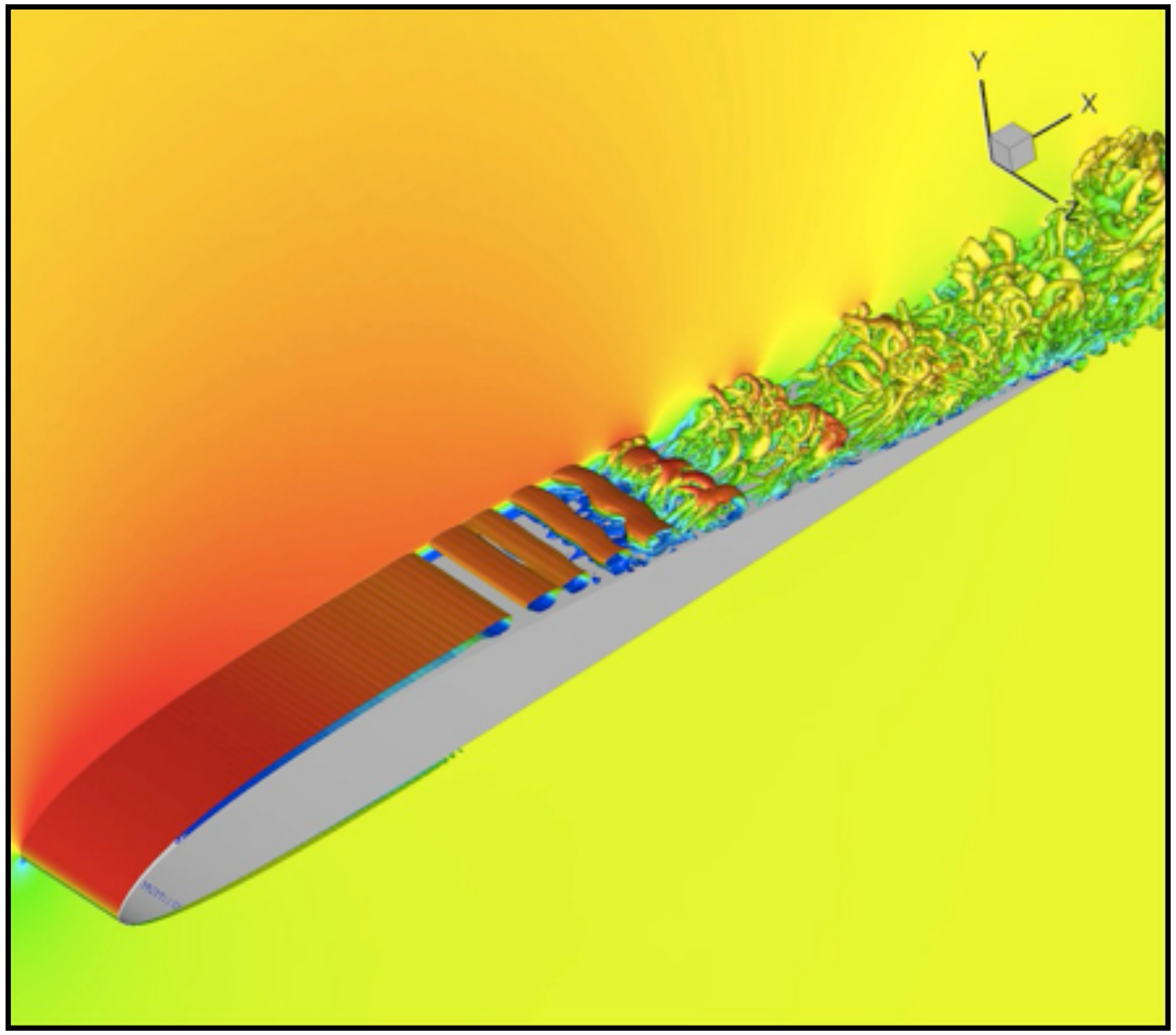

Iso-Q colored by Ma

Re=6×10^4, AoA=4°, 2.2×10^7 DoF

***1.7×10^6 DoF**

Castonguay, et al. (2010). AIAA P., 2010-4626; Radespiel, et al. (2007). AIAA J., 45(6); Ol, et al. (2005). AIAA P., 2005-5149; Galbraith, Visbal (2008). AIAA P., 2008-225; Uranga, et al. (2009). AIAA P., 2009-4131;

Transitional Flow over SD7003 Airfoil

	Freestream Turbulence	Separation x_{sep}/c	Transition x_{tr}/c	Reattach. x_r/c
Radespiel et al.	0.08%	0.30	0.53	0.64
Ol et al.	0.10%	0.18	0.47	0.58
Galbraith Visbal	0%	0.23	0.55	0.65
Uranga et al.	0%	0.23	0.51	0.60
Present ILES*	**0%**	**0.23**	**0.53**	**0.64**

Experiments in green

SD scheme, N=4

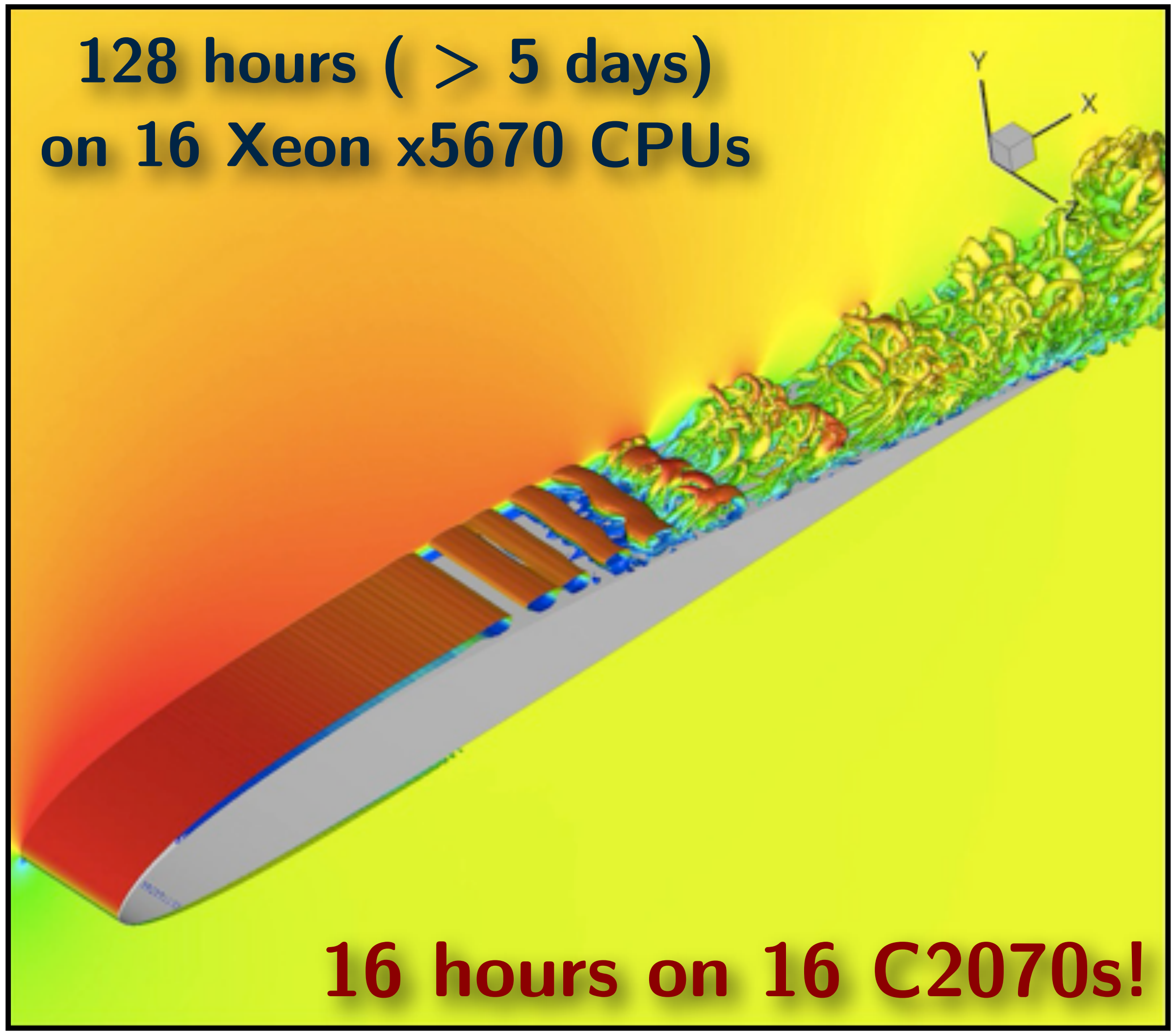

Iso-Q colored by Ma

Re=6×10^4, AoA=$4°$, 2.2×10^7 DoF

$^*1.7\times10^6$ DoF

Castonguay, et al. (2010). AIAA P., 2010-4626; Radespiel, et al. (2007). AIAA J., 45(6); Ol, et al. (2005). AIAA P., 2005-5149; Galbraith, Visbal (2008). AIAA P., 2008-225; Uranga, et al. (2009). AIAA P., 2009-4131;

Study of Flapping Wing Sections

SD, 2D, N=5 on deforming grid

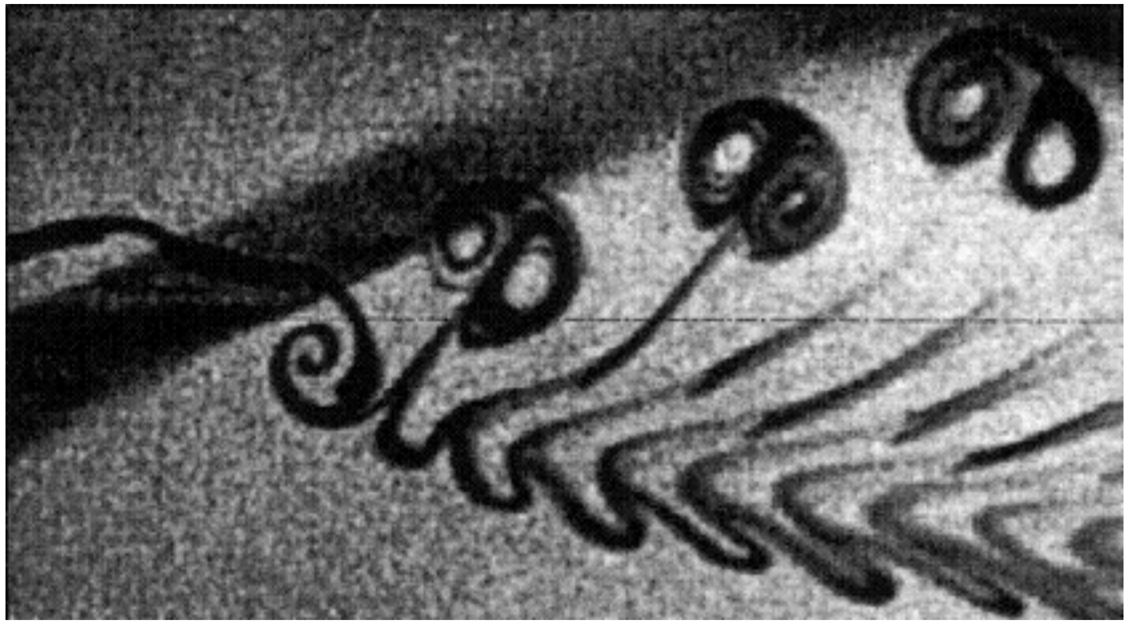

Experiment (Jones, et al.)

NACA0012, Re=1850, Ma=0.2, St=1.5, ω=2.46, h=0.12c

Jones, et al. (1998). AIAA J., 36(7)

Study of Flapping Wing Sections

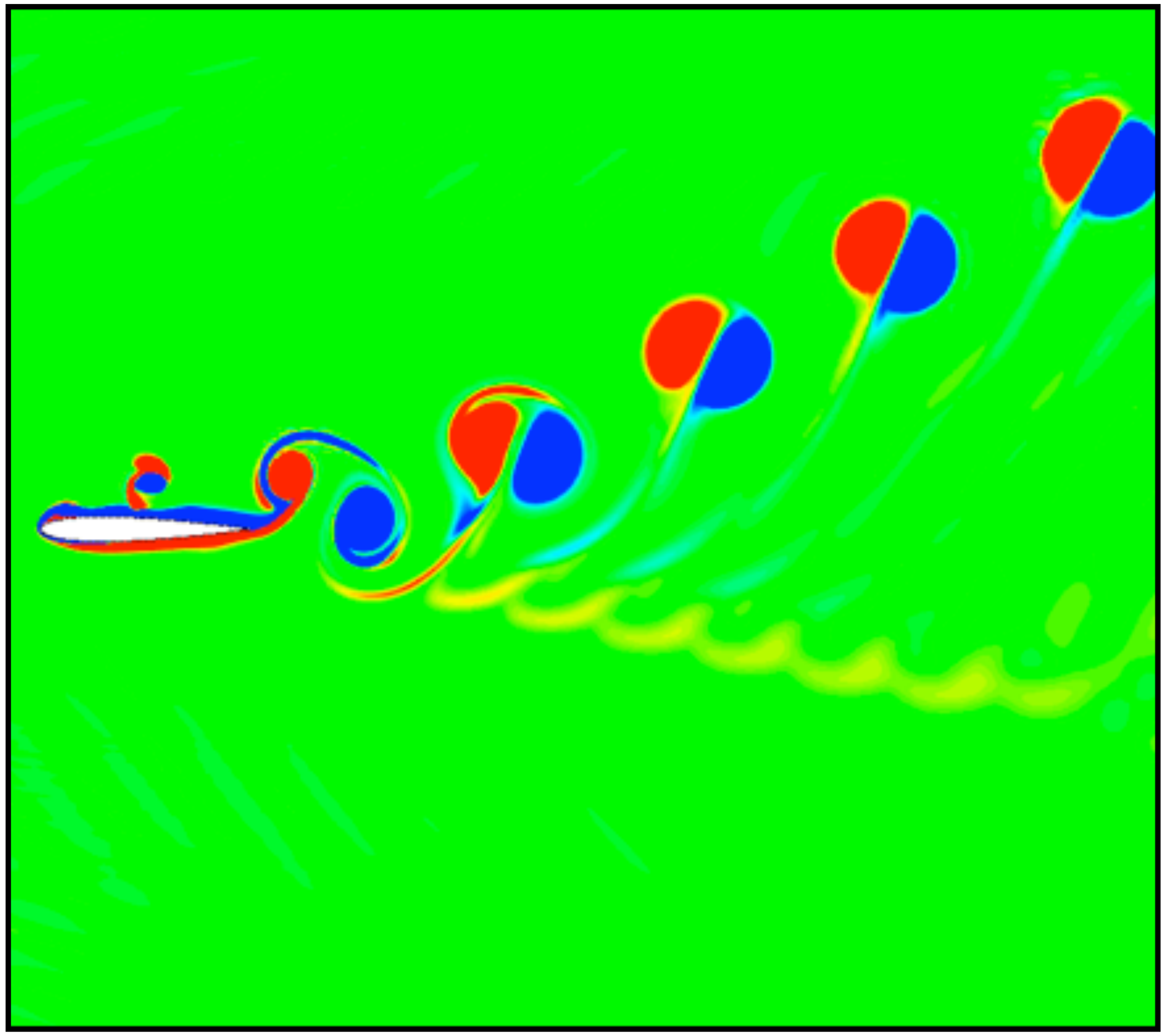

SD, 2D, N=5 on deforming grid

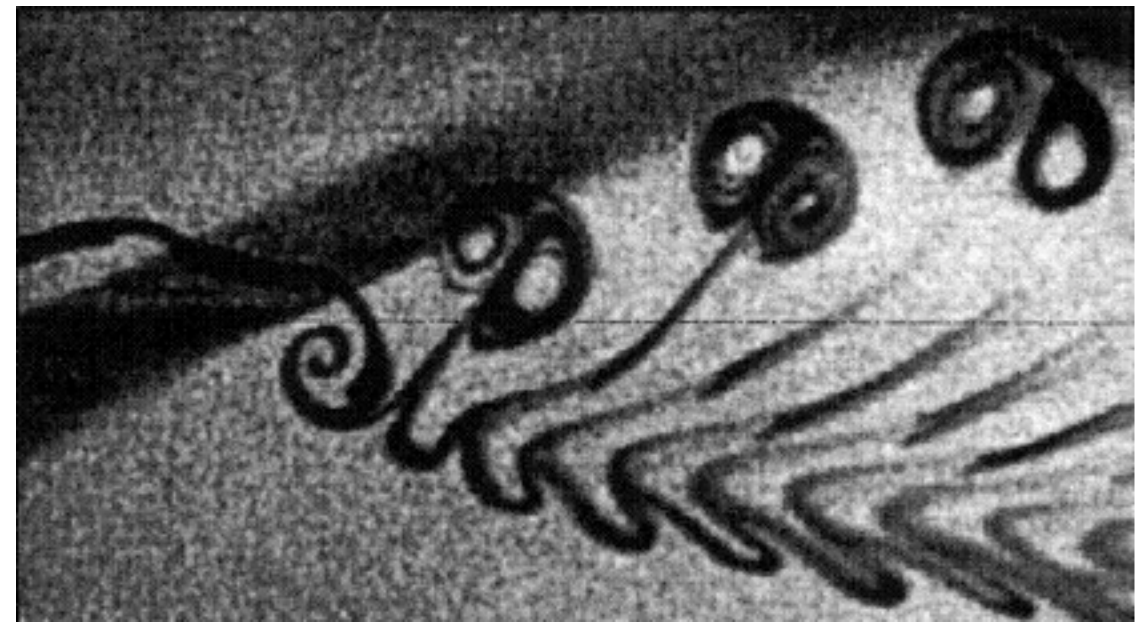

Experiment (Jones, et al.)

NACA0012, Re=1850, Ma=0.2, St=1.5, ω=2.46, h=0.12c

Jones, et al. (1998). AIAA J., 36(7)

Outline

Explicit Filtering in the SD Element

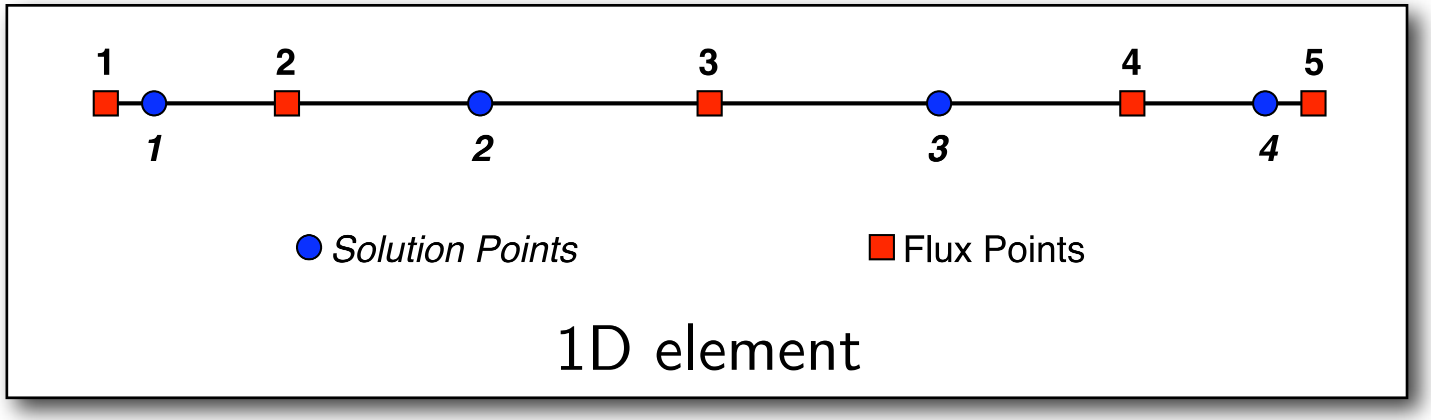

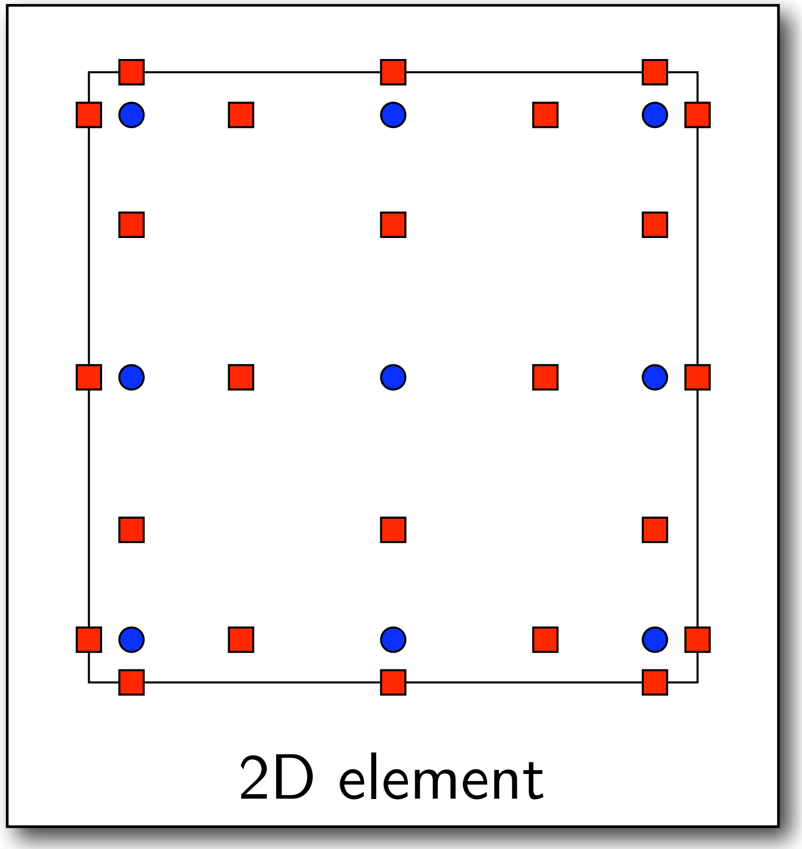

Key issues:

- non-uniform and staggered distribution of points
- the filter stencil shall not lie across elements
- filter width shall be prescribed and constant

Filtering Strategy:

1. The filtered solution is computed at solution points
2. The SGS model term is evaluated at solution points
3. The SGS model term is extrapolated at flux points via Lagrange basis

Discrete Filtering Operators

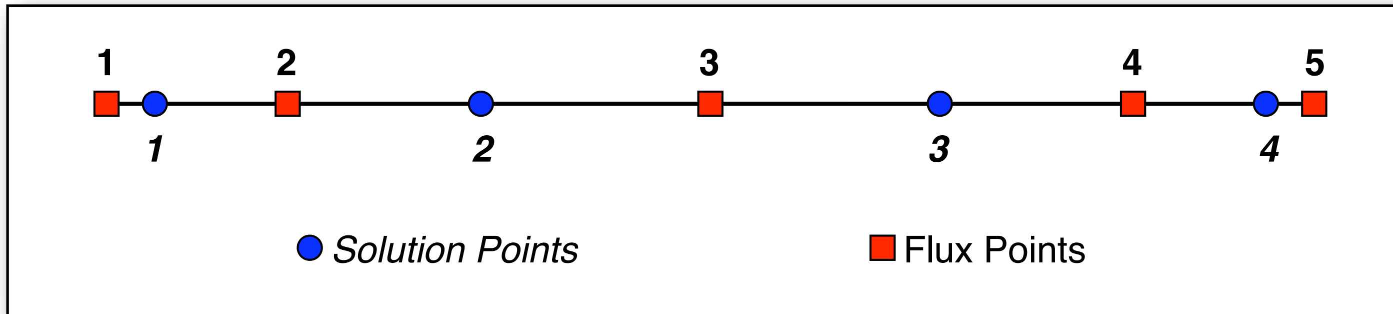

The filtering operator for the 1D standard element is defined as

$$\overline{\phi}_s = \sum_{i=1}^{N} w_i^s \phi_i, \quad (s = 1, \ldots, N)$$

The kernel of the above discrete filter can be written as

$$\widehat{G}_s(k) = \sum_{i=1}^{N} w_i^s \exp(-\mathrm{j}\beta_i^s k\Delta), \quad \text{with} \quad \beta_i^s = \frac{\xi_i - \xi_s}{\Delta}$$

Δ=1/N is assumed to be the actual resolution within the SD element

Vasilyev, et al. (1998). J. Comput. Phys. 146(1); Berland, et al. (2007). J. Comput. Phys. 224(2); Sagaut, Grohens (1999). Int. J. Numer. Meth. Fl. 31(8)

The Restriction-Prolongation Filter

Sharp cutoff in modal space:

The solution is first projected on a lower order polynomial (**restriction** step) and then extrapolated back to the original solution points (**prolongation** step)

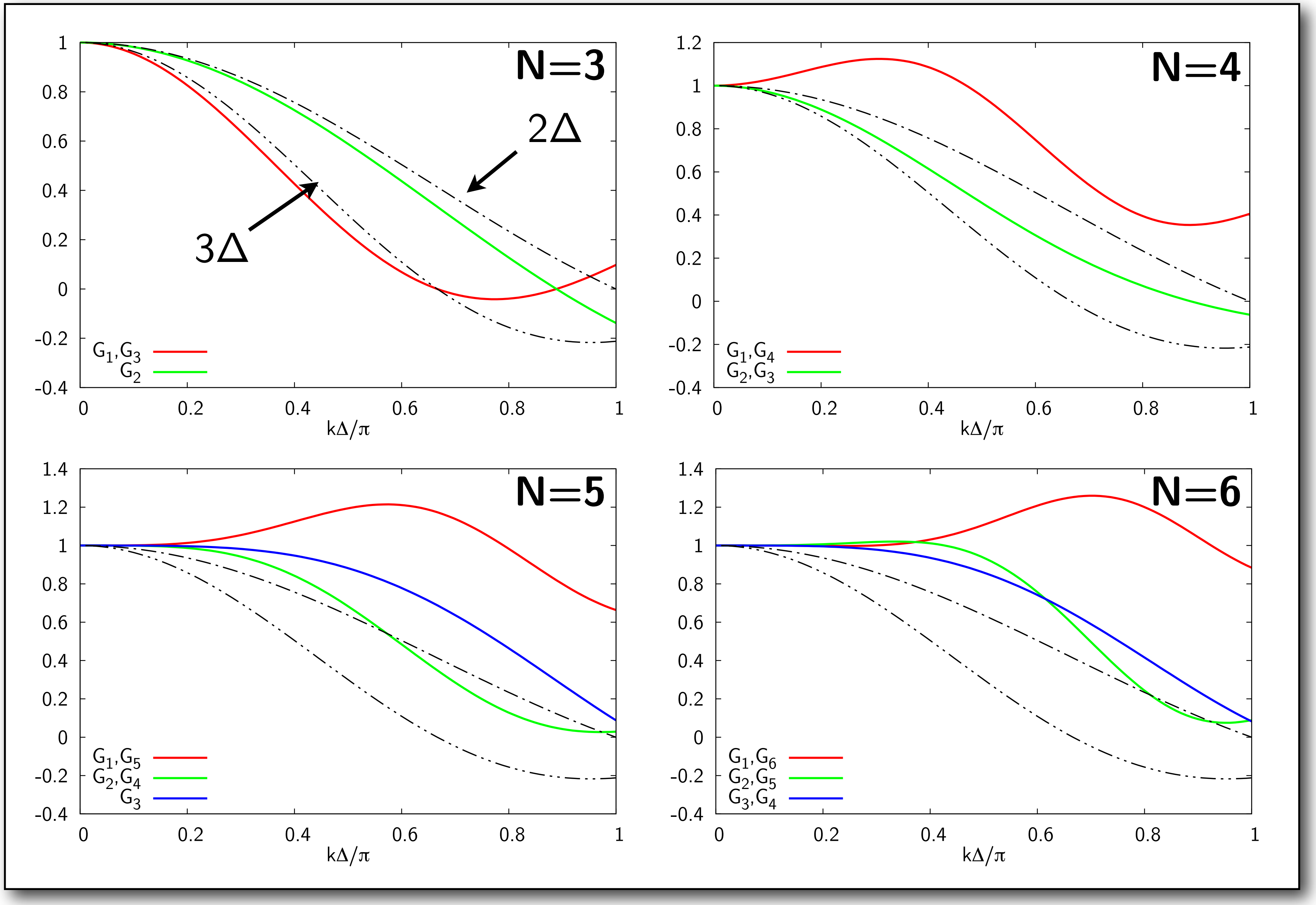

Premasuthan, et al. (2009). AIAA P., 2009-3785

The Restriction-Prolongation Filter

Sharp cutoff in modal space:

The solution is first projected on a lower order polynomial (**restriction** step) and then extrapolated back to the original solution points (**prolongation** step)

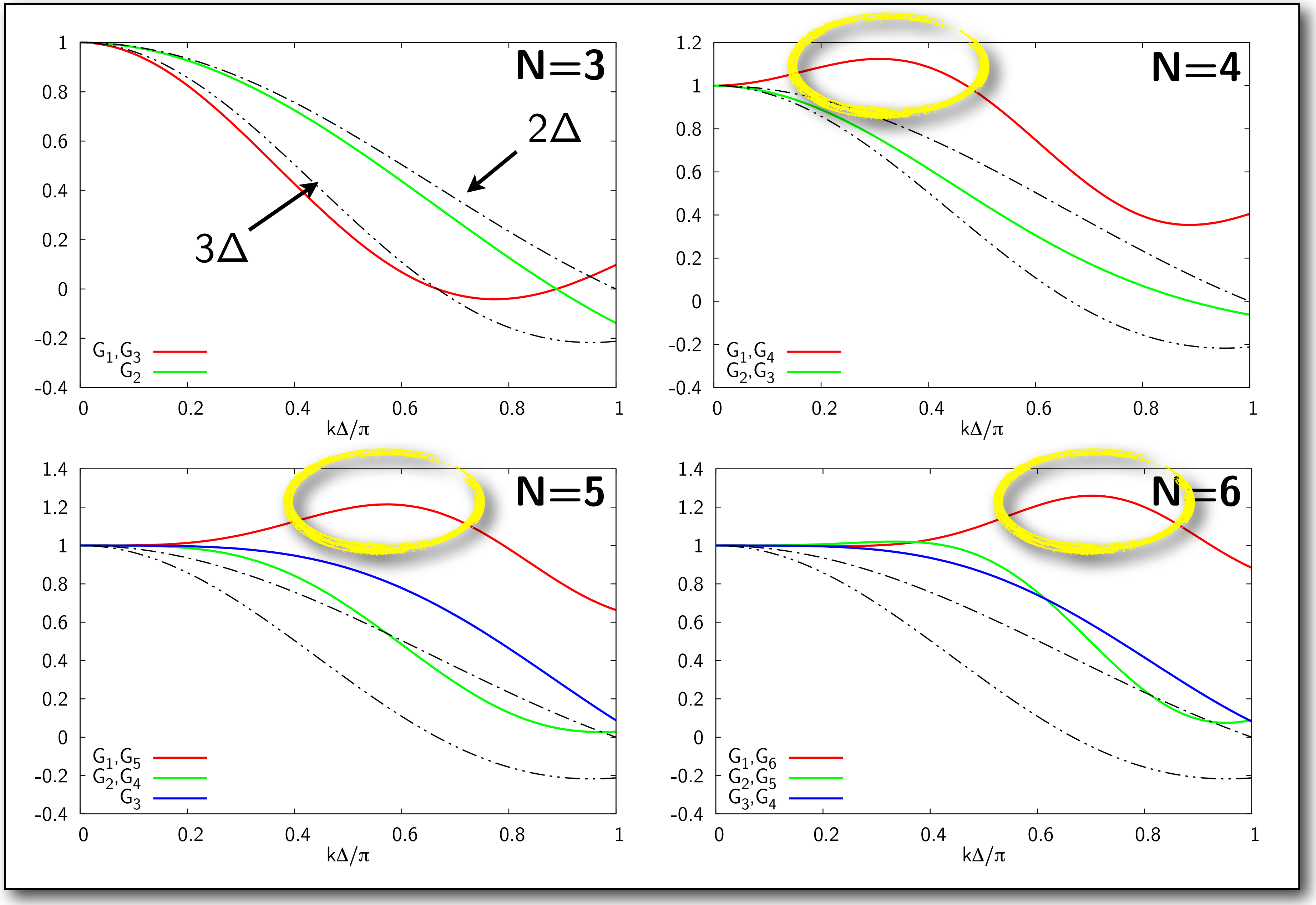

Premasuthan, et al. (2009). AIAA P., 2009-3785

Discrete Filters by Gauss Quadrature

Gauss-Legendre quadrature points:

- The discrete filter is obtained by analytical integration of a selected filter kernel
- Cutoff is enforced iteratively by checking the filter's 2nd moment in physical space

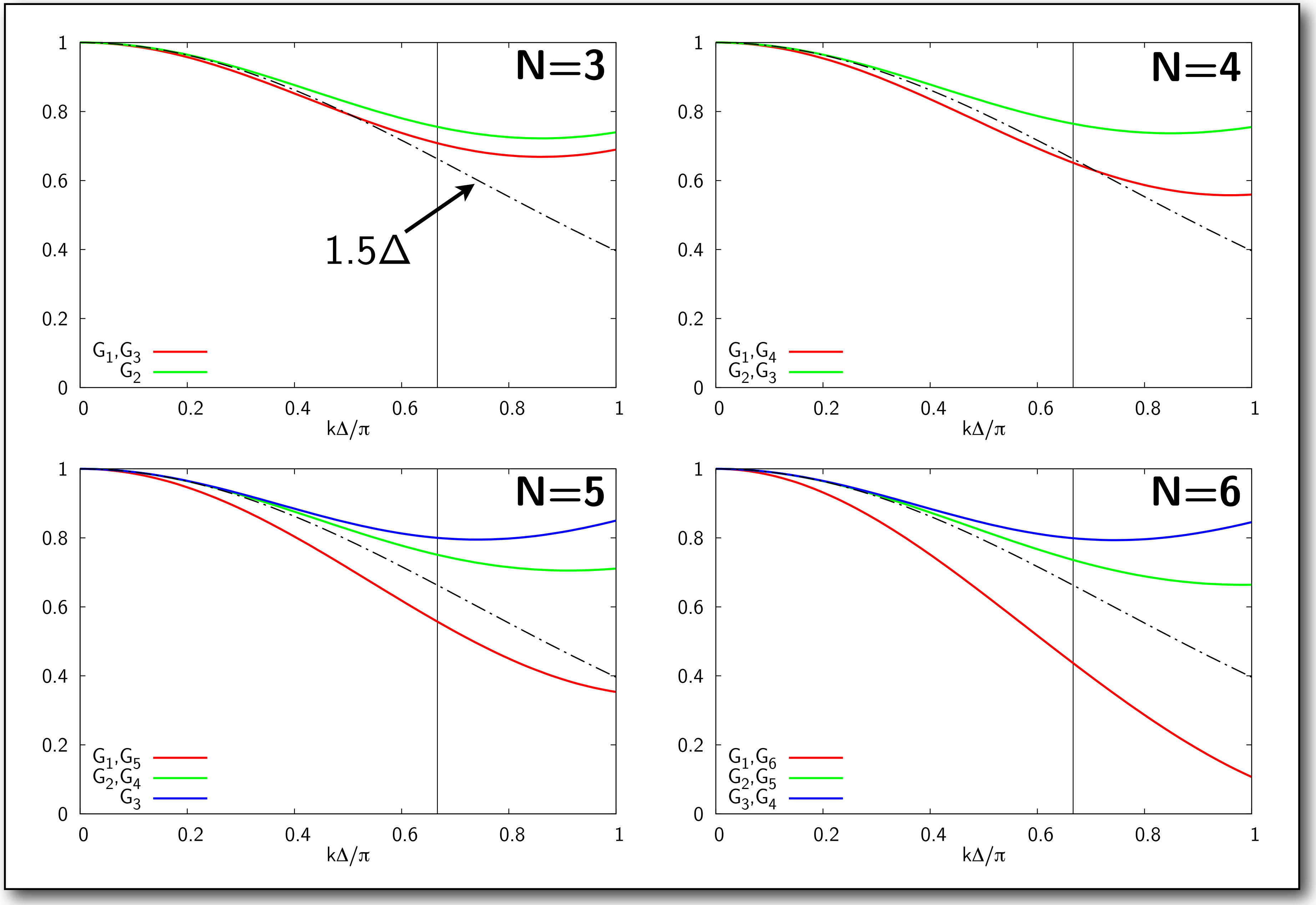

Lodato, Castonguay, Jameson (in preparation)

Discrete Filters for Arbitrary Points

Generalized method of Vasilyev et al. (1998):

- Value and slope at cutoff are enforced using a selected filter kernel (2)
- Higher moments are set to zero (N-3) + preservation of constant variable (1)

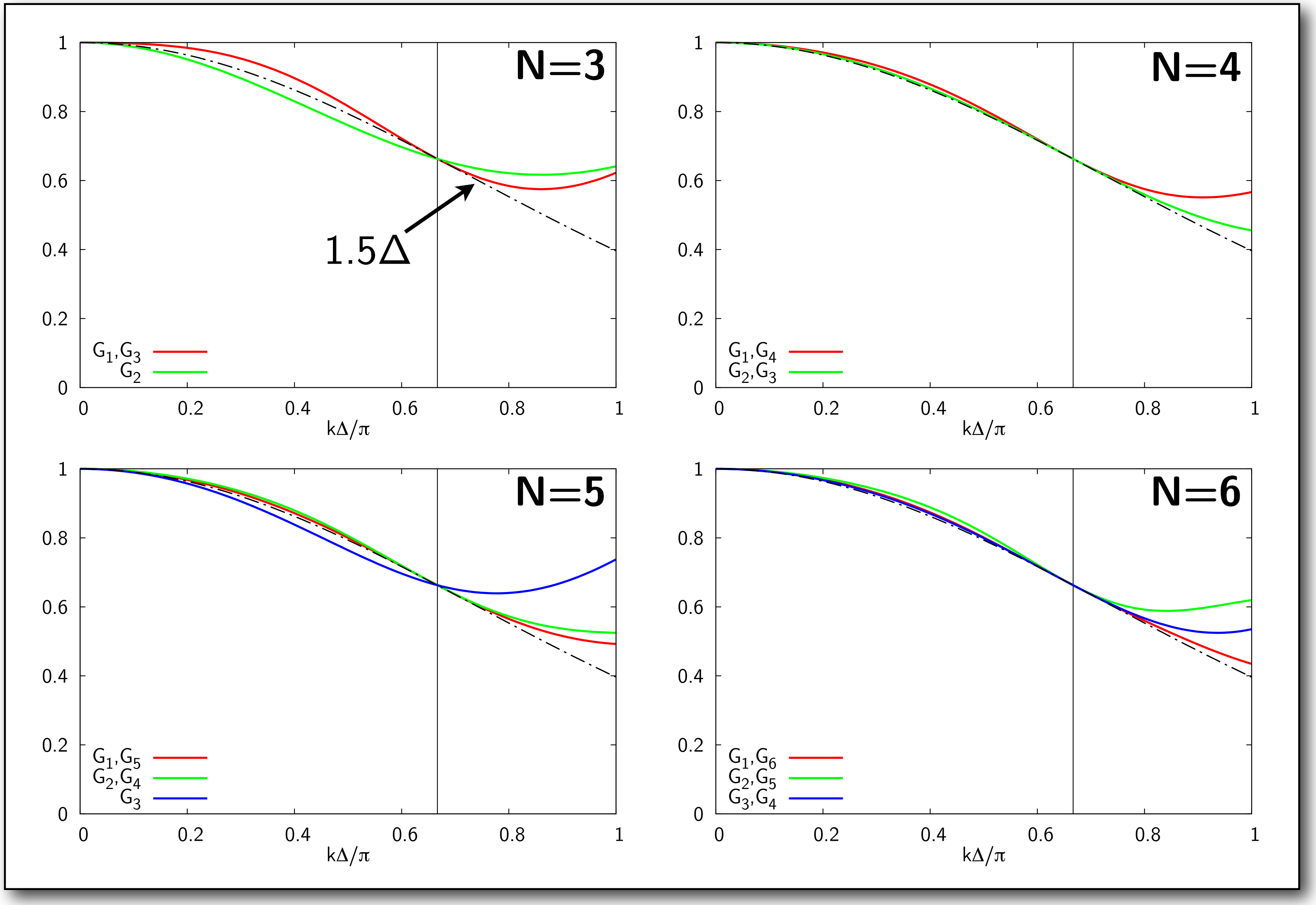

Lodato, Castonguay, Jameson (2011), CTR Annual Research Briefs; Vasilyev et al. (1998), J. Comput. Phys., 146(1)

Outline

Wall-Resolved Turbulent Channel Flow

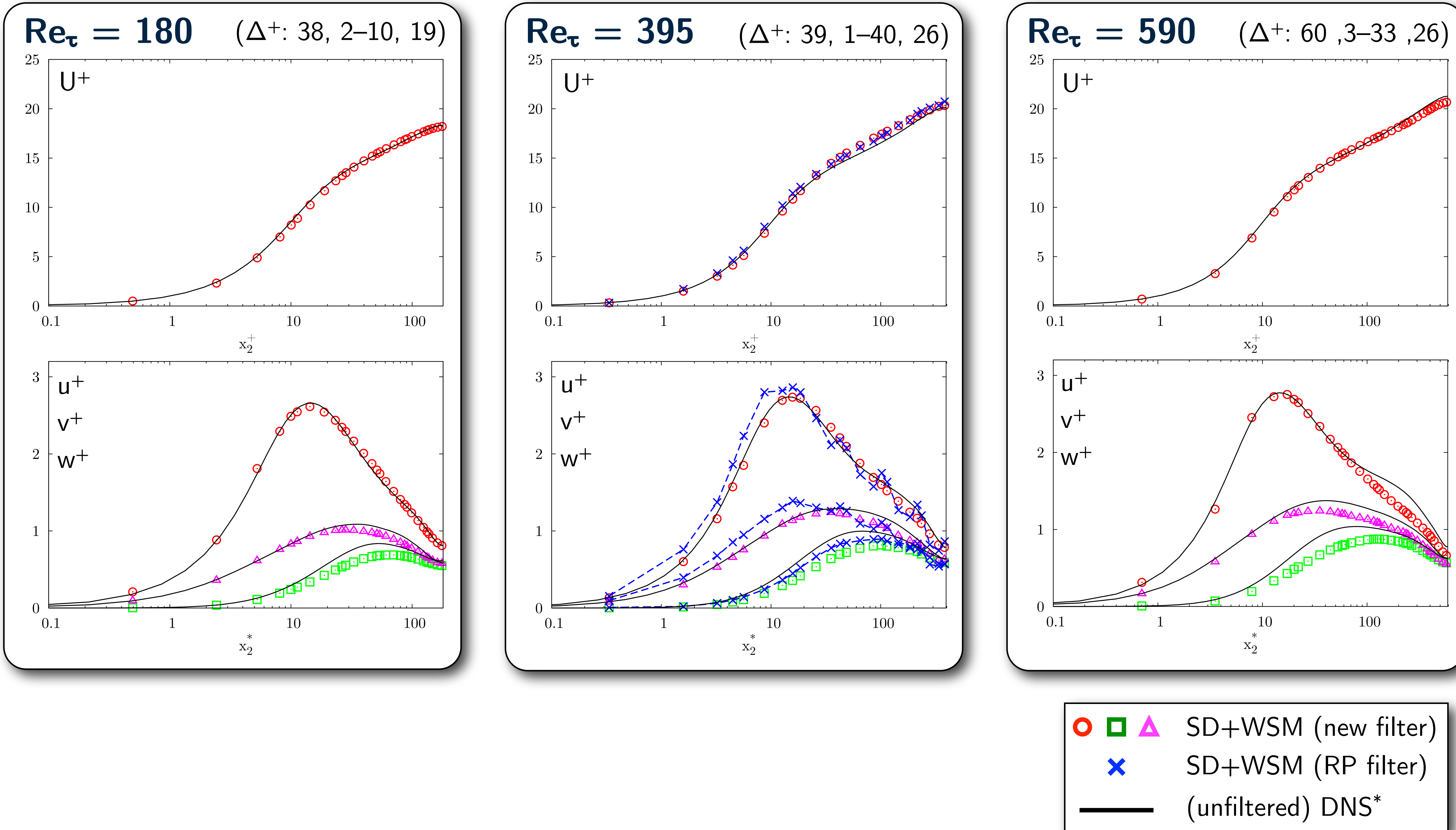

*Moser, et al. (1999). Phys. Fluids, 11(4); Lodato, et al. (2009). Phys. Fluids, 21(3); Premasuthan, et al. (2009). AIAA P., 2009-3785

Wall-Resolved Turbulent Channel Flow

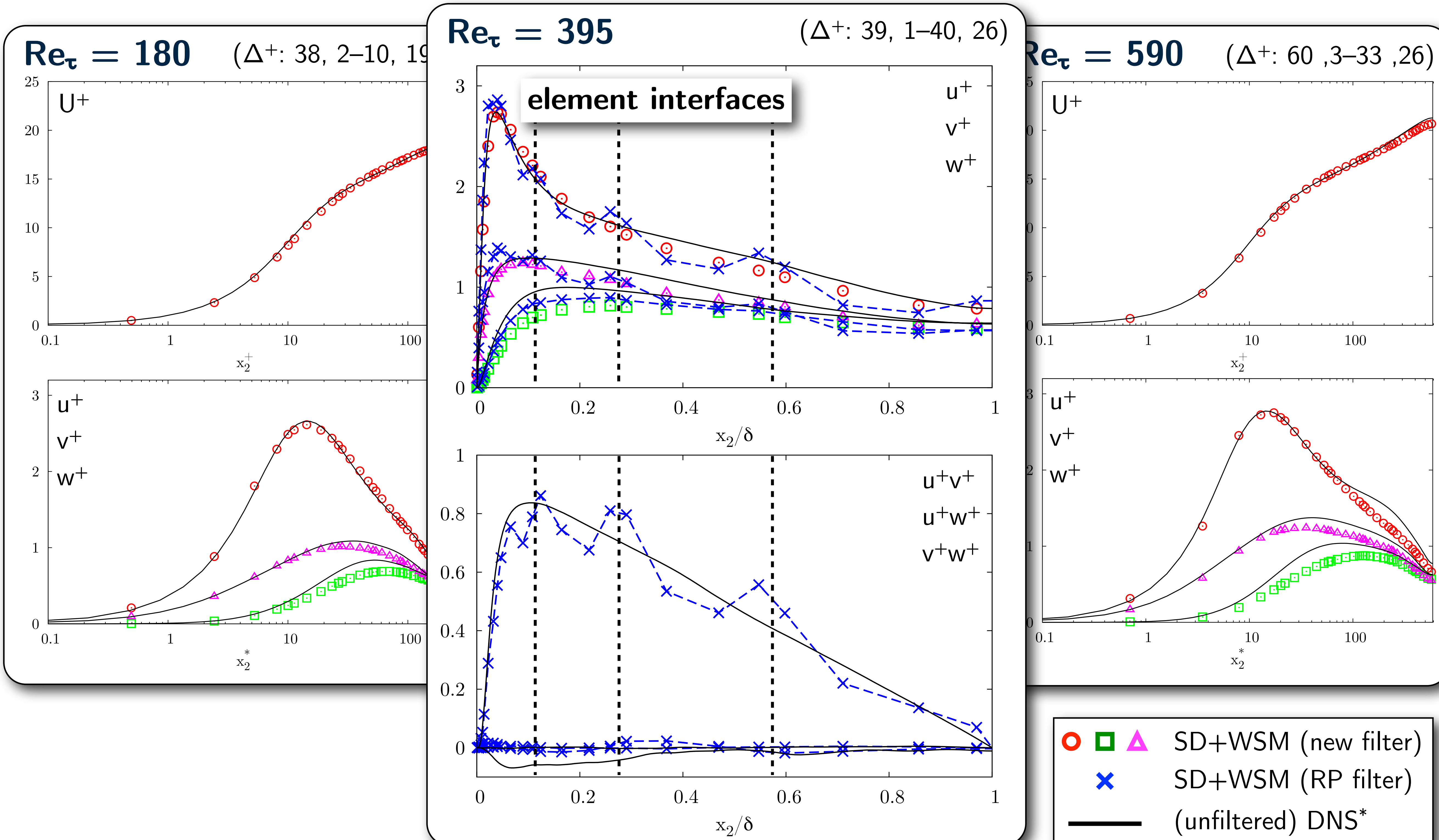

*Moser, et al. (1999). Phys. Fluids, 11(4); Lodato, et al. (2009). Phys. Fluids, 21(3); Premasuthan, et al. (2009). AIAA P., 2009-3785

Wall-Resolved Turbulent Channel Flow

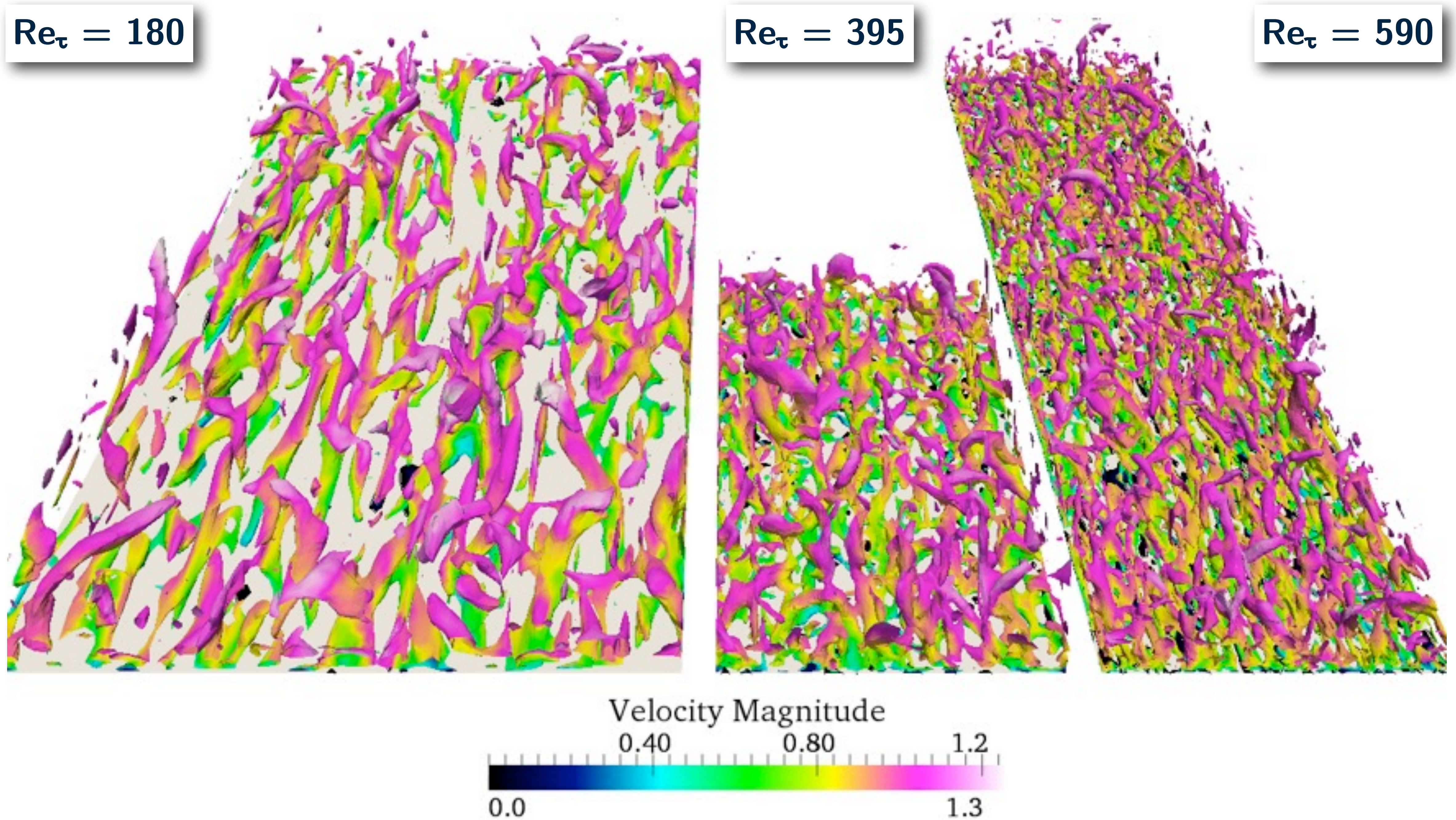

Lodato, Castonguay, Jameson (2011), CTR Annual Research Briefs; Lodato, et al. (2009). Phys. Fluids, 21(3)

A Wall-Modeling Strategy

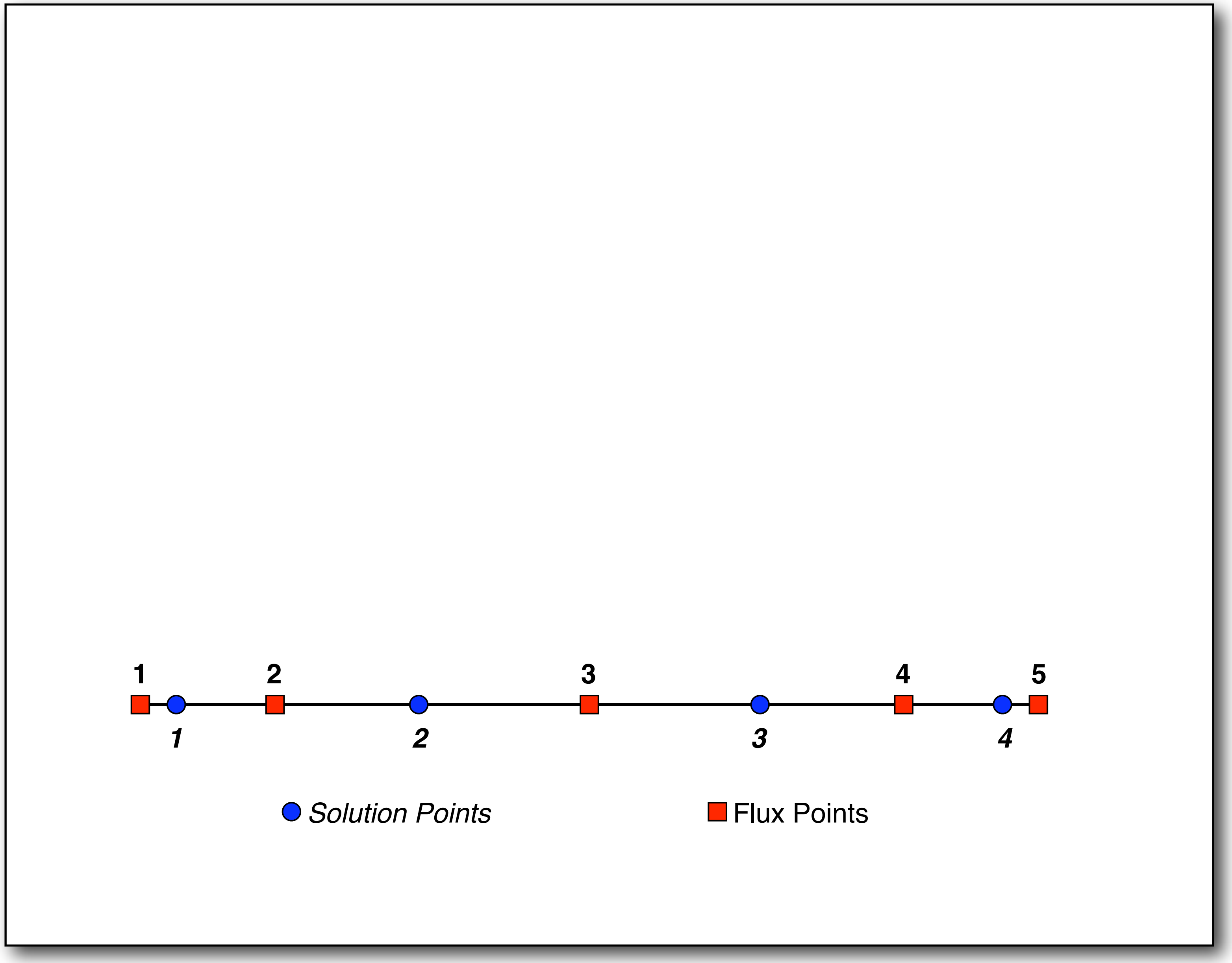

Breuer and Rodi (1996)

A Wall-Modeling Strategy

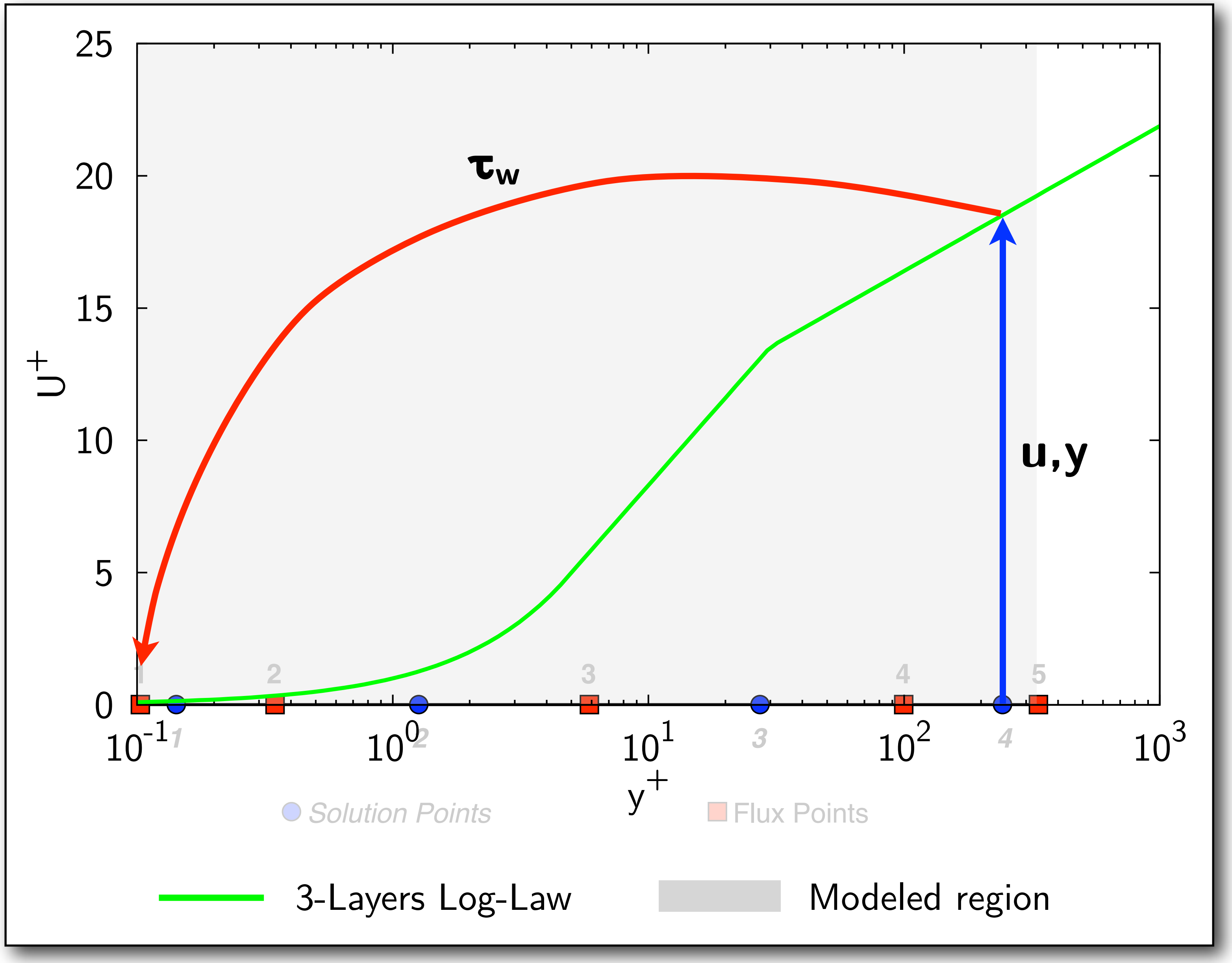

Breuer and Rodi (1996)

Wall-Modeled Turbulent Channel Flow

$Re_\tau = 590$ (Δ^+: 58, 24–47, 58)

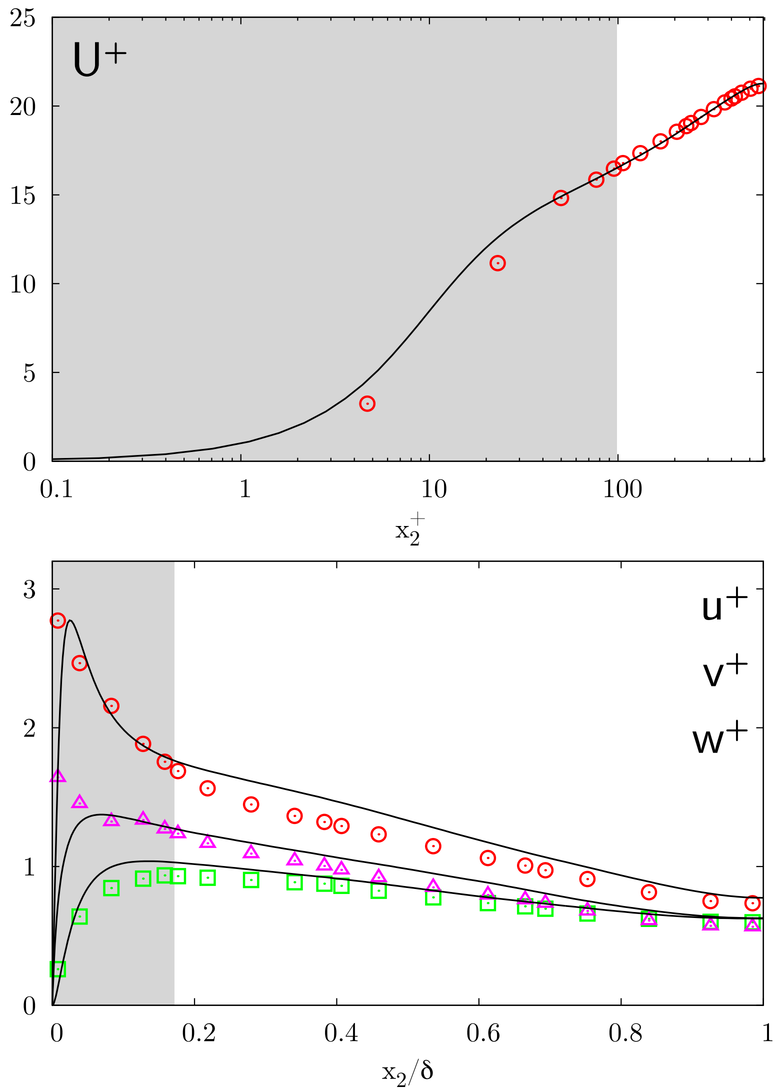

$Re_\tau = 2000$ (Δ^+: 98, 22–102, 98)

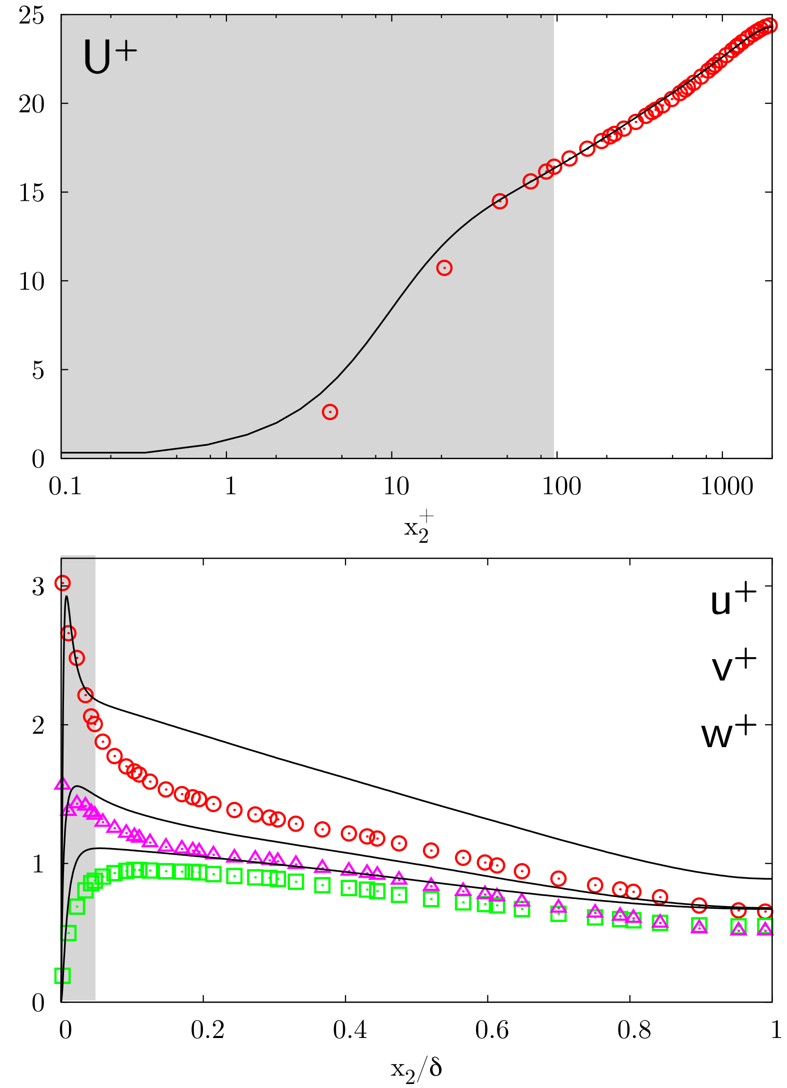

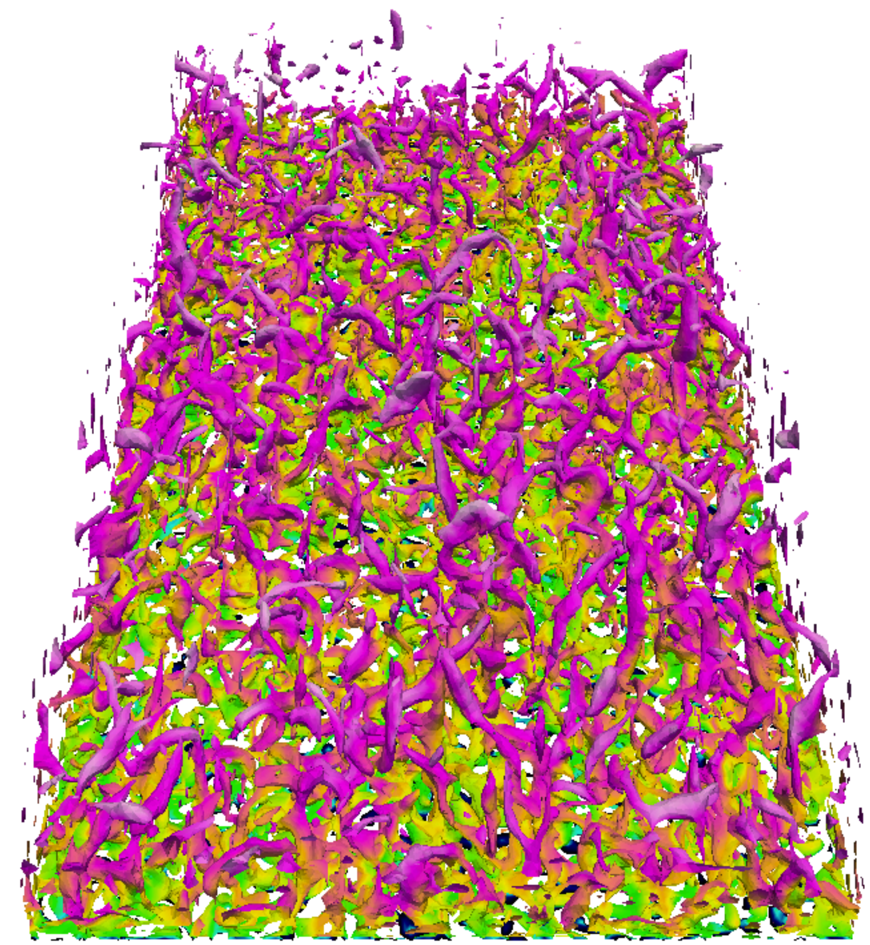

Iso-Q colored by velocity magnitude

○ □ △	LES with SD+WSM+LW
——	DNS Moser, et al., 1999 (Re_τ 590) DNS Hoyas, Jiménez, 2006 (Re_τ 2000)
(grey)	Modeled region

Moser, et al. (1999). Phys. Fluids, 11(4); Hoyas, Jiménez (2006). Phys. Fluids, 18; Breuer, Rodi (1996)

Wall-Modeled Turbulent Channel Flow

$Re_\tau = 590$

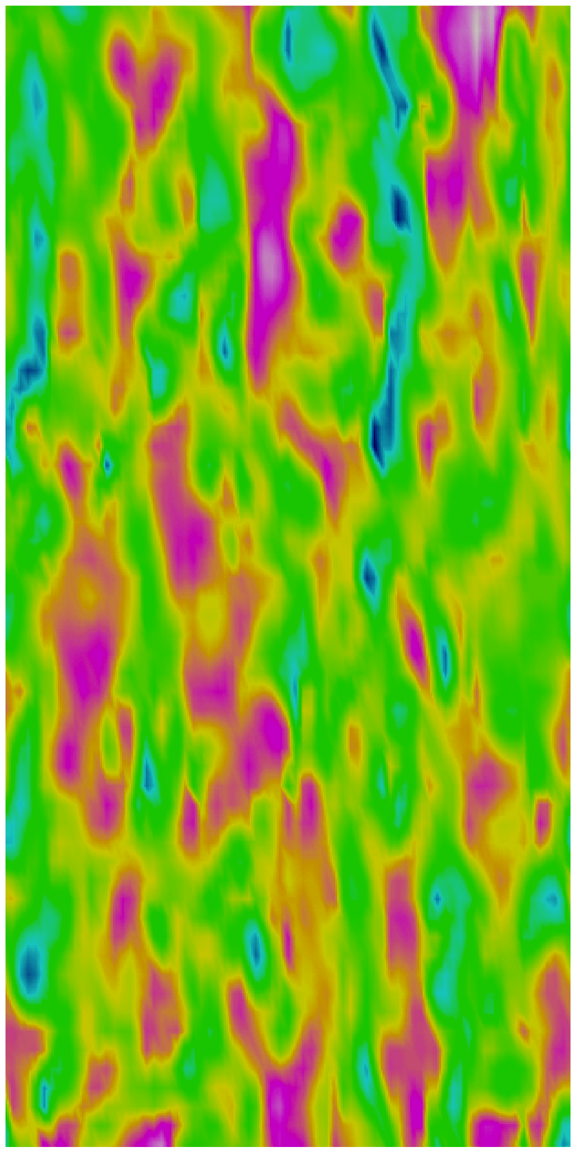

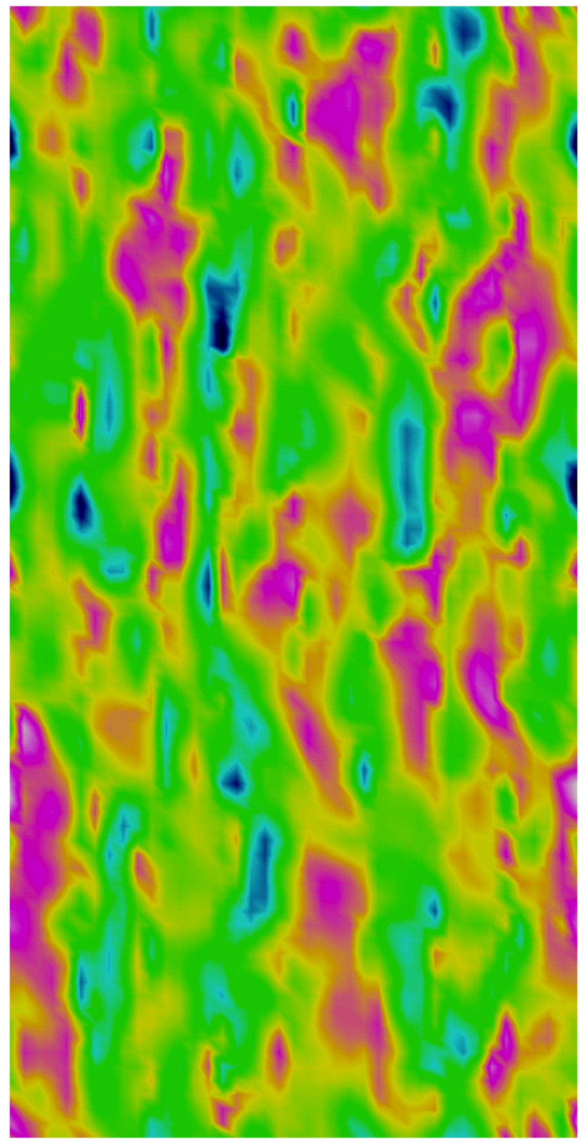

u at y^+=100

Wall-Resolved

Wall-Modeled

$Re_\tau = 2000$

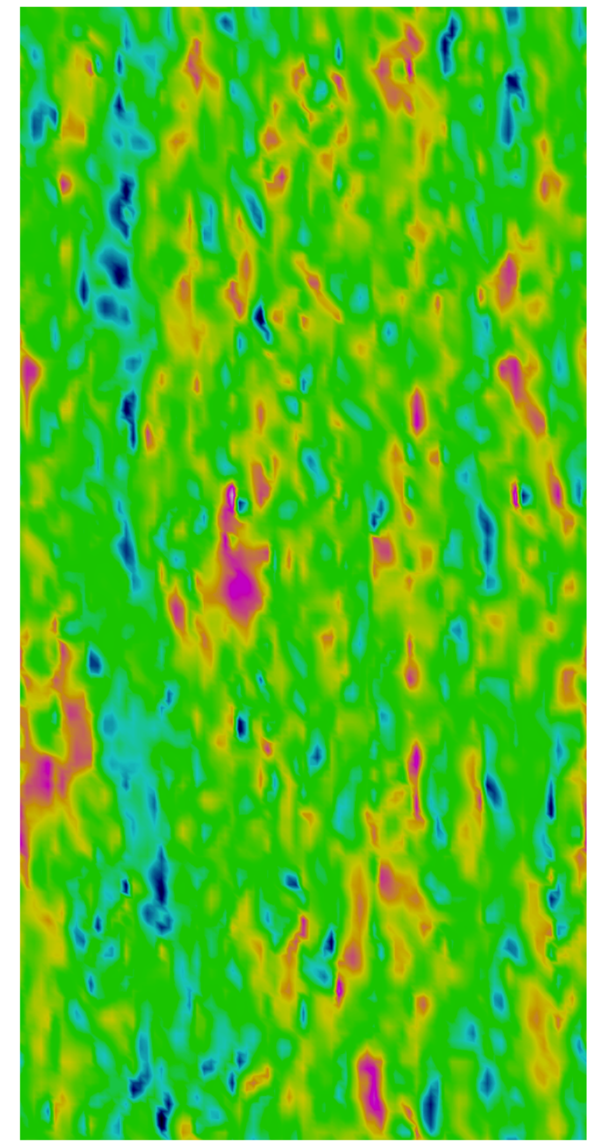

u at y^+=100

Flow Past Square Cylinder: Re = 21400

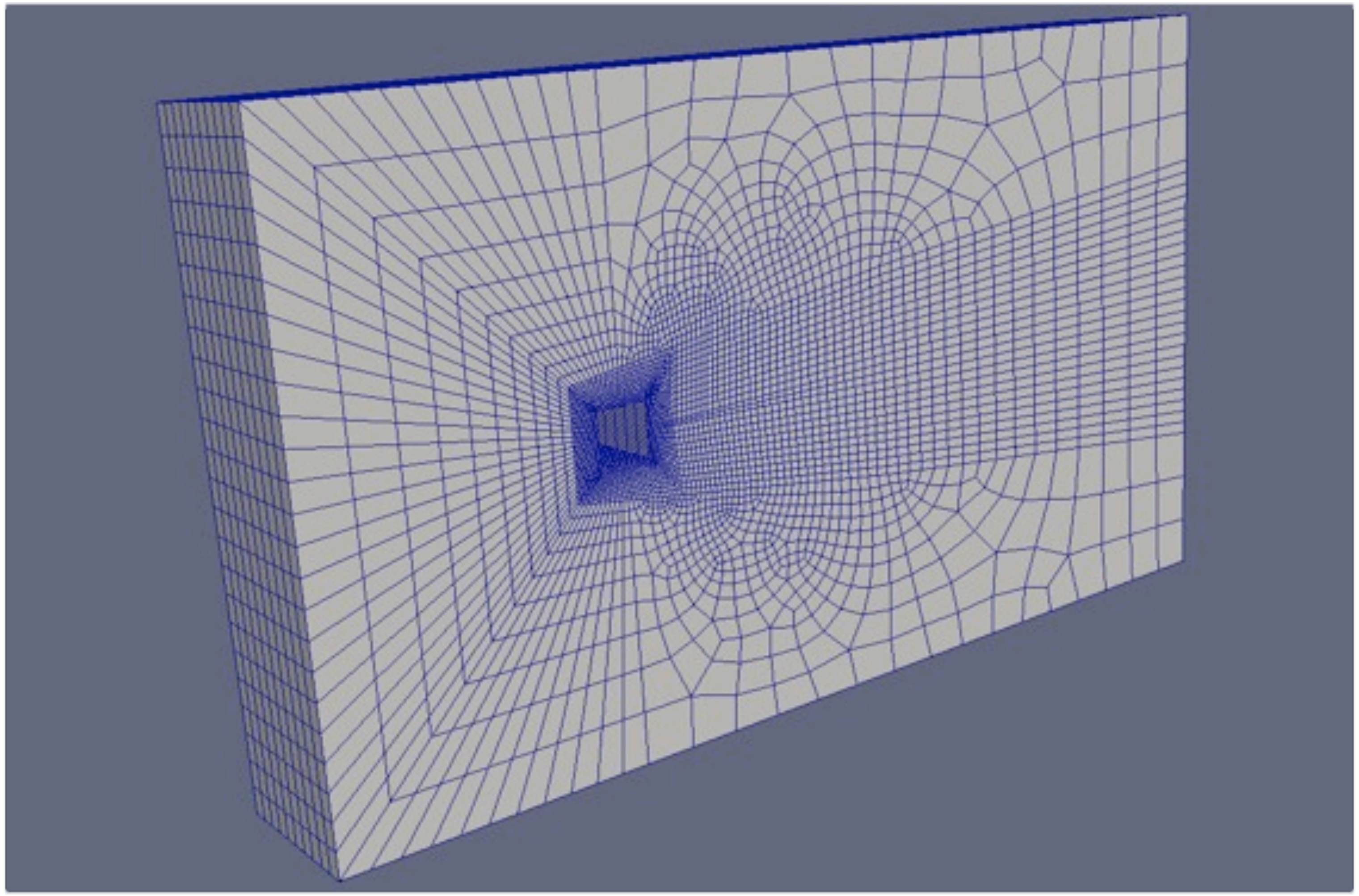

- Time integration: **RK3**
- Nº of elements: **35760** (2.3×10^6 DoF)
- Grid dimensions: **$21D \times 12D \times 3.2D$**
- Reynolds: **21400**
- Mach: **0.3**
- Statistics: **16 T_0**

Flow Past Square Cylinder: Re = 21400

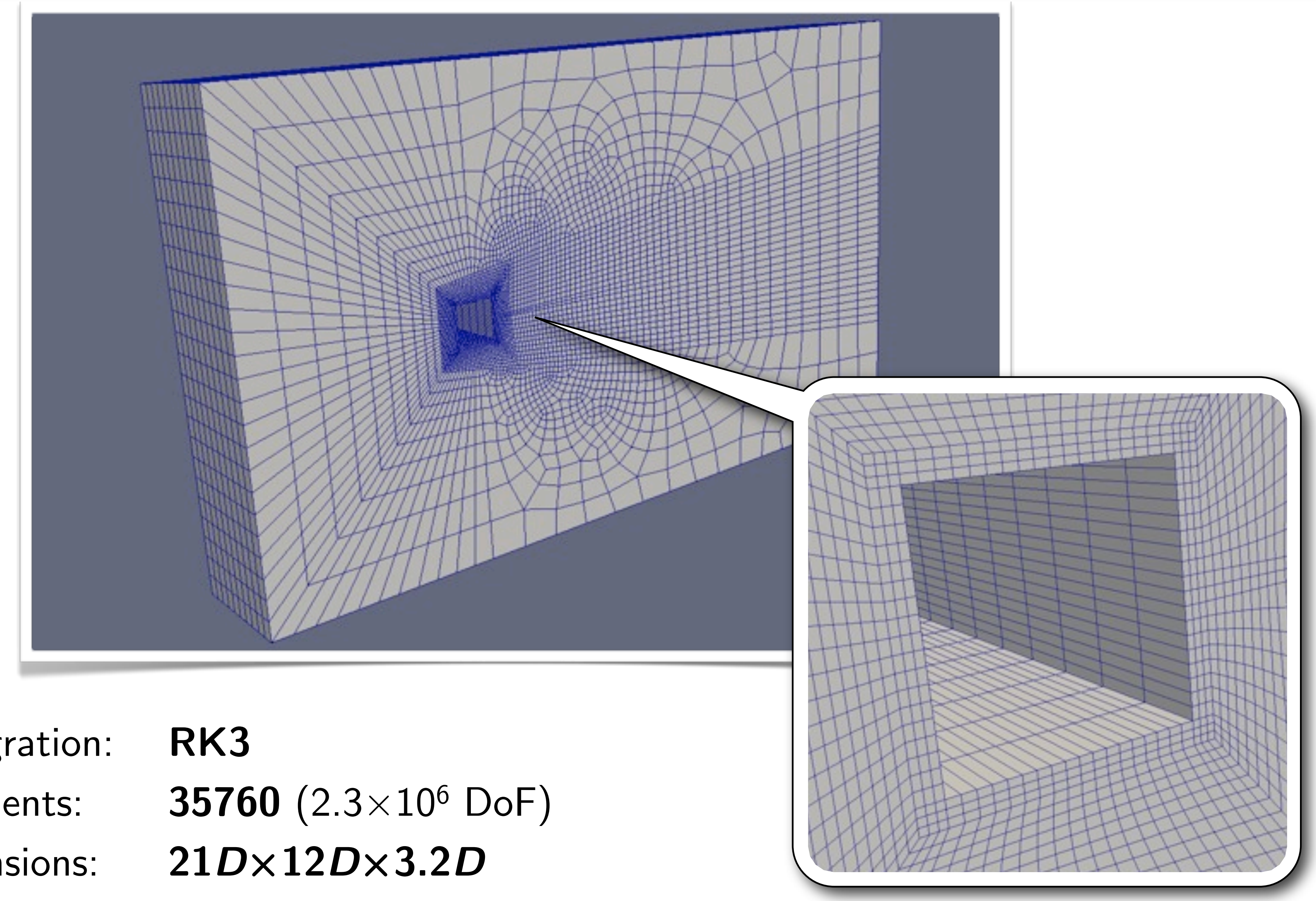

elements view

- Time integration: **RK3**
- Nº of elements: **35760** (2.3×10^6 DoF)
- Grid dimensions: $\mathbf{21D\times12D\times3.2D}$
- Reynolds: **21400**
- Mach: **0.3**
- Statistics: $\mathbf{16\ T_0}$

Flow Past Square Cylinder: Re = 21400

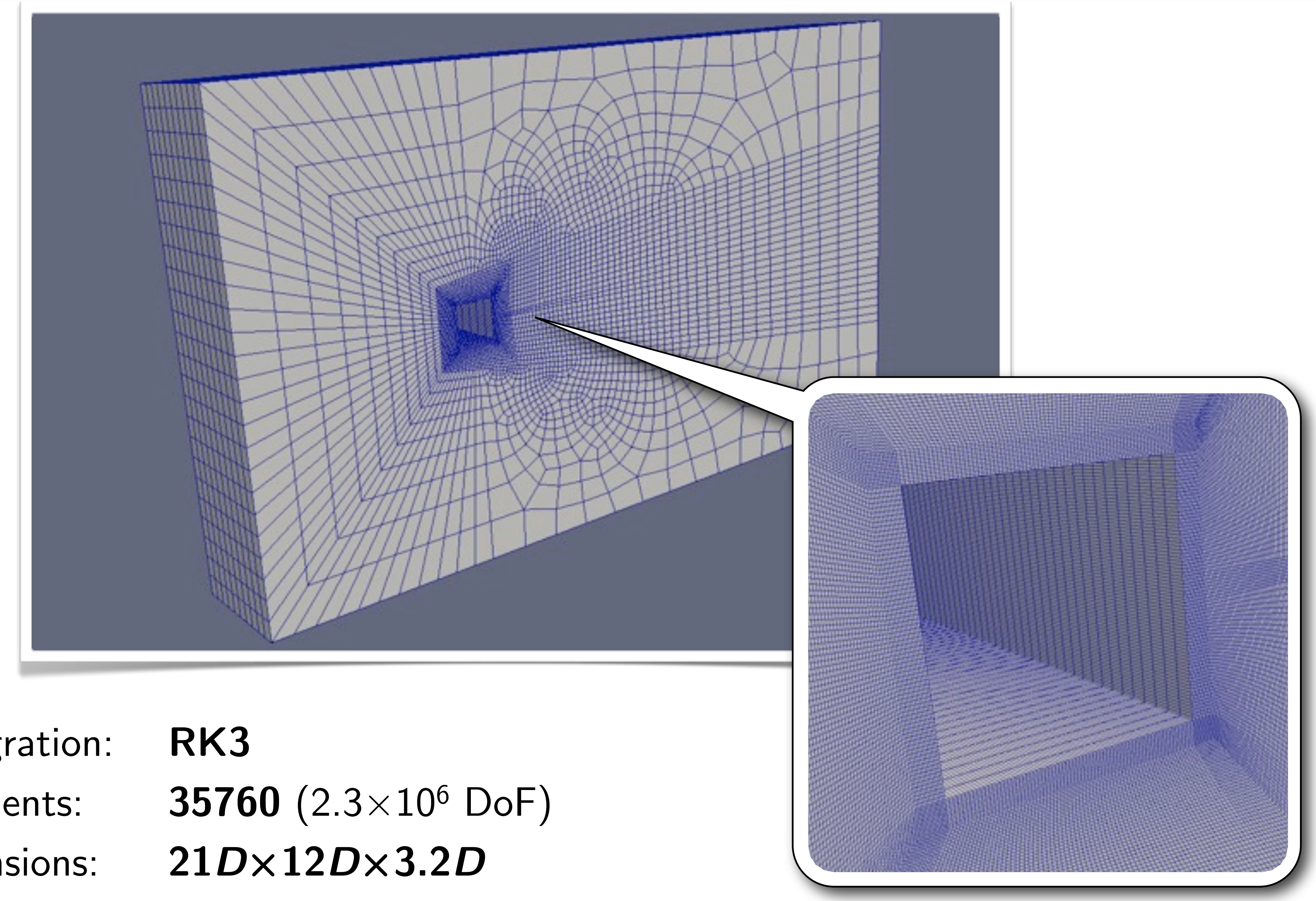

actual resolution

- Time integration: **RK3**
- Nº of elements: **35760** (2.3×10^6 DoF)
- Grid dimensions: **$21D\times12D\times3.2D$**
- Reynolds: **21400**
- Mach: **0.3**
- Statistics: **16 T_0**

Flow past a Square Cylinder: $Re_D = 21400$

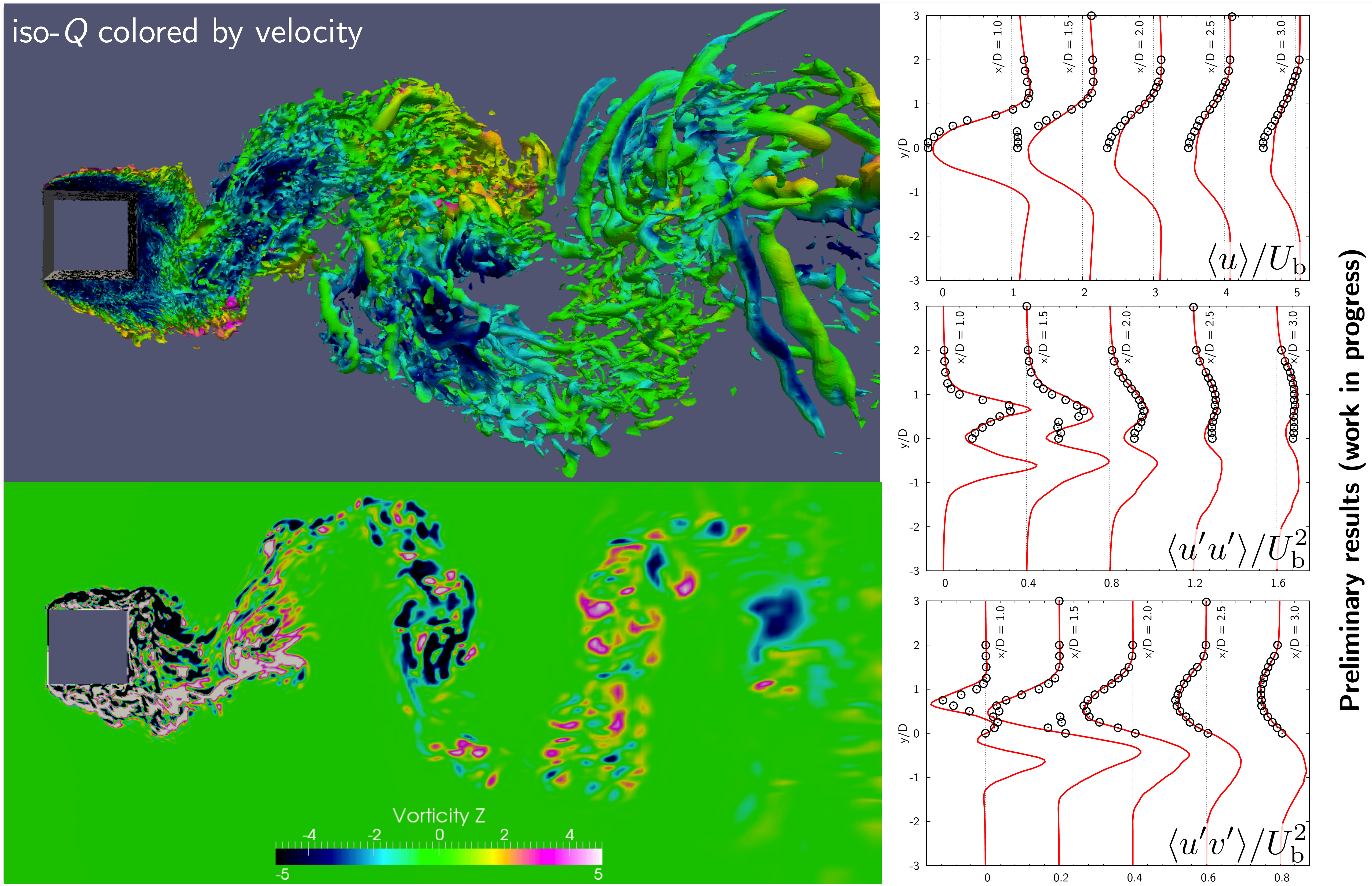

Summary and Conclusions

Predicting the future is generally ill advised.

However, the following are the author's opinions:

Summary and Conclusions

Predicting the future is generally ill advised.
However, the following are the author's opinions:

- The early development of CFD in the Aerospace Industry was primarily driven by the need to calculate steady transonic flows: ***this problem is quite well solved***
- CFD has been on a plateau for the last 15 years with 2nd-order accurate FV methods for the RANS equations almost universally used in both commercial and government codes which can treat complex configurations
- These methods cannot reliably predict complex separated, unsteady and vortex dominated flows
- Ongoing advances in both numerical algorithms and computer hardware and software should enable an advance to LES for industrial applications within the foreseeable future
- Research should focus on high-order methods with minimal numerical dissipation for unstructured meshes to enable the treatment of complex configurations
- Eventually DNS may become feasible for high Reynolds number flows

hopefully with a smaller power requirement than a wind tunnel

Acknowledgement

The current research is a combined effort by

- *Postdocs*: Charlie Liang, Peter Vincent, Guido Lodato
- *Ph.D. students*: Sachin Premasuthan, Kui Ou, Patrice Castonguay, David Williams, Yves Allenau, Lala Li, Manuel Lopez, and Andy Chan

It is made possible by the support of

- the *Airforce Office of Scientific Research* under grant FA9550-10-1-0418 by Dr. Fariba Fahroo
- the *National Science Foundation* under grants 0708071 and 0915006 monitored by Dr. Leland Jameson

A Review of the Literature from ACL

1. Castonguay, P., D. Williams, P. Vincent, M. Lopez, and A. Jameson (2011). On the development of a high-order, multi-GPU enabled, compressible viscous flow solver for mixed grids. *AIAA P.*, **vol. 2011-3229**
2. Jameson, A. (2010). A proof of the stability of the spectral difference method for all orders of accuracy. *J. Sci. Comput.*, **vol. 45**(1)
3. Jameson, A. (2011). Advances in bringing high-order methods to practical applications in computational fluid dynamics. *AIAA P.*, **vol. 2011-3226**
4. Jameson, A., P. Vincent, and P. Castonguay (2012). On the non-linear stability of flux reconstruction schemes. *J. Sci. Comput.*, **vol. 50**(2)
5. Lodato, G., P. Castonguay, and A. Jameson, Structural LES modeling with high-order spectral difference schemes. In *Annual Research Briefs* (Center for Turbulence Research, Stanford University, 2011)
6. Ou, K. and A. Jameson (2011). Unsteady adjoint method for the optimal control of advection and Burger's equations using high-order spectral difference method. *AIAA P.*, **vol. 2011- 24**
7. Vincent, P., P. Castonguay, and A. Jameson (2010). A new class of high-order energy stable flux reconstruction schemes. *J. Sci. Comput.*, **vol. 47**(1)
8. Vincent, P., P. Castonguay, and A. Jameson (2011). Insights from von Neumann analysis of high-order flux reconstruction schemes. *J. Comput. Phys.*, **vol. 230**(22)
9. Vincent, P. and A. Jameson (2011). Facilitating the adoption of unstructured high-order methods amongst a wider community of fluid dynamicists. *Math. Model. Nat. Phenom.*, **vol. 6**(3)
10. Williams, D., P. Castonguay, P. Vincent, and A. Jameson (2011). An extension of energy stable flux reconstruction to unsteady, non-linear, viscous problems on mixed grids. *AIAA P.*, **vol. 2011-3405**